# Performance Analysis of MIMO Systems: Transmit Antenna Selection, Cooperative Communications and Spatial Modulation

*A*

*Thesis Submitted*

*in Partial Fulfilment of the Requirements*

*for the Degree of*

**DOCTOR OF PHILOSOPHY**


**By**

**Brijesh Kumbhani**

Department of Electronics and Electrical Engineering

Indian Institute of Technology Guwahati

Guwahati - 781 039, INDIA.


October, 2015

# Certificate

This is to certify that the thesis entitled "**Performance Analysis of MIMO Systems: Transmit Antenna Selection, Cooperative Communications and Spatial Modulation**", submitted by **Brijesh Kumbhani** (10610212), a research scholar in the *Department of Electronics & Electrical Engineering, Indian Institute of Technology Guwahati*, for the award of the degree of **Doctor of Philosophy**, is a record of an original research work carried out by him under my supervision and guidance. The thesis has fulfilled all requirements as per the regulations of the institute and in my opinion has reached the standard needed for submission. The results embodied in this thesis have not been submitted to any other University or Institute for the award of any degree or diploma.

Dated:

Guwahati.

Dr. Rakhesh Singh Kshetrimayum
Dept. of Electronics & Electrical Engg.
Indian Institute of Technology Guwahati
Guwahati - 781039, Assam, India.

# Acknowledgements

I would like to express my sincere gratitude to my supervisor, Dr. Rakhesh Singh Kshetrimayum, for his excellent guidance and support throughout the course for this work. My heartfelt thanks to him for the unlimited support and patience shown to me. I would particularly like to thank for all his help in patiently and carefully correcting all my manuscripts.

I would like to thank my doctoral committee members Dr. P. R. Sahu, Dr. A. Rajesh, Dr. B. K. Rai and Dr. A. Sahu for sparing their precious time to evaluate the progress of my work. Their suggestions have been valuable. I would also like to extend my thanks to other faculty members of the department for their kind help during my academic studies. My special thanks to Mr. Sanjib, Mr. Sarma and all the members of the Communication Laboratory for maintaining an excellent computing facility and providing various resources useful for the research work.

I had a great time with my many friends and seniors at IIT Guwahati, including (but not limited to) Parveen, Atul, Vinay, Somen, Shivanshu, Murli, Anand, Ripudaman, Dhaval, Varun, Jaimeen, Suresh, Dharamashibhai, Piyush, Shrenik and the list goes on. I thank them for their support, encouragement and time to have fun with in the instances of boredom at my home away from home. The company of my friends at IIT Guwahati proved to be a great asset which helped me stay relaxed.

I also gratefully acknowledge MHRD, Govt. of India for financing my studies at IIT Guwahati. Finally, I would like to thank the Almighty for bestowing me this opportunity and showering his blessings on me to come out successful against all odds.

*(Brijesh Kumbhani)*

# Abstract

It is well known that multiple input multiple output (MIMO) systems improve transmission capacities and performance of wireless systems. But, with the increasing number of antennas, the required computation for detection at the receiver and the hardware at both the transmitter and the receiver ends becomes highly complex. To deal with this, MIMO systems that activate single antenna at a time were proposed namely transmit antenna selection (TAS) and spatial modulation (SM). TAS can achieve full diversity order. SM is a MIMO technique which can improve spectral efficiency up to a certain level. In this thesis, we consider TAS with maximal ratio combining at receiver (TAS/MRC), cooperative communications (CC) and SM aspects integrated with MIMO systems. Performance analysis of TAS/MRC MIMO systems is carried out over $\kappa-\mu$ and $\eta-\mu$ fading channels. It may be noted that $\kappa-\mu$ and $\eta-\mu$ fading distributions are better fit to practical fading conditions for line of sight and non line of sight conditions respectively. We derived closed form expressions for outage probability and infinite series expressions for SER and capacity of TAS/MRC MIMO systems. The expressions derived in this thesis for TAS/MRC systems are also applicable to TAS with selection combining at receiver (TAS/SC) systems. Simple expressions in the form of elementary functions are derived for approximate SER of SM MIMO systems over $\kappa-\mu$ and $\eta-\mu$ fading channels. The expressions are also given for other fading channels as special cases of $\kappa-\mu$ and $\eta-\mu$ fading channels. The application of TAS on two hop CC systems and SM MIMO systems have also been studied. Expressions for BER of TAS CC systems are derived using the analysis of TAS/MRC systems. Finally, closed form expression for outage probability is derived for SM MIMO systems with TAS over Rayleigh fading channels. All the expressions derived in the thesis are validated by

Monte Carlo simulation results. It is also shown that the infinite series expressions are converging fast enough to achieve sufficient accuracy by truncating them up to practically computable number of terms.

# CONTENTS

# List of Figures

# List of Tables

# LIST OF ACRONYMS

| | |
|---|---|
| ADC | Analog to Digital Converter |
| AF | Amplify and Forward |
| AWGN | Additive White Gaussian Noise |
| BER | Bit Error Rate |
| BFSK | Binary Frequency Shift Keying |
| BPSK | Binary Phase Shift Combining |
| CC | Cooperative Communication |
| CDF | Cumulative Distribution Function |
| COAS | Capacity Optimized Antenna Selection |
| CPE | Conditional Probability of Error |
| CSI | Channel State Information |
| DAC | Digital to Analog Converter |
| DF | Decode and Forward |
| EDAS | Euclidean Distance Optimized Antenna Selection |
| EGC | Equal Gain Combining |
| GSM | Global System for Mobile Communications |
| i.i.d. | Independent and identically distributed |
| LOS | Line of Sight |
| MGF | Moment Generating Function |
| MIMO | Multiple Input Multiple Output |
| MISO | Multiple Input Single Output |

| | |
|---|---|
| ML | Maximum Likelihood |
| MPAM | M-ary Pulse Amplitude Modulation |
| MPSK | M-ary Phase Shift Keying |
| MQAM | M-ary Quadrature Amplitude Modulation |
| MRC | Maximal Ratio Combining |
| MRP | Maximum Received Power |
| NLOS | Non Line of Sight |
| OFDM | Orthogonal Frequency Division Multiplexing |
| OP | Outage Probability |
| PDF | Probability Density Function |
| QoS | Quality of Service |
| QPSK | Quadrature Phase Shift Keying |
| RF | Radio Frequency |
| SC | Selection Combining |
| SER | Symbol Error Rate |
| SISO | Single Input Single Output |
| SIMO | Single Input Multiple Output |
| SM | Spatial Modulation |
| SNR | Signal to Noise Ratio |
| STBC | Space Time Block Codes |
| STTC | Space Time Trellis Codes |
| TAS | Transmit Antenna Selection |
| TAS/MRC | Transmit Antenna Selection with Maximal Ratio Combining |
| TAS/SC | Transmit Antenna Selection with Selection Combining |
| V-BLAST | Vertical Bell Laboratories Layered Space Time |

# CHAPTER 1

# INTRODUCTION

Wireless communication has revolutionized the communication technology in present era. Each generation of wireless technology is improving the speed and performance of wireless communication systems. But, the most challenging and pertaining aspect of wireless systems is fading, the temporal variation in received signal strength due to constructive and destructive combination of multipath components. It results on the account of the received signal being collection of different components reaching the receiver after reflections and scattering from different objects in the path between transmitter and receiver. These multipath components arriving almost at the same instant to the receiver can not be differentiated. Fading causes severe degradation in the performances of wireless communication systems, the most important is erroneously received data. The most commonly studied methods to overcome the effect of fading are the diversity combining schemes such as spatial diversity scheme, temporal diversity scheme, spectral diversity scheme, polarization diversity scheme, etc. of which spatial diversity techniques are the most commonly used and highly studied diversity techniques. Spatial diversity techniques take advantage of spatial variation in the signal strength due to multipath components and combine them accordingly using multiple antennas at the receiver. The commonly used spatial diversity combining schemes are: selection combining (SC), equal gain combining (EGC) and maximal ratio combining (MRC). Each of these combining techniques is discussed in brief as follows.

**Selection Diversity**

It is the simplest of all spatial diversity schemes. It takes advantage of the spatial diversity that the signals may have different strengths at different points in space. So, it is highly likely that the signal has sufficient strength at one of the antennas at the receiver. Keeping this fact into consideration, signal received at the antenna having the highest strength is passed to the detector and decoded to recover the transmitted signal.

**Equal Gain Combining**

Equal gain combining also takes advantage of different strengths at different locations. But unlike selection diversity scheme, it uses all the received signals including the weaker signals. Before passing the signal to the detector, received signals from all the receiver antennas are cophased and added. The resultant signals are then used to recover the transmitted message. Equal gain combining gives better performance compared to selection combining because it used less strong signals also in addition to the strongest signal.

**Maximal Ratio Combining**

This is a more complex combining scheme to implement. It has been inspired from equal gain combining to further improve the system performance. In addition to cophasing the received signals, each signal is amplified such that after combining the signal to noise (SNR) gets maximized. With added complexity MRC gives the best error performance among all the spatial diversity combining schemes. So, sometimes it is also referred to as optimal combining scheme, i.e. the combining scheme that gives optimum error performance.

In each of the spatial diversity schemes, transmitter employs single antenna which in turn improves performance of the communication systems but does not change the spectral efficiency which is number of bits transmitted per channel usage. Multiple antennas at the transmitter resulting to multiple input multiple output (MIMO) systems [4] were seen as a possible way to get even better information carrying capacities. Spatial multiplexing techniques [5], such as Vertical-Bell Laboratories Layered Space-Time (V-BLAST) [6] can achieve spectral efficiency which is linearly proportional to the number of transmitting antennas. Space time block codes (STBC) [7] or space time trellis codes (STTC) [8] use transmit diversity scheme and can achieve full diversity order (same as product of number of antennas at transmitter and receiver). In spatially multiplexed MIMO systems, information is converted into multiple data streams that are transmitted simultaneously through the multiple antennas of transmitter [9]. This simultaneous transmission requires parallel radio frequency (RF) chains. Parallel RF chains at the transmitter and/or receiver of MIMO systems comes with added cost in terms of hardware complexity, power and size [10]. It becomes difficult to integrate such complex hardware in the mobile units simultaneously retaining their easy handling and compactness. Moreover, simultaneous transmission from multiple antennas have inherent disadvantages of interantenna interference, requirement of synchronization, etc [11]. These disadvantages can be overcome by the MIMO systems with single RF chain at transmitter which in turn activate single antenna at a time for transmission. Possible candidates for such systems are transmit antenna selection (TAS) and spatial modulation (SM) in which only one antenna is made active at the transmitter to send information at any time instant, thus helps to reduce power consumption, size and cost [12]. TAS and SM systems may activate more than one antennas at the transmitter but this will have the same problems mentioned above like interantenna interference, synchronization requirement, etc. At receiver, any of the spatial diversity combining technique can be used.

Antenna selection uses a subset of total available antennas of any MIMO system at the transmitter, receiver or both sides simultaneously. The technique of antenna selection has been very effective in reducing the hardware complexity as the number of RF chains required will be reduced. With these advantages, TAS systems are found to achieve full diversity order unlike other MIMO systems such as V-BLAST which achieves diversity order of the number of antennas at the receiver. These advantages are achieved at the cost of spectral efficiency. TAS does not give any spectral efficiency gain like V-BLAST which is capable of improving spectral efficiency as the order of number of antennas at the transmitter at the cost of hardware and decoding complexity. Alamouti space time coding achieves full diversity order. However, it requires same number of RF chains at the transmitter as the number of antennas in addition to synchronization. Different selection criteria either based on maximizing channel capacity or maximizing SNR may be employed. TAS can be used with any of the diversity combining techniques at the receiver such as MRC, SC, etc. depending on the allowed level of complexity and the performance quality of service (QoS) requirements.

Another system with single transmit RF chain is SM MIMO system. Unlike TAS systems, SM can not achieve full diversity. However, SM systems achieve gain in terms of spectral efficiency by a factor of logarithm of number of transmitter antennas to the base 2 which is less than V-BLAST systems but in addition, SM systems need single RF chain which overcomes the disadvantage of V-BLAST systems. SM systems select antenna to transmit data based on the incoming bit sequence. The bit sequences are mapped with antenna index and corresponding antenna is used to transmit information. Recently generalized SM [13] has been proposed in which multiple antennas are activated at a time but it has higher decoding complexity than SM with single antenna activation.

## 1.1 Thesis Contribution

Some of the contributions of this thesis are enlisted below:

1. Performance analysis of TAS systems over $\eta - \mu$ fading channels

   (a) TAS systems with MRC receiver are analyzed over i.i.d. fading channels. Infinite series expressions are derived for error performance and ergodic capacity.

   (b) The derived expressions have been validated through extensive Monte Carlo simulation results.

2. Performance analysis of TAS systems over $\kappa-\mu$ fading channels

   (a) TAS systems with MRC receiver are analyzed over i.i.d. fading channels. Closed form expression for outage probability and infinite series expressions for error performance and ergodic capacity are derived.

   (b) The derived expressions have been validated through extensive Monte Carlo simulation results.

3. Simplified expressions for approximate error analysis of SM MIMO systems over $\eta-\mu$ and $\kappa-\mu$ fading channels

   (a) SM MIMO systems are analyzed over i.i.d. $\eta-\mu$ and $\kappa-\mu$ fading channels. Closed form expressions for approximate error performance in terms of elementary functions are derived.

   (b) The accuracy of analytical expressions has been verified by Monte Carlo simulation results.

4. Application of TAS systems in two hop relaying systems

   (a) TAS scheme applied on two hop relaying systems with MIMO nodes and their error performance is analyzed over $\eta-\mu$ and $\kappa-\mu$ fading channels

   (b) The derived expressions have been validated through extensive Monte Carlo simulation results.

5. Application of TAS systems in SM based MIMO systems

   (a) TAS scheme applied on SM based MIMO systems and their outage probability is analyzed over Rayleigh fading channels.

   (b) A closed form expression for OP is derived and validated through extensive Monte Carlo simulation results.

## 1.2 Thesis Organization

This thesis is divided into eight Chapters. A brief description of content of each Chapter is given below.

In chapter 2, we give overview of TAS and generalized fading channels. It introduces TAS criterion for different receive diversity combining schemes, different generalized fading distributions and the fading parameters of generalized fading channels to represent some well known fading distributions as their special cases.

In chapter 3, we present OP, BER/SER and channel capacity analysis of TAS/MRC systems for arbitrary number of transmit and receive antennas over $\kappa-\mu$ fading channels. Closed form expression for calculation of OP for TAS based MIMO systems over $\kappa-\mu$ fading channels and computationally efficient expressions of OP over Nakagami-m and Rayleigh fading channels in comparison to those reported in [14] and [1] are presented. Infinite series expressions for exact SER, ergodic capacity and simple expression for asymptotic SER of TAS/MRC systems for several modulation schemes are derived. We also present the results of Monte Carlo simulations to validate our analytical results.

Chapter 4 presents analysis of SER performance and ergodic capacity of TAS/MRC systems over $\eta-\mu$ fading channels. We derive expressions for SER (exact, approximate and asymptotic) for several modulation schemes and ergodic capacity. The exactness of all the expressions has been validated with the help of Monte Carlo simulation results. The variation of ergodic capacity with fading parameters ($\eta$ and $\mu$) is also studied.

In chapter 5, we derive infinite series expression for end to end BER of two-hop relaying DF cooperative communication (CC) systems over generalized $\eta-\mu$ and $\kappa-\mu$ fading channels for BPSK modulation scheme with transmit antenna selection at source node and relay node as well such that the received SNR at the destination node is maximized.

In chapter 6, performance analysis of SM MIMO systems is presented. Simple analytical expressions for approximate SER in terms of elementary functions are derived over $\kappa-\mu$ and

$\eta - \mu$ fading channels for various modulation schemes.

In chapter 7, we analyze the outage probability of TAS SM MIMO systems. A closed form expression for outage probability of TAS SM MIMO systems over flat Rayleigh fading environment is derived. Analytical results are validated using Monte Carlo simulations and they are in close agreement.

Summary of the work presented in this thesis with conclusions and possible future directions have been presented in chapter 8.

# Chapter 2

# Overview of Transmit Antenna Selection and Generalized Fading Channels

Multiple antennas at transmitter and receiver bring drastic improvement in the capacity and performance of wireless communication systems compared to single antenna systems. But the disadvantage being multiple RF chains consisting of filters, frequency up and/or down converters, low noise amplifiers, analog to digital converters (ADCs) and digital to analog converters (DACs) bring hardware complexity and increased power consumption. In addition, detection at the receiver also becomes computationally complex, the decoding complexity is of the exponential order of product of number of antennas at the transmitter and receiver. To overcome these issues, the technique of transmit antenna selection was proposed at the same time exploiting the advantage of all the antennas being in the system. In antenna selection, only a subset of total available antennas is made active at a time. In this thesis, unless it is mentioned, we consider single antenna selection at the transmitter.

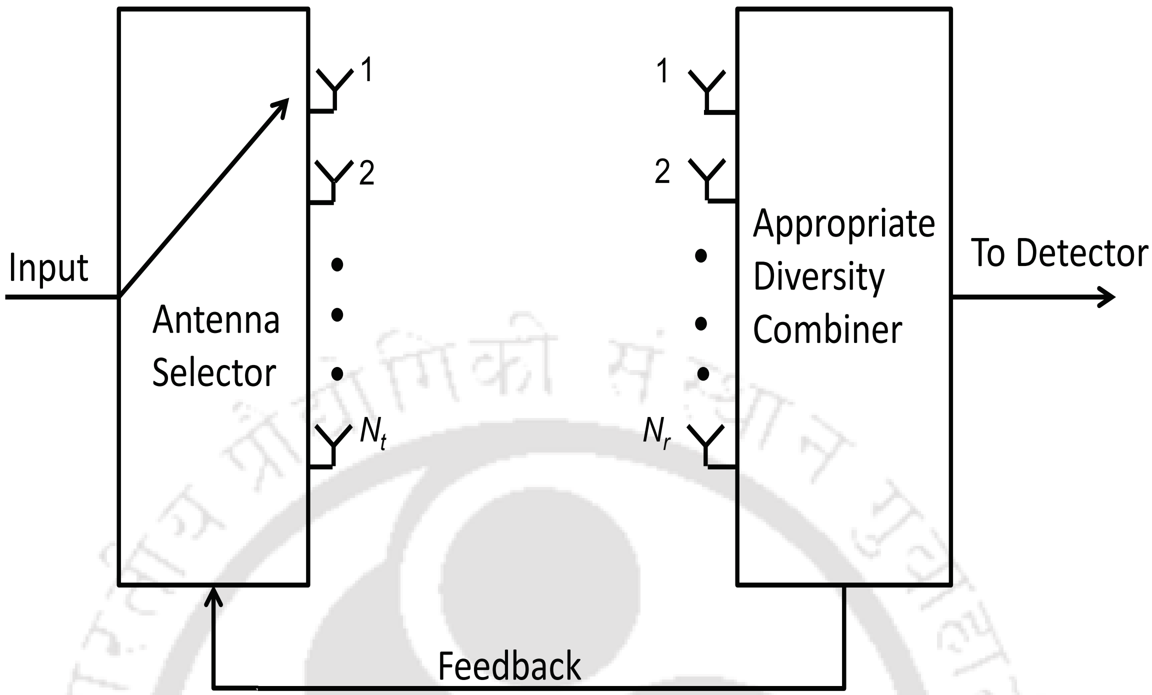


Figure 2.1: System Model of TAS MIMO Systems [1]

## 2.1 Antenna Selection

Different criteria for TAS explored in the literature are received SNR, channel capacity and Euclidian distance [15, 16]. In this thesis, we have limited ourselves to TAS based on received SNR in which single antenna is selected at the transmitter which maximizes the received instantaneous SNR. However, it does not require the estimation or knowledge of channel state information at the transmitter. The transmit antenna which maximize received SNR is estimated at the receiver and the information is made available to transmitter through very low rate feedback link. Different diversity combining techniques can be used at the receiver with TAS of which MRC and SC are most commonly explored in literature because of optimality of MRC and simplicity of SC. The block diagram of TAS system with spatial diversity combining at receiver is shown in Figure 2.1. It consists of a feedback link from receiver to transmitter so that receiver can send information about the antenna that maximizes the received instantaneous

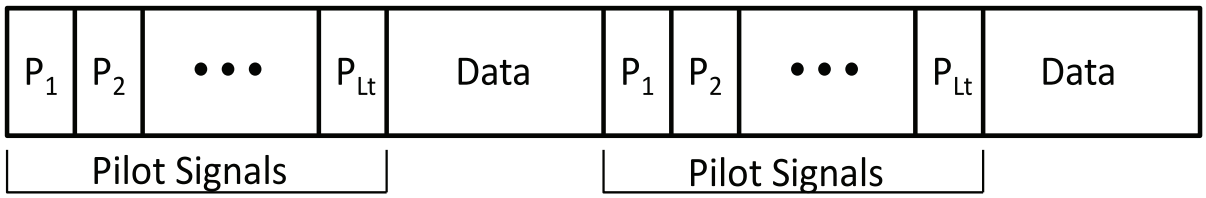


Figure 2.2: Frame structure of TAS MIMO Systems [1]

SNR. According to this feedback information, the antenna selector connects to corresponding antenna and sends appropriately modulated data. Note that the antenna selector block is an RF switch and hence it does not require the complete set of RF chain for each antenna at the transmitter. To select an antenna at the transmitter, a set of pilot sequence is transmitted from each transmitter antenna one by one and for each transmission receiver compares the antenna selection criteria as per diversity scheme to be implemented and intimate the transmitter about the antenna maximizing SNR as in Figure 2.2. The antenna selection criterion for both these combining schemes are discussed in the following sections:

### 2.1.1 Selection Combining at the Receiver

SC is the simplest diversity combining scheme. In SC, only the strongest received signal among all the received copies is processed further to detect the information. When SC is used with TAS, only the antennas corresponding to the link which gives maximum received SNR are activated. The link which gives the highest received SNR is determined by

$$I_{SC} = \arg\max_{\substack{1\leq i\leq N_t \\ 1\leq j\leq N_r}} \left\{\gamma_{j,i}\right\} \tag{2.1}$$

where $I_{SC}$ denote the link which gives maximum instantaneous SNR at the receiver and $\gamma_{j,i}$ is the instantaneous SNR of the link between $i^{th}$ transmitting antenna and $j^{th}$ receiver antenna. Only the antennas that correspond to the best link are made active at a time in this case. We refer to such systems as $(N_t,1;N_r,1)$ joint transmit and receive antenna selection systems. The advantage of SC at the receiver is that it requires only one RF chain at the receiver and hence it is easy to implement.

### 2.1.2 MRC at the Receiver

In this case, it is assumed that the number of RF chains at receiver is same as the number of receiver antennas. MRC is used at the receiver. The resulting received SNR for MRC combining scheme is given by $\gamma_t = \sum_{n=1}^{N_r} \gamma_n$, where $\gamma_n$ is the instantaneous SNR of the $n^{th}$ branch. The transmitting antenna that maximizes SNR at the receiver can be determined by

$$I_{MRC} = \arg\max_{1 \le i \le N_t} \left\{ \gamma_{t,i} = \sum_{j=1}^{N_r} \gamma_{j,i} \right\} \tag{2.2}$$

where $\gamma_{t,i}$ denote total received instantaneous SNR when $i^{th}$ transmitting antenna is selected and $I_{MRC}$ denotes antenna index which corresponds to the transmitting antenna that maximizes the received SNR. We refer to such systems as ($N_t$,1;$N_r$) TAS/MRC systems. MRC requires as many RF chains at the receiver as the number of receiving antennas. With this hardware complexity, it promises optimum performance in terms of probability of error among all the diversity combining schemes.

## 2.2 Generalized Fading Channels

The well-known fading distributions are obtained assuming homogeneous environment consisting of point scatters which certainly is an assumption. In practical, the reflecting surfaces are spatially correlated most of the time characterizing a non-homogeneous environment. Yacoub proposed two fading distributions namely $\eta-\mu$ distribution and $\kappa-\mu$ distribution to model generalized fading conditions in NLOS as well as LOS scenarios in wireless links for non-homogeneous environment [17–19]. These distributions are also shown to be better fit to the experimental data in their respective wireless scenario. Moreover, the well known distributions like Nakagami-m, one sided Gaussian, Rayleigh, Nakagami-q, etc. can be represented as special cases of $\kappa-\mu$ and/or $\eta-\mu$ distributions. These features are the key points to consider

$\kappa-\mu$ and/or $\eta-\mu$ fading environments in this thesis. The detailed description of $\eta-\mu$ and $\kappa-\mu$ distribution can be found in the following subsections.

### 2.2.1 $\eta-\mu$ Distribution

It is assumed that the multi-path components are received in the form of clusters and the clusters does not have any dominating or LOS component in $\eta-\mu$ distribution. With this assumption, it is best suited to model the practical fading channels in NLOS conditions. The probability density function (PDF) of $\eta-\mu$ distributed normalized envelope can be given by

$$f_{X_{\eta-\mu}}(x) = \frac{4\sqrt{\pi}\mu^{\mu+\frac{1}{2}}h^{\mu}}{\Gamma(\mu)H^{\mu-\frac{1}{2}}}x^{2\mu}e^{-2\mu hx^2}I_{\mu-\frac{1}{2}}\left(2\mu Hx^2\right) \tag{2.3}$$

where $\mu > 0$ is a fading parameter defined as $\mu = \frac{1}{2V\left(X^2_{\eta-\mu}\right)}\left[1+\left(\frac{H}{h}\right)^2\right]$, $\Gamma(\cdot)$ is the Gamma function, $I_\nu(\cdot)$ is the modified Bessel function of first kind and order $\nu$, $V(\cdot)$ denotes the variance operator, $H$ and $h$ are the functions of fading parameter $\eta$ defined for two formats as follows:

**Format 1**

In this format, the in phase and quadrature phase components of the envelope are assumed to be independent and with different powers. $\eta$ is defined as the ratio of power of in phase component to the power of quadrature component. In this case, $0 < \eta < \infty$, $H = \frac{\eta^{-1}-\eta}{4}$ and $h = \frac{2+\eta^{-1}+\eta}{4}$. It can be shown that the values of $h$ and $H$ are symmetrical around $\eta = 1$. Therefore, it suffices to consider either $0 < \eta \leq 1$ or $1 \leq \eta < \infty$.

**Format 2**

In this format, the in phase and quadrature phase components of the envelope are assumed to be correlated and with equal powers. $\eta$ is defined as the correlation coefficient between in phase

Table. 2.1: Values of fading parameters to represent different fading distributions as special case of $\eta-\mu$ fading distribution

| Distribution | Value of $\eta$ | Value of $\mu$ |
|---|---|---|
| One sided Gaussian | 1 | 0.25 |
| Rayleigh | 1 | 0.5 |
| Nakagami-m | 1 | $m/2$ |
| Nakagami-q (Hoyt) | $q^2$ | 0.5 |

component and the quadrature component. In this case, $-1<\eta<1$, $H=\frac{\eta}{1-\eta^2}$ and $h=\frac{1}{1-\eta^2}$. It can be shown that the values of $h$ and $H$ are symmetrical around $\eta=0$. Therefore, it suffices to consider either $0\leq\eta<1$ or $-1<\eta\leq 0$.

### $\eta-\mu$ **Distributed Power Variate**

The normalized power variate of $\eta-\mu$ distribution is the square of $\eta-\mu$ distributed normalized envelope. Thus, the PDF of $\eta-\mu$ distributed normalized power variate can be given as

$$f_{P_{\eta-\mu}}(\omega)=\frac{2\sqrt{\pi}\mu^{\mu+\frac{1}{2}}h^{\mu}}{\Gamma(\mu)H^{\mu-\frac{1}{2}}}\omega^{\mu-\frac{1}{2}}e^{-2\mu h\omega}I_{\mu-\frac{1}{2}}(2\mu H\omega) \tag{2.4}$$

where $\mu>0$ is a fading parameter defined as $\mu=\frac{1}{2V(P_{\eta-\mu})}\left[1+\left(\frac{H}{h}\right)^2\right]$

$\eta-\mu$ distribution includes one-sided Gaussian, Rayleigh, Nakagami-m and Hoyt fading distributions as its special cases. The values of $\eta-\mu$ fading parameters corresponding to these special cases are listed in Table 2.1. The PDFs for special cases of $\eta-\mu$ distributed normalized envelope corresponding to values of fading parameters are plotted and can be observed in Figure 2.3.

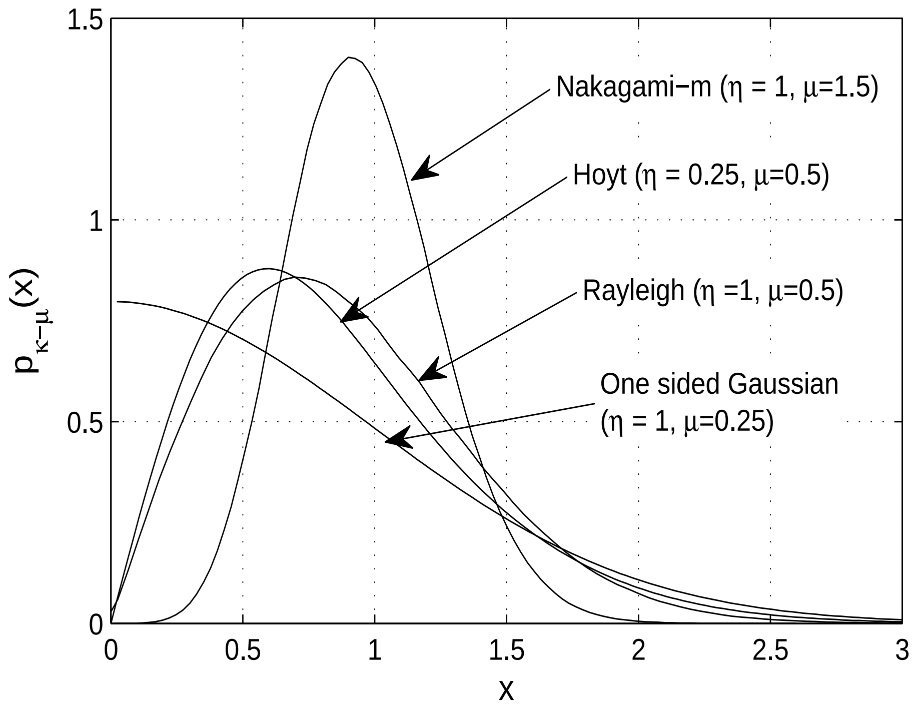


Figure 2.3: PDFs of some special cases of $\eta-\mu$ distribution

### 2.2.2 $\kappa-\mu$ Distribution

Unlike in $\eta-\mu$ fading, in $\kappa-\mu$ fading, it is assumed that the in-phase and quadrature phase components are independent and have equal powers. But, it has some dominant components considered to be LOS components. So, $\kappa-\mu$ distribution is best suited to model the practical fading channels in presence of LOS component. PDF of $\kappa-\mu$ distributed normalized envelope can be given by

$$f_{X_{\kappa-\mu}}(x) = \frac{2\mu(1+\kappa)^{\frac{\mu+1}{2}}}{\kappa^{\frac{\mu-1}{2}}e^{\mu\kappa}} x^{\mu} e^{-\mu(1+\kappa)x^2} I_{\mu-1}\left(2\mu x\sqrt{\kappa(1+\kappa)}\right) \tag{2.5}$$

where $\kappa$ is the ratio of power in the dominant (LOS) components to that of scattered components and $\mu = \frac{1}{V\left(X_{\kappa-\mu}^2\right)}\frac{1+2\kappa}{(1+\kappa)^2}$.

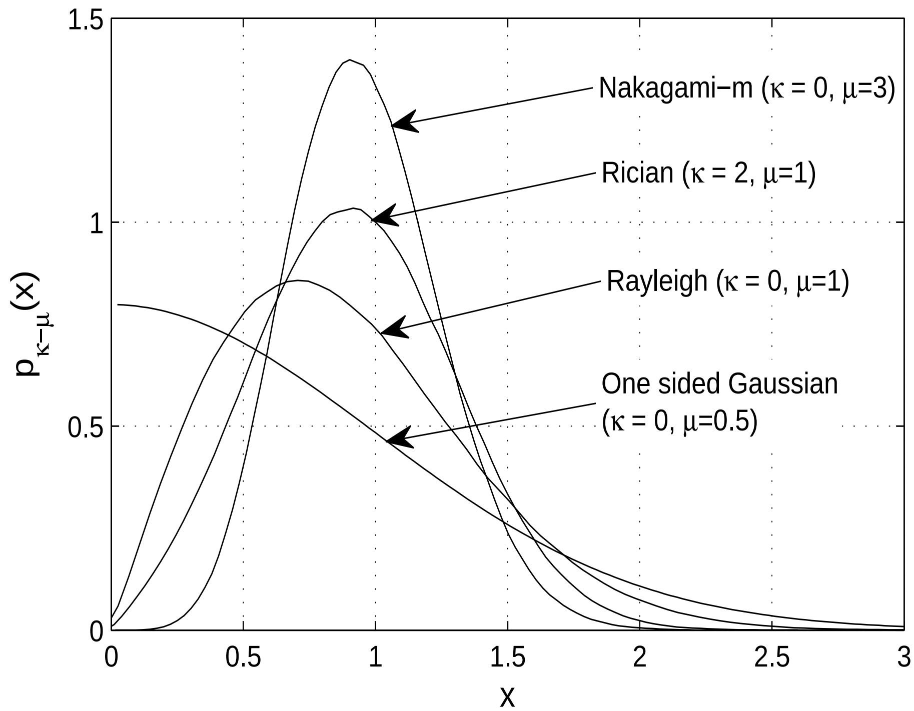


Figure 2.4: PDFs of some special cases of $\kappa-\mu$ distribution

### $\kappa-\mu$ Distributed Power Variate

The power variate of $\kappa-\mu$ distribution is the square of $\kappa-\mu$ distributed envelope. Thus, the PDF of $\kappa-\mu$ distributed normalized power variate can be given as

$$f_{P_{\kappa-\mu}}(p) = \frac{\mu(1+\kappa)^{\frac{\mu+1}{2}}}{\kappa^{\frac{\mu-1}{2}} e^{\mu\kappa}} p^{\frac{\mu-1}{2}} e^{-\mu(1+\kappa)p} I_{\mu-1}\left(2\mu\sqrt{\kappa(1+\kappa)p}\right) \tag{2.6}$$

where $\mu = \frac{1}{V\left(P_{\kappa-\mu}\right)} \frac{1+2\kappa}{(1+\kappa)^2}$.

$\kappa-\mu$ distribution includes one-sided Gaussian, Rayleigh, Rician and Nakagami-m fading distributions as its special cases. The values of $\kappa-\mu$ fading parameters for these special cases are listed in Table 2.2. The PDFs for special cases of $\kappa-\mu$ distributed normalized envelope corresponding to values of fading parameters are plotted and can be observed in Figure 2.4. It can be observed that the PDF curves shift towards right for non zero values of $\kappa$ when compared with the same value of $\mu$ (see Rayleigh and Rician case in Figure 2.4).

Table. 2.2: Values of fading parameters to represent different fading distributions as special case of $\kappa-\mu$ fading distribution

| Distribution | Value of $\kappa$ | Value of $\mu$ |
|---|---|---|
| One sided Gaussian | 0 | 0.5 |
| Rayleigh | 0 | 1 |
| Nakagami-m | 0 | $m$ |
| Rice | $K$ | 1 |

## 2.3 Literature Review

The existing literature on SM, TAS with MRC at receiver (TAS/MRC) and joint transmit and receive antenna selection systems have reported closed form or infinite series expressions for different performance metrics such as bit error rate (BER) or symbol error rate (SER) and outage probability (OP) over various fading channels for several modulation schemes. Summary of some of the existing literatures on TAS, SM, application of TAS on various wireless communication systems and others related to this thesis is given in brief as follows.

The technique of TAS has become popular since Sollenberger proposed TAS with SC at the receiver (TAS/SC) in 1993 [20]. Thoen et. al. modified the system model further to take advantage of MRC diversity and proposed TAS/MRC [21]. Both [20] and [21] show that TAS/SC and TAS/MRC systems achieve full diversity order without affecting the spectral efficiency of the basic modulation scheme being used. Analytical closed form expressions for OP and BER of TAS/MRC systems with binary phase shift keying (BPSK) modulation over independent and identically distributed (i.i.d.) Rayleigh fading channels are derived in [1]. It is also shown that TAS/MRC systems provide better SNR gain and BER performance when compared with STBC systems with same number of antennas at the transmitter and the receiver. This performance improvement is justified by the fact that in STBC, total energy per symbol is shared among the transmit antennas while in TAS/MRC single antenna being active, it transmits with the full transmit power. The performance of TAS systems over Nakagami-m fading channels is analyzed and reported in [14, 22–24]. In [22], authors assumed Nakagami-m fading channels with integer values of fading parameter $m$ to analyze the error performance of TAS/MRC systems with various coherent modulation schemes and derived closed form expression for the exact BER. With the same assumptions, TAS systems with SC at receiver are analyzed in [23]. TAS/MRC systems over Nakagami-m fading channels with real values of fading parameter $m$ are analyzed and infinite series expressions for OP and BER (exact and asymptotic) are derived for M-ary phase shift keying (MPSK) modulation and M-ary quadrature amplitude modulation (MQAM) schemes in [14]. In [25], the OP analysis of multiuser TAS/MRC systems over arbitrary Nakagami-m fading channels has been analyzed. Recently, error performance and channel capacity of TAS/MRC systems over Hoyt fading channels is investigated and closed form expressions are reported for two receiving antennas in [26]. There are literatures which reported performance analysis of TAS based MIMO systems over correlated fading channels [27–29], but in this thesis, we limit to the literatures related to TAS based MIMO systems over independent fading channels.

M. D. Yacoub proposed $\eta-\mu$ and $\kappa-\mu$ distributions to model the fading channels in non line of sight (NLOS) and line of sight (LOS) conditions respectively [17–19]. It is also shown that these distributions are better fit to the experimental data and these are capable of representing the classical fading models such as Rayleigh, Nakagami-m, Nakagami-q (Hoyt), Rician and one sided Gaussian distributions as their special cases. Several previous works have analyzed the BER/SER performances of single input single output (SISO) and single input multiple output (SIMO), also known as diversity combining schemes over i.i.d. $\kappa-\mu$ and $\eta-\mu$ fading channels [30–36]. Closed form expressions of moment generating function (MGF) of $\eta-\mu$ and $\kappa-\mu$ distributions in the form of elementary functions are reported in [35]. Using the closed form expressions of MGF, closed form expressions are derived for error performance analysis of digital modulation schemes over $\eta-\mu$ and $\kappa-\mu$ fading channels [36], the same analysis is applicable to analyze error performance of diversity combined digital modulation techniques. BER/SER performance of MRC system is analyzed with closed form expressions for MQAM schemes with MRC diversity combining technique over $\kappa-\mu$ and $\eta-\mu$ fading channels in [30, 31]. The L branch SC SIMO systems with binary coherent and non-coherent modulation schemes are analyzed for SER over $\kappa-\mu$ and $\eta-\mu$ fading channels in [32] but it does not consider MQAM modulation scheme which is being implemented in next generation wireless communication technologies, even the channel capacity has not been reported. Recently, the multiple input single output (MISO) systems were analyzed for throughput over $\kappa-\mu$ fading channels [33]. Closed form expressions for probability of error and channel capacity for selection diversity combining has been reported in [34], but it restricted the analysis only to integer values of $\mu$.

Some of the literature also explored the effect of TAS on cooperative relaying systems based on both Amplify and forward (AF) and Decode and forward (DF) protocols [37–47]. Most of the existing literature on TAS based relaying systems analyzing error performance considered AF protocol at the relay node over Rayleigh and Nakagami-m fading channels [46,47]. Whereas much work is done on OP analysis of DF based relaying with TAS at source and/or relay [41–43, 45]. BER of TAS based relaying systems with DF protocol at relay node has been analyzed in [44], however, it does not consider a direct link between source and the destination.

Some of the advances in research towards implementation and improvements of SM MIMO systems reported in literature is summarized as follows. SM MIMO systems have been proposed and analysed in [48, 49]. It is already reported that, SM MIMO systems outperform the other MIMO systems like Alamouti STBC and V-BLAST for the same spectral efficiencies with computationally much simpler decoding algorithms [49]. In [50], an optimum detection technique for SM is proposed with added computational complexity in detection algorithm that gives better performance in terms of error rate. It also reported expression for BER of SM MIMO systems with BPSK modulation over Rayleigh fading channels. Later, computationally efficient decoding algorithms are proposed in the literature for optimal detection technique, they are signal vector based detection scheme and generalized sphere decoding. Signal vector based detection [51] is a decoding technique for SM MIMO in which computational complexity is independent of signal constellation size and depends only on the number of antennas at transmitter and receiver but it gives error performances comparable to the optimal maximum likelihood (ML) detection technique only for lower SNRs when QAM scheme is used [52]. Generalized sphere decoding [53] also brings reduction in computational complexity with almost similar error performance as that of ML detection scheme. In [54], authors analyzed performance of SM MIMO systems over Nakagami-m fading channels for high SNR conditions and derived expressions for upper bound on BER. Generalized SM (GSM) with multiple active antennas simultaneously at transmitter is proposed in [13] to achieve higher spectral efficiency than that of SM but it has added disadvantages of inter antenna synchronization and more complex detection process. Recently, improved spatial modulation is proposed that achieves further reduction in hardware complexity at receiver [55]. Performance analysis of SM MIMO systems over generalized fading has been reported in [56] and it reported analytical results over Rician, Rayleigh and Nakagami-m fading channels. In [57], authors analyzed BER of SM MIMO systems over generalized $\eta-\mu$ fading channels. TAS has been recently applied to SM based MIMO systems [16, 58] and it is reported that TAS based SM MIMO systems show improved performance.

# CHAPTER 3

# PERFORMANCE ANALYSIS OF MIMO SYSTEMS WITH ANTENNA SELECTION OVER GENERALIZED $\kappa-\mu$ FADING CHANNELS

Performance analysis of TAS based MIMO systems and related research is available in [1, 14, 22–24, 26] over fading channels like Rayleigh, Nakagami-m and Hoyt. These analysis considered MRC and SC diversity combining techniques at the receiver. However, no study has been reported over the fading channels with LOS component like Rician and $\kappa-\mu$. $\kappa-\mu$ distribution is better fit to experimental data and it includes Rician channel as its special case as well [17].

In this chapter, we present OP, BER/SER and channel capacity analysis of TAS/MRC systems for arbitrary number of transmit and receive antennas over $\kappa-\mu$ fading channels. We derive closed form expression for calculation of OP of wireless MIMO systems with antenna selection at transmitter as well as receiver over $\kappa-\mu$ fading channels. We further give expressions for OP over Nakagami-m and Rayleigh fading channels as special cases of $\kappa-\mu$ fading which are computationally efficient than those reported in [14] for Nakagami-m and in [1] for

Rayleigh fading channels. We derive the infinite series expressions for exact and asymptotic SER of TAS/MRC systems for several modulation schemes. The expression for ergodic channel capacity for TAS/MRC systems over $\kappa-\mu$ fading channels is derived. It is important to note that all the expressions derived in this chapter for performance analysis of TAS/MRC systems are also applicable to joint transmit and receive antenna selection systems. We also present the results of Monte Carlo simulations to validate our analytical results. Through simulations, we compared OP, SER and ergodic capacity of TAS MIMO systems with MRC and selection diversity combining strategies at the receiver to demonstrate the superiority of TAS/MRC systems over joint transmit and receive antenna selection systems. We also studied the variation in ergodic capacity with increasing values of fading parameters, $\kappa$ and $\mu$. It is found that the ergodic capacity degrades with increase in the strength of LOS component and/or reduction in the severity of fading, i.e increasing the values of $\kappa$ and $\mu$.

Further, this chapter is organized as follows. In the next section, we describe system and channel model. We derive the PDF of received SNR for TAS/MRC system over $\kappa-\mu$ fading channels. Closed form expression for OP calculation is derived in section 3.2. The expressions for exact or approximate and asymptotic error probabilities of TAS/MRC systems for various modulation schemes over $\kappa-\mu$ fading channels have been derived in section 3.3. In section 3.4, we derive expression for ergodic capacity of TAS/MRC and joint transmit and receive antenna selection systems over $\kappa-\mu$ fading channels. In section 3.5, we present the analytical and simulation results with related discussion and the chapter is summarized in section 3.6.

## 3.1 System and Channel Model

### 3.1.1 System Model

We considered an $N_t \times N_r$ MIMO system having $N_t$ antennas at transmitter side and $N_r$ antennas at the receiver side. It is assumed that only one RF chain is available at the transmitter. The antenna which maximizes the received SNR is selected at the transmitter to send the information. Assuming that the fading coefficients from $i^{th}$ transmitting antenna to $j^{th}$ receiving antenna is represented by $h_{j,i}$ for $i \in (1,2,...,N_t)$ and $j \in (1,2,...,N_r)$. TAS criterion for SC and MRC diversity schemes at the receiver are discussed as follows:

**Selection Combining at the Receiver**

In this case, we select only one antenna at the receiver and the instantaneous SNR becomes $\overline{\gamma}\left|h_{j,i}\right|^2$ for an average SNR of $\overline{\gamma}$. Using (2.1), the link which gives the highest received SNR is determined by

$$\begin{aligned} I_{SC} &= \underset{\substack{1\leq i\leq N_t \\ 1\leq j\leq N_r}}{\arg\max}\left\{\gamma_{t,ji} = \overline{\gamma}\left|h_{j,i}\right|^2\right\} \\ &= \underset{\substack{1\leq i\leq N_t \\ 1\leq j\leq N_r}}{\arg\max}\left\{\gamma_{t,ji} = \left|h_{j,i}\right|^2\right\} \end{aligned} \tag{3.1}$$

where $\gamma_{t,ji}$ denotes the instantaneous received SNR of the link form $i^{th}$ transmitting antenna and $j^{th}$ receiving antenna.

**MRC at the Receiver**

In this case, the resulting instantaneous received SNR after MRC is given by $\sum_{n=1}^{N_r}\gamma_n = \overline{\gamma}\sum_{j=1}^{N_r}\left|h_{j,i}\right|^2$, where $\gamma_n$ is the instantaneous SNR of the $n^{th}$ branch. The transmitting antenna that maximizes SNR at the receiver can be determined by using (2.2) as

$$\begin{aligned} I_{MRC} &= \underset{1\leq i\leq N_t}{\arg\max}\left\{\gamma_{t,i} = \overline{\gamma}\sum_{j=1}^{N_r}\left|h_{j,i}\right|^2\right\} \\ &= \underset{1\leq i\leq N_t}{\arg\max}\left\{\gamma_{t,i} = \sum_{j=1}^{N_r}\left|h_{j,i}\right|^2\right\} \end{aligned} \tag{3.2}$$

### 3.1.2 Channel Model

In this chapter, we assume the fading envelope $\left(\left|h_{j,i}\right|\right)$ to be $\kappa-\mu$ distributed. We already discussed about the PDFs of $\kappa-\mu$ distributed envelope and square variate in the previous chapter. The PDF of $\kappa-\mu$ distributed instantaneous SNR at each receiver antenna can be obtained by scaling of $\kappa-\mu$ distributed random variable in (2.6) by a factor of average SNR, $\overline{\gamma}$ [17]. It can be given as

$$p_{\gamma_{\kappa-\mu}}(\gamma)=\frac{\mu(1+\kappa)^{\frac{\mu+1}{2}}\gamma^{\frac{\mu-1}{2}}}{\kappa^{\frac{\mu-1}{2}}\overline{\gamma}^{\frac{\mu+1}{2}}e^{\mu\kappa}}e^{-\frac{\mu(1+\kappa)\gamma}{\overline{\gamma}}}I_{\mu-1}\left(2\mu\sqrt{\frac{\kappa(1+\kappa)\gamma}{\overline{\gamma}}}\right) \tag{3.3}$$

where $\kappa>0$ and $\mu>0$ are fading parameters as defined in Chapter 2 for $\kappa-\mu$ square variate of $\kappa-\mu$ distribution.

The cumulative distribution function (CDF) of received SNR at each receiver antenna can be given by

$$P_{\gamma_{\kappa-\mu}}(\gamma)=1-Q_{\mu}\left(\sqrt{2\kappa\mu},\sqrt{\frac{2\mu(1+\kappa)\gamma}{\overline{\gamma}}}\right) \tag{3.4}$$

where $Q_{\ddot{m}}(\alpha,\beta)$ is Generalized Marcum Q function with the arguments $\ddot{m}$, $\alpha$ and $\beta$ to be positive real valued numbers.

### 3.1.3 PDF of Received SNR after Antenna Selection

Each $\gamma_{t,ji}$ or $\gamma_{t,i}$ for $i\in(1,2,...,N_t)$ and $j\in(1,2,...,N_r)$ obtained from (3.1) or (3.2) are arranged in ascending order such that $\gamma_{t,(1)}\leq\gamma_{t,(2)},\cdots\leq\gamma_{t,(N)}$ where $\gamma_{t,(l)}$ is the random variable obtained after the arrangement in ascending order and $N=N_tN_r$ or $N_t$ for joint transmit and receive antenna selection or TAS/MRC systems respectively. In TAS/MRC system, we select the transmitting antenna corresponding to the highest received SNR $\left(\gamma_{t,(N_t)}\right)$ when MRC diversity technique is used at the receiver. In joint transmit and receive antenna selection, the transmit antenna and the receive antenna that maximizes the received SNR $\left(\gamma_{t,(N_tN_r)}\right)$ are selected. The PDF of received SNR in such a system assuming all $\left(\left|h_{j,i}\right|\right)$'s are to be i.i.d. can be given by [59]

$$\begin{aligned} p_{\gamma_{t(N)}}(\gamma) &= N\{P_{\gamma_t}(\gamma)\}^{N-1} p_{\gamma_t}(\gamma) \\ &= N\left(1-Q_{\mu}\left(\sqrt{2\kappa\mu},\sqrt{\frac{2\mu(1+\kappa)\gamma}{\bar{\gamma}}}\right)\right)^{N-1} \\ &\quad \times \frac{\mu(1+\kappa)^{\frac{\mu+1}{2}}\gamma^{\frac{\mu-1}{2}}}{\kappa^{\frac{\mu-1}{2}}\bar{\gamma}^{\frac{\mu+1}{2}}e^{\mu\kappa}} e^{-\frac{\mu(1+\kappa)\gamma}{\bar{\gamma}}} I_{\mu-1}\left(2\mu\sqrt{\frac{\kappa(1+\kappa)\gamma}{\bar{\gamma}}}\right) \end{aligned} \tag{3.5}$$

It should be noted that (3.5) applies to TAS/MRC as well as joint transmit and receive antenna selection schemes. $N=N_t$ for TAS/MRC and $N=N_tN_r$ for joint transmit and receive antenna selection and $P_{\gamma_t}(\gamma)$ is the CDF of $\gamma_t$. For TAS/MRC $\gamma_t$ is $\kappa-N_r\mu$ distributed as it is sum of $N_r$ i.i.d. $\kappa-\mu$ square variates [17]. Hence, in all subsequent expressions $\mu$ shall be interpreted as $N_r\mu$ for TAS/MRC systems and it remains as it is for joint transmit and receive antenna selection systems.

## 3.2 Outage Probability

In this section, a closed form expression for OP of MIMO systems with antenna selection is derived for $\kappa-\mu$ fading channels. The closed form expression is evaluated for different fading scenarios as special cases of $\kappa-\mu$ fading. OP is the probability that the instantaneous SNR at the receiver is less than a certain threshold SNR, $\gamma_{th}$ [60]. Thus, outage probability can be given by

$$P_{out}(\bar{\gamma},\gamma_{th}) = P(\gamma<\gamma_{th}) \tag{3.6}$$

So, the OP which is the CDF of (3.5) can be given as

$$\begin{aligned} P_{out}(\bar{\gamma},\gamma_{th}) = \int_0^{\gamma_{th}} \Bigg\{ & N\left(1-Q_{\mu}\left(\sqrt{2\kappa\mu},\sqrt{\frac{2\mu(1+\kappa)x}{\bar{\gamma}}}\right)\right)^{N-1} \\ & \times \frac{\mu(1+\kappa)^{\frac{\mu+1}{2}}x^{\frac{\mu-1}{2}}}{\kappa^{\frac{\mu-1}{2}}\bar{\gamma}^{\frac{\mu+1}{2}}e^{\mu\kappa}} e^{-\frac{\mu(1+\kappa)x}{\bar{\gamma}}} I_{\mu-1}\left(2\mu\sqrt{\frac{\kappa(1+\kappa)x}{\bar{\gamma}}}\right)\Bigg\} dx \end{aligned} \tag{3.7}$$

Following the steps discussed in appendix A.1, the integral of (3.7) can be solved to get a compact closed form expression for OP as

$$P_{out}\left(\overline{\gamma},\gamma_{th}\right)=\left(1-Q_{\mu}\left(\sqrt{2\kappa\mu},\sqrt{\frac{2\mu\left(1+\kappa\right)\gamma_{th}}{\overline{\gamma}}}\right)\right)^{N} \tag{3.8}$$

The above expression of OP is in the form of Marcum Q function which can be easily evaluated using the computation tools like MATLAB and MATHEMATICA. Using [61, (4.71)] and $\kappa\to 0$ and the fading parameter values, $\mu=m$, the OP of TAS/MRC systems over Nakagami-m fading channels can be given by

$$P_{out}\left(\overline{\gamma},\gamma_{th}\right)=\left(1-\frac{\Gamma\left(m,\frac{m\gamma_{th}}{\overline{\gamma}}\right)}{\Gamma\left(m\right)}\right)^{N} \tag{3.9}$$

where $\Gamma\left(a,b\right)$ is the upper incomplete Gamma function. The above expression for OP is computationally simpler than (8) of [14] which is a summation of infinite series. The expression (3.9) is valid for integer and non-integer values of Nakagami fading parameter, $m$. For integer values of $m$, it can be alternatively represented in form of finite sum series as

$$P_{out}\left(\overline{\gamma},\gamma_{th}\right)=\left(1-e^{-\frac{m\gamma_{th}}{\overline{\gamma}}}\sum_{k=0}^{m-1}\frac{\left(\frac{m\gamma_{th}}{\overline{\gamma}}\right)^{k}}{k!}\right)^{N} \tag{3.10}$$

In (3.9) and (3.10), the fading parameter $m$ is to be interpreted as $mN_r$ and $m$ for TAS/MRC systems and joint transmit and receive antenna selection systems respectively. Using $m=1$ in (3.10), it gives the OP of TAS/MRC systems over Rayleigh fading channels as

$$P_{out}\left(\overline{\gamma},\gamma_{th}\right)=\left(1-e^{-\frac{N_r\gamma_{th}}{\overline{\gamma}}}\sum_{k=0}^{N_r-1}\frac{\left(\frac{N_r\gamma_{th}}{\overline{\gamma}}\right)^{k}}{k!}\right)^{N} \tag{3.11}$$

The above expression involves $N_r$ addition operations and two power operations. Hence, it is computationally more efficient than (9) of [1] which involves number of addition and power operations of the order $N_tN_r$. This difference will become more significant when we consider large MIMO systems [62] with hundreds of antennas at the transmitter and receiver.

## 3.3 Error Performance

In this section, we derive expressions for exact SER of TAS/MRC systems for BPSK, binary frequency shift keying (BFSK) and M-ary pulse amplitude modulation (MPAM) schemes and approximate SER of TAS/MRC systems for MQAM, MPSK and quadrature phase shift keying (QPSK) schemes. BER of a wireless communication system can be calculated by averaging the conditional probability of error (CPE) over the PDF of output SNR. The exact CPE for various modulation schemes and approximate CPE for MPSK can be given by

$$P_e(\gamma) = aQ\left(\sqrt{b\gamma}\right) - cQ^2\left(\sqrt{b\gamma}\right) \tag{3.12}$$

where $Q(\cdot)$ is the Gaussian Q function which gives the area under the tail of a Gaussian curve and is defined as $Q(\hbar) = \frac{1}{\sqrt{2\pi}}\int_{\hbar}^{\infty} e^{-\left(\frac{u^2}{2}\right)}du$, $\gamma$ is SNR and $a$, $b$ and $c$ are modulation dependent parameters listed in Table 3.1.

The SER can be given by

$$\overline{P_e} = \int_0^\infty P_e(\gamma)\, p_{\gamma_{t(N)}}(\gamma)\, d\gamma = -\int_0^\infty P_e'(\gamma)\, P_{\gamma_{t(N)}}(\gamma)\, d\gamma \tag{3.13}$$

where $P_e'(\cdot)$ is the first derivative of CPE and $P_{\gamma_{t(N)}}(\gamma)$ is the CDF of output SNR.

### 3.3.1 BPSK and MPSK Modulation Schemes

From (3.12) and Table 3.1, the CPE for BPSK and MPSK can be given in the form $P_e(\gamma) = aQ\left(\sqrt{b\gamma}\right)$ with $a = 1$, and $b = 2$ for BPSK and $a = 2$, and $b = \sin(\pi/M)$ for MPSK, respectively. So, SER can be given as

Table. 3.1: Modulation parameters for various modulation schemes [2, 3]

| Modulation Scheme | $a$ | $b$ | $c$ |
|---|---|---|---|
| BPSK | 1 | 2 | 0 |
| BFSK | 1 | 1 | 0 |
| MPSK | 2 | $2\sin^2\left(\frac{\pi}{M}\right)$ | 0 |
| MPAM | $2\frac{M-1}{M}$ | $\frac{6}{M^2-1}$ | 0 |
| QPSK or MSK | 2 | 2 | 1 |
| Coherent DPSK | 2 | 2 | 2 |
| MQAM | $4\frac{\sqrt{M}-1}{\sqrt{M}}$ | $\frac{3}{M-1}$ | $4\left(\frac{\sqrt{M}-1}{\sqrt{M}}\right)^2$ |

$$\overline{P_e} = \frac{a}{2}\sqrt{\frac{b}{2\pi}}\int_0^{\infty}\frac{e^{-\frac{b\gamma}{2}}}{\sqrt{\gamma}}\left(1-Q_\mu\left(\sqrt{2\kappa\mu},\sqrt{\frac{2\mu\left(1+\kappa\right)\gamma}{\bar{\gamma}}}\right)\right)^N d\gamma \tag{3.14}$$

$Q_{\ddot{m}}(\cdot,\cdot)$ can be represented in the form of infinite series for integer as well as non integer values of $\ddot{m}$ as [61]

$$Q_{\ddot{m}}\left(\alpha,\beta\right) = 1-e^{-\frac{\alpha^2+\beta^2}{2}}\sum_{r=\ddot{m}}^{\infty}\left(\frac{\beta}{\alpha}\right)^r I_r\left(\alpha\beta\right) \tag{3.15}$$

and the modified Bessel function in the series representation of $Q_{\ddot{m}}(\cdot,\cdot)$ can also be represented as an infinite series as follows [63, (8.406.1), (8.402)].

$$I_r\left(\omega\right) = \sum_{s=0}^{\infty}\frac{1}{s!\Gamma\left(r+s+1\right)}\left(\frac{\omega}{2}\right)^{r+2s} \tag{3.16}$$

Using (3.15) and (3.16) in (3.14), the SER can be given by

$$\overline{P_e} = \frac{a}{2}\sqrt{\frac{b}{2\pi}}\sum_{R_N}\sum_{S_N}\frac{(\kappa\mu)^{\sum_{i=1}^{N}s_i}\left(\frac{K'}{N}\right)^{N'_\mu}e^{-N\kappa\mu}}{\prod_{i=1}^{N}s_i!\Gamma(s_i+r_i+\mu+1)}\int_0^\infty \frac{e^{-\left(\frac{b}{2}+K'\right)\gamma}}{\sqrt{\gamma}}\gamma^{N'_\mu}d\gamma \qquad (3.17)$$

where $N'_\mu = N\mu + \sum_{i=1}^{N} r_i + \sum_{i=1}^{N} s_i$, $K' = \frac{N\mu(1+\kappa)}{\overline{\gamma}}$, $\sum_{R_N} = \sum_{r_1=0}^{\infty}\sum_{r_2=0}^{\infty}\ldots\sum_{r_N=0}^{\infty}$ and $\sum_{S_N} = \sum_{s_1=0}^{\infty}\sum_{s_2=0}^{\infty}\ldots\sum_{s_N=0}^{\infty}$. Then SER can be evaluated as

$$\overline{P_e} = \frac{a}{2}\sqrt{\frac{b}{2\pi}}\sum_{R_N}\sum_{S_N}\frac{(\kappa\mu)^{\sum_{i=1}^{N}s_i}\left(\frac{K'}{N}\right)^{N'_\mu}e^{-N\kappa\mu}}{\prod_{i=1}^{N}s_i!\Gamma(s_i+r_i+\mu+1)}\frac{\Gamma\left(N'_\mu+\frac{1}{2}\right)}{\left(\frac{b}{2}+K'\right)^{N'_\mu-\frac{1}{2}}} \qquad (3.18)$$

We evaluated the above infinite summation by truncating each summation to first $P$ terms, i.e. $\sum_{R_N} \cong \sum_{r_1=0}^{P}\sum_{r_2=0}^{P}\ldots\sum_{r_N=0}^{P}$ and $\sum_{S_N} \cong \sum_{s_1=0}^{P}\sum_{s_2=0}^{P}\ldots\sum_{s_N=0}^{P}$. Figure 3.1 shows the BER for different values of $P$ for the SNR values of 0dB, 5dB, 10dB and 15dB for BPSK modulation scheme. It is observed that the BER values converge very fast and $P >= 10$ gives sufficient accuracy in the numerical values.

The expression (3.18) can be simplified by truncating $P$ to zero for each of the summation variables ($r_1, r_2, \ldots, r_N$ and $s_1, s_2, \ldots, s_N$) to give the asymptotic error probability.

$$\overline{P_e} \geq \frac{a}{2}\sqrt{\frac{b}{2\pi}}\frac{\left(\frac{K'}{N}\right)^{N\mu}e^{-N\kappa\mu}}{\Gamma(\mu+1)}\frac{\Gamma\left(N\mu+\frac{1}{2}\right)}{\left(\frac{b}{2}+K'\right)^{N\mu-\frac{1}{2}}} \qquad (3.19)$$

The above asymptotic expression is a lower bound to the exact BER/SER and it approaches the exact value at high SNR conditions. The expressions, (3.18) and (3.19) are valid for any values of fading parameters, number of transmitter antennas and number of receiver antennas. (3.18) gives exact BER for BPSK modulation scheme and approximate SER for MPSK modulation scheme. (3.19) gives asymptotic BER for BPSK and asymptotic SER for MPSK modulation schemes applied to TAS/MRC MIMO systems. One may use the appropriate values of $a$ and $b$ as listed in Table 3.1 for specific modulation scheme like BPSK and MPSK.

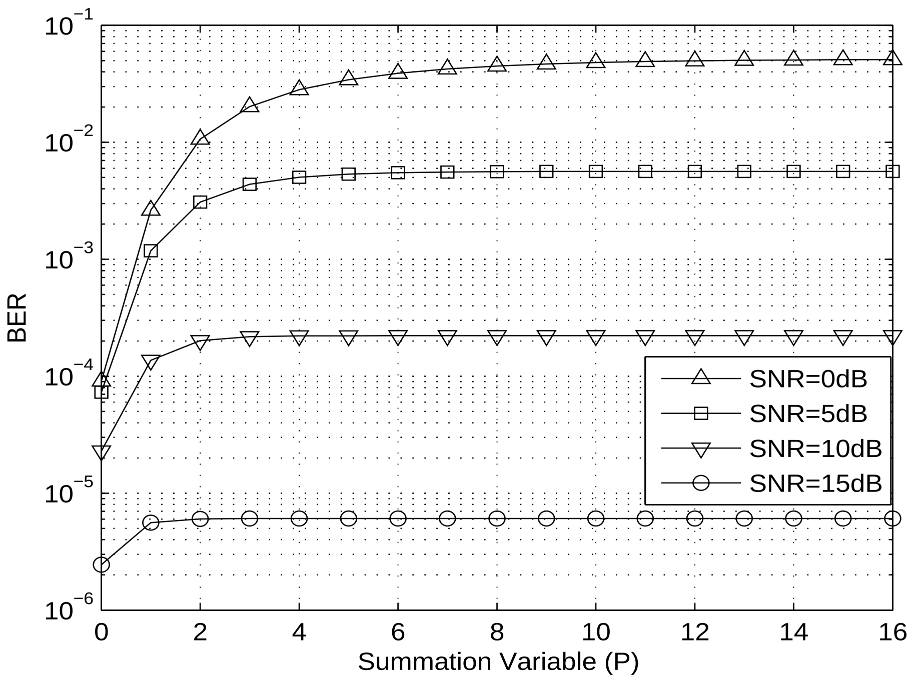


Figure 3.1: Plot showing fast convergence of (3.18), BER of (3,1;1) TAS/MRC system for $\kappa = 1.5$ and $\mu = 1$

### 3.3.2 MQAM and QPSK Modulation Schemes

In this subsection, we derive expressions to analyze approximate error performance of TAS/MRC MIMO systems with MQAM and QPSK modulation schemes. We use MGF based approach to derive the expressions for SER. The CPE of (3.12) can be approximated as a sum of two exponential functions [64]. The derivative of approximate CPE can be given as

$$P_e^{'} \cong -\frac{ab}{2\sqrt{2\pi b}}\frac{e^{-\frac{b\gamma}{2}}}{\sqrt{\gamma}} - \frac{bc}{12\sqrt{2\pi b}}\frac{e^{-b\gamma}}{\sqrt{\gamma}} - \frac{bc}{4\sqrt{2\pi b}}\frac{e^{-\frac{7b\gamma}{6}}}{\sqrt{\gamma}} \quad (3.20)$$

Substituting $P_e^{'}$ of (3.20) in the expression of SER (3.13) and comparing the resulting expression with the definition of Laplace transform, one can find that SER can be represented in the form of Laplace transform of $\frac{P_{\gamma_{t(N)}}(\gamma)}{\sqrt{\gamma}}$.
The Fourier transform of $\frac{P_{\gamma_{t(N)}}(\gamma)}{\sqrt{\gamma}}$ can be given as

$$M_{\gamma_t}(s) = \sum_{R_N}\sum_{S_N} \frac{(\kappa\mu)^{\sum_{i=1}^{N} s_i}\Gamma\left(N'_\mu + \frac{1}{2}\right)}{\prod_{i=1}^{N} s_i!\Gamma(s_i + r_i + \mu + 1)} \left(\frac{e^{-N\kappa\mu}\sqrt{\bar{\gamma}}}{\sqrt{\mu(1+\kappa)}}\right)\left(\frac{\mu(1+\kappa)}{N\mu(1+\kappa)+s\bar{\gamma}}\right)^{\left(N'_\mu+\frac{1}{2}\right)} \tag{3.21}$$

Then, using above equation, the SER can be given by

$$\overline{P}_e \cong \frac{ab}{2\sqrt{2\pi b}} M_{\gamma_t}\left(\frac{b}{2}\right) + \frac{bc}{12\sqrt{2\pi b}} M_{\gamma_t}(b) + \frac{bc}{4\sqrt{2\pi b}} M_{\gamma_t}\left(\frac{7b}{6}\right) \tag{3.22}$$

From (3.21) and (3.22), the asymptotic error performance (lower bound) can be evaluated by truncating the values of all summation variables to be zero, i.e. ($r_1,\ r_2,\ \ldots,\ r_N = 0$ and $s_1,\ s_2,\ \ldots,\ s_N = 0$).

## 3.4 Channel Capacity

The maximum data rate for reliable transmission or the channel capacity is one of the measure for performance analysis of wireless communication systems. In this section, we consider ergodic channel capacity as a performance measure and compare ergodic capacities of TAS/MRC and joint transmit and receive antenna selection systems over $\kappa-\mu$ fading channels. The instantaneous capacity of the channel ($C_{inst}$) can be given by [61]

$$C_{inst} = B\log_2(1+\gamma) \quad \text{bits/s} \tag{3.23}$$

where B is the channel bandwidth. It can be averaged over the PDF of received SNR to obtain ergodic capacity per unit bandwidth as

$$\frac{\bar{C}_{erg}}{B} = \int_0^\infty \log_2(1+\gamma)\, p_{\gamma_{t(N)}}(\gamma)\, d\gamma \tag{3.24}$$

Using (3.15) and (3.16) in (3.5), the pdf of received SNR, $p_{\gamma_{t(N)}}(\gamma)$ can be given as

$$p_{\gamma_{t(N)}}(\gamma)=Ne^{-N\mu\kappa}\sum_{S_N}\sum_{R_{N-1}}\frac{e^{-\left(K'\gamma\right)}\gamma^{\left(N'_\mu-1\right)}}{\prod_{i=1}^{N-1}\Gamma\left(s_i+r_i+\mu+1\right)}\frac{(\kappa\mu)^{\sum_{i=1}^{N}s_i}\left(\frac{K'}{N}\right)^{N'_\mu}}{\Gamma\left(s_N+\mu\right)\prod_{i=1}^{N}s_i!} \tag{3.25}$$

Using (3.25) in (3.24), the ergodic capacity per unit bandwidth can be evaluated using Mathematica as

$$\begin{aligned}\frac{\bar{C_{erg}}}{B}=&\frac{Ne^{-N\mu\kappa}}{\ln(2)}\sum_{S_N}\sum_{R_{N-1}}\frac{(\kappa\mu)^{\sum_{i=1}^{N}s_i}}{\Gamma\left(s_N+\mu\right)\prod_{i=1}^{N}s_i!}\frac{\left(\frac{1}{N}\right)^{N'_\mu}}{\prod_{i=1}^{N-1}\Gamma\left(s_i+r_i+\mu+1\right)}\\&\left(-\frac{\Gamma\left(N'_\mu,K'\right)}{\sin\left(N'_\mu\pi\right)}+(-1)^{N'_\mu}K'\ {}_2F_2\left(\{1,1\},\left\{2,2-N'_\mu\right\},K'\right)\right.\\&\left.+\Gamma\left(N'_\mu\right)\left(\frac{\pi}{\sin\left(N'_\mu\pi\right)}-(-1)^{N'_\mu}\left(\ln\left(K'\right)+\psi^{(0)}\left(N'_\mu\right)\right)\right)\right)\end{aligned} \tag{3.26}$$

where $\ln(\cdot)$ is natural logarithm, $\psi^{(i)}(\cdot)$ is the $(i+1)^{th}$ derivative of logarithm of Gamma function and ${}_pF_q\left(\{a_1,a_2,...a_p\},\{b_1,b_2,...,b_q\},z\right)$ is the generalized Hypergeometric function.

However, for integer values of $\mu$, following the steps of [65], it can be evaluated as

$$\frac{\bar{C_{erg}}}{B}=\frac{Ne^{-N\mu\kappa}}{\ln(2)}\sum_{S_N}\sum_{R_{N-1}}\frac{(\kappa\mu)^{\sum_{i=1}^{N}s_i}\left(\frac{K'}{N}\right)^{N'_\mu}}{\Gamma\left(s_N+\mu\right)\prod_{i=1}^{N}s_i!}\frac{\Gamma\left(N'_\mu\right)e^{K'}}{\prod_{i=1}^{N-1}\Gamma\left(s_i+r_i+\mu+1\right)}\sum_{m=1}^{N'_\mu}\frac{\Gamma\left(m-N'_\mu\right)}{\left(K'\right)^m} \tag{3.27}$$

## 3.5 Results and Discussion

In this section, numerical and simulation results are presented for OP, BER or SER and ergodic capacity of TAS/MRC systems as well as joint transmit and receive antenna selection systems. We simulated TAS/MRC systems and joint transmit and receive antenna selection systems for various values of fading parameters ($\kappa$ and $\mu$).

In Figure 3.2, the analytical and simulation OP results are shown for a (3,1;2) TAS/MRC

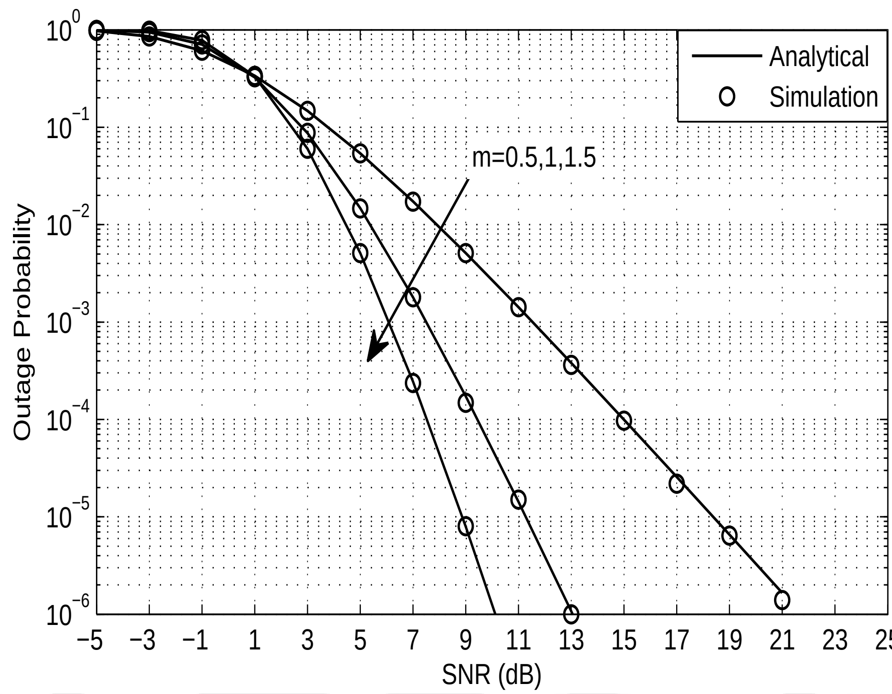


Figure 3.2: Outage Probability of (3,1;2) TAS/MRC system over $\kappa-\mu$ fading for $\kappa = 0$, $\mu = m$ for $\gamma_{th} = 3$

system for Nakagami-m fading case with $\kappa \to 0$ and $\mu = m$ (a special case of $\kappa-\mu$ fading). The analytical and simulation results are plotted for m= 0.5, 1 and 1.5 for R=2 bits/s/Hz. It can be found that the results are the same as shown in [14, Fig. 1]. We compare the OP of TAS/MRC and joint transmit and receive antenna selection in Figure 3.3. For this comparison, we have considered $2\times 2$ MIMO systems. It is observed from the slopes of curves that both TAS/MRC and joint transmit and receive antenna systems give full diversity order but TAS/MRC systems are superior than the joint transmit and receive antenna selection systems. TAS/MRC systems in the presented case give 1.5-2dB SNR gain over joint transmit and receive antenna selection systems.

We simulated $(3,1;N_r)$ TAS/MRC systems for $\kappa = 0$ and $\mu = 1, 1.5$ and 2 with BPSK modulation scheme. The exact, asymptotic and simulation results of BER for different values of SNR are given in Figure 3.4. It is observed that with increase in the value of fading parameter ($\mu$), BER performance of TAS/MRC systems shows improvement. It is also important to note

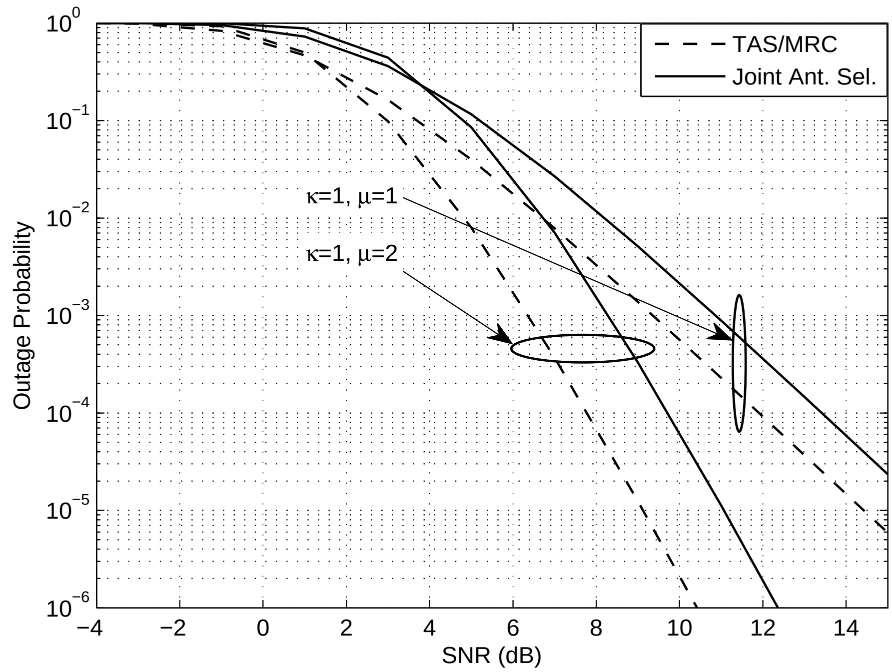


Figure 3.3: Outage Probability comparison of TAS/MRC and joint transmit and receive antenna selection systems over $\kappa-\mu$ fading channels for $\gamma_{th}=3$

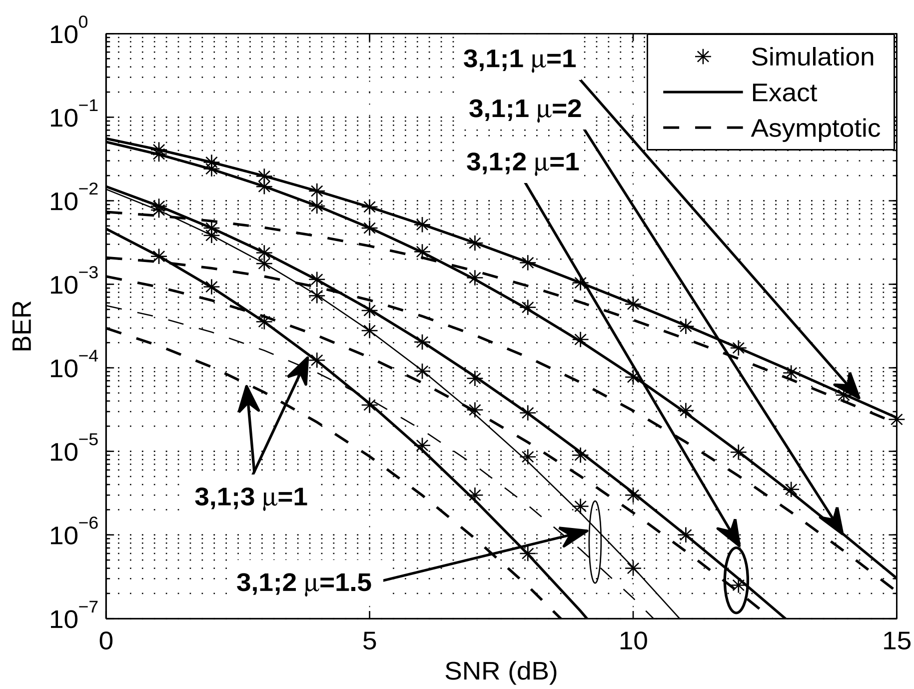


Figure 3.4: BER performance of TAS/MRC systems over $\kappa-\mu$ fading channels for BPSK modulation

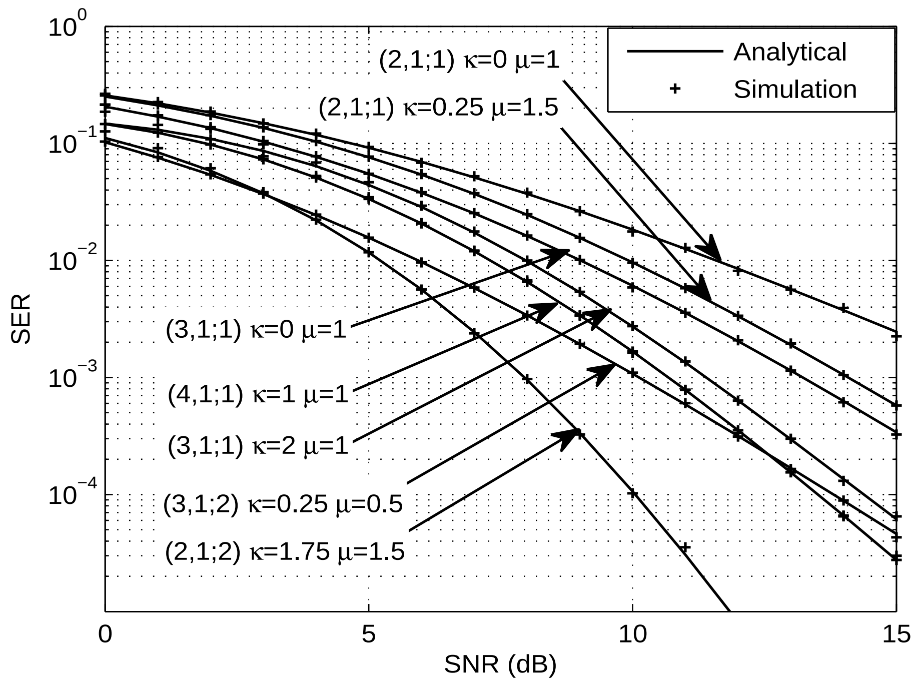


Figure 3.5: SER performance of $(N_t, 1; N_r)$ TAS/MRC systems over $\kappa-\mu$ fading channels with 4-QAM modulation

that the asymptotic performance shown is a lower bound on BER on the account of truncating the infinite series expression by first term.

The TAS/MRC systems were also simulated with different number of antennas at transmitter and receiver $(N_t, 1; N_r)$ for different values of fading parameters with 4-QAM modulations to validate the expression (3.22) derived in previous section for approximate SER. The analytical and simulation results for various values of fading parameters are shown in Figure 3.5. The approximate SER obtained analytically is found to be in close agreement with the simulation results. In this case, we also show the results for non integer values of fading parameters ($\kappa$ and $\mu$) to verify that the expressions derived in this chapter applies equally good for integer and non integer values of fading parameters.

For the sake of comparison, we present the simulation results of $(2, 1; N_r)$ TAS/MRC and $(2, 1; N_r, 1)$ joint transmit and receive antenna selection systems with 4-QAM modulation for various values of fading parameters. The SER performance comparison is given in Figure

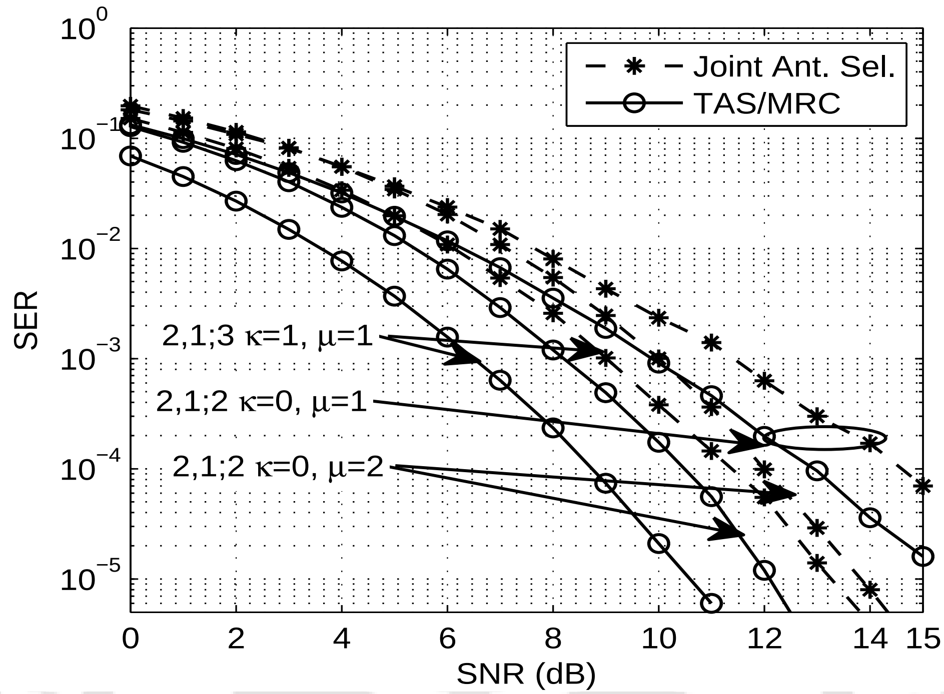


Figure 3.6: SER performance comparison of $(2,1;N_r)$ TAS/MRC systems and $(2,1;N_r,1)$ Joint transmit and receive antenna selection systems over $\kappa-\mu$ fading channels with 4-QAM modulation

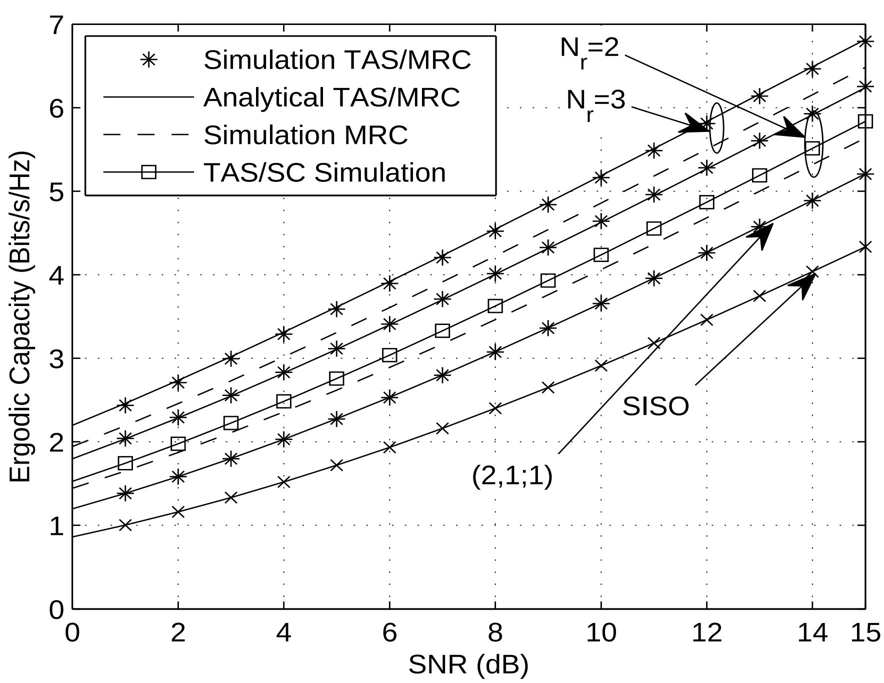


Figure 3.7: Ergodic capacity comparison of SISO, MRC, TAS/SC and TAS/MRC systems

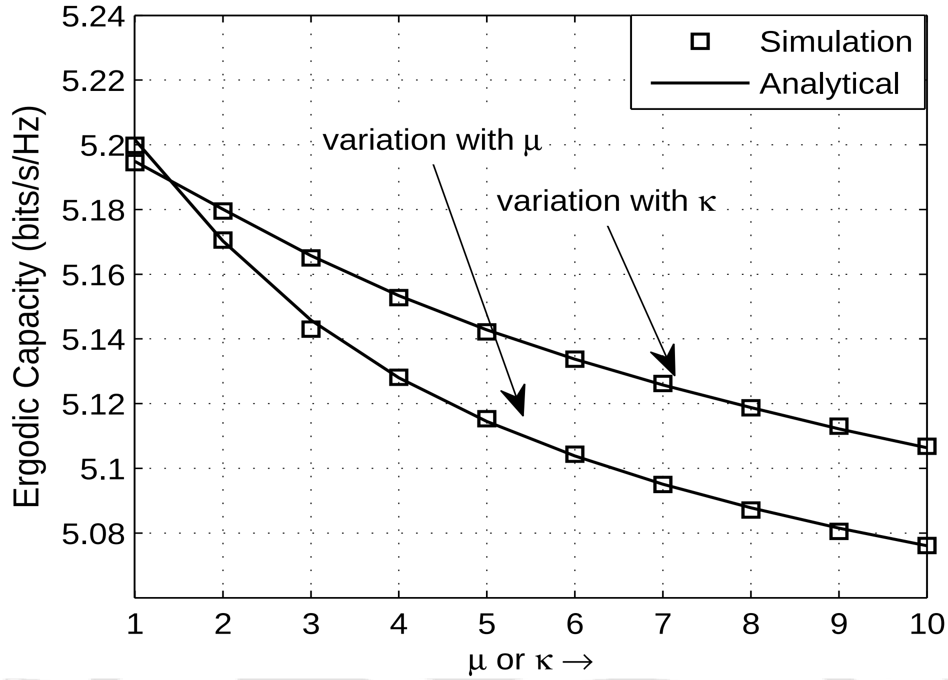


Figure 3.8: Capacity variation of $(2,1;3)$ TAS/MRC system with different values of $\kappa$ and $\mu$

3.6. Again, TAS/MRC systems perform better than joint transmit and receive antenna selection systems. At SER of $10^{-4}$, an SNR gain of about 2dB and 3dB is observed for TAS/MRC systems compared to joint transmit and receive antenna selection systems for $N_r = 2$ and $N_r = 3$ respectively. Furthermore, the slopes of SER curves of both the systems is observed to be the same indicating the same diversity orders of both the systems.

Figure 3.7 shows the simulation and analytical results for ergodic capacity of TAS/MRC and joint transmit and receive antenna selection systems. We also show the ergodic capacity of MRC diversity scheme and SISO system for comparison purpose. The results are shown considering $1 \times N_r$ MRC system, $(2,1;N_r)$ TAS/MRC system and $(2,1;N_r,1)$ joint transmit and receive antenna selection system. It can be observed that the ergodic capacities improve as we move from system to system following the order: SISO systems, MRC diversity scheme, TAS/SC systems and TAS/MRC systems.

A (2,1;3) TAS/MRC system was simulated to investigate the variation in ergodic capacity for different values of fading parameters ($\kappa$ and $\mu$). The results are plotted in Figure 3.8.

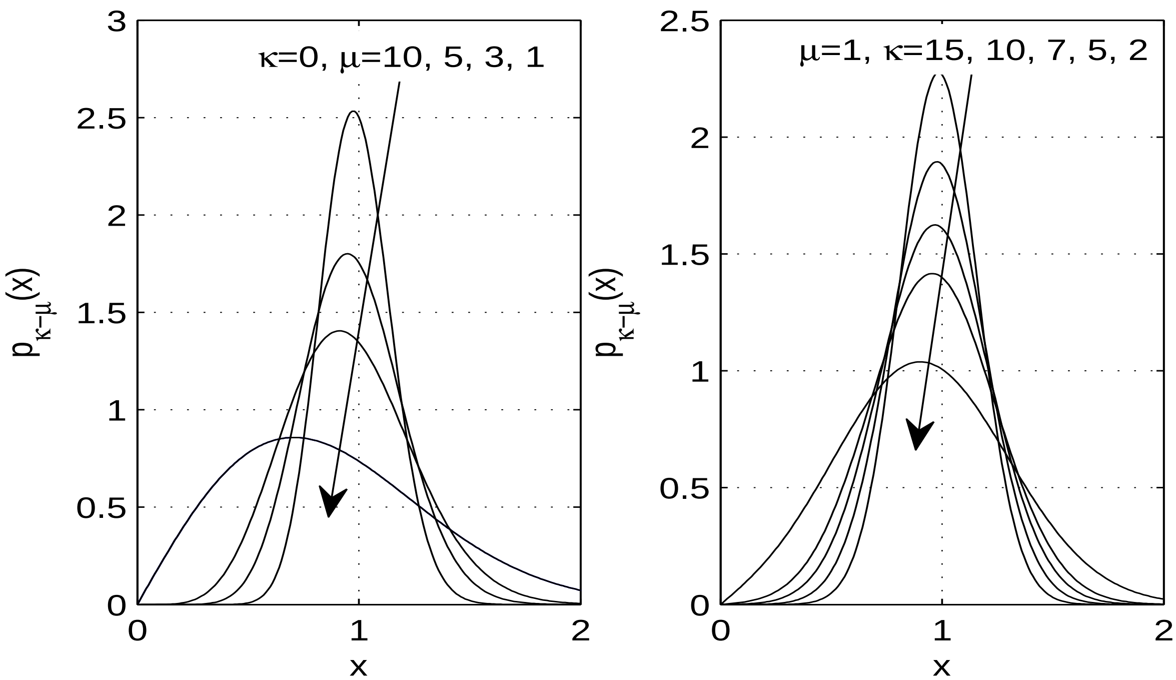


Figure 3.9: Figure to show reduction in the variability of fading coefficients with increasing values of $\kappa$ and/or $\mu$.

The results are obtained for two cases, (a) $\kappa = 0$ and $\mu$ varying from 1 to 10 and (b) $\mu = 1$ and $\kappa$ varying from 1 to 10. It is observed that the ergodic capacity of TAS/MRC systems degrades when the values of $\kappa$ and/or $\mu$ increase. From these results, it can be concluded that the capacity degrades when the fading conditions become severe to less severe or the LOS component becomes stronger. This can be explained by the fact that when $\kappa \to \infty$ and/or $\mu \to \infty$, the channel becomes additive white Gaussian noise (AWGN) channel and hence the variability of fading coefficients reduce with increasing values of $\kappa$ and/or $\mu$ as observed in Figure 3.9.

## 3.6 Summary

In this chapter, we derived closed form expression for OP and infinite series expressions for exact and approximate SER and capacity of MIMO transmit antenna selection over generalized i.i.d. $\kappa-\mu$ fading channels. We presented expressions for OP over Nakagami-m and

Rayleigh fading channels as special cases of $\kappa-\mu$ fading channels. The expressions of OP over Nakagami-m and Rayleigh fading channels reported in this chapter are computationally efficient than the existing expressions. The closed form expressions are in the form of elementary functions or finite sum of elementary functions which can be easily evaluated using software packages like MATLAB and MATHEMATICA. We also derived expressions for exact/approximate and asymptotic BER/SER with arbitrary number of transmitting and receiving antennas for various modulation schemes. The expression of ergodic channel capacity for TAS/MRC systems is derived. Simulation results for various fading parameter values have been shown to validate the exactness of analytical expressions. We also compared the outage probabilities of TAS/MRC systems with joint transmit and receive antenna selection systems to show the superiority of TAS/MRC systems. The superiority of TAS/MRC over joint transmit and receive antenna selection systems in terms of error performance is demonstrated. The superiority of TAS/MRC systems can also be observed from the results obtained for ergodic channel capacity analysis. It is also shown that the less severe fading and/or better LOS component degrades the ergodic capacity of TAS/MRC channels but it improves the BER/SER performance of TAS/MRC systems. This is similar to the findings of [26] over Hoyt fading channels, that the TAS/MRC systems take advantage of antenna selection at transmitter and the channel capacity increases with severity of fading.

# CHAPTER 4

# PERFORMANCE ANALYSIS OF MIMO SYSTEMS WITH ANTENNA SELECTION OVER GENERALIZED $\eta - \mu$ FADING CHANNELS

The analysis reported in the literature for the SER and capacity of TAS based MIMO systems have not considered $\eta - \mu$ fading channels. Though, in a very recent paper, performance analysis of selection combining over $\eta - \mu$ fading is reported for integer values of $\mu$ [34]. To the best of our knowledge, SER and capacity analysis has not been reported in the literature for TAS based MIMO systems with non integer values of fading parameter $\mu$.

In this chapter, we analyze the SER performance and ergodic capacity of TAS/MRC systems over $\eta - \mu$ fading channels. We derive expressions for exact, approximate and asymptotic SER performance for several modulation schemes. For our analysis, we use MGF based approach to derive the expressions of SER. We derive expression of approximate SER by approximating the Gaussian Q function as a sum of two exponential functions [64]. The analytical expressions are also applicable to the performance analysis of TAS/SC systems in which only the best link is active at a time. An expression for ergodic capacity of TAS/MRC system over $\eta - \mu$ fading channels is also derived for integer values of $2\mu$. The exactness of all the expressions has been validated with the help of Monte Carlo simulation results. Finally, the BER performance of TAS/MRC systems and TAS/SC systems have been compared and superiority of TAS/MRC systems over TAS/SC systems has been demonstrated. The variation of ergodic capacity with fading parameters ($\eta$ and $\mu$) is studied. It is found through simulations that the ergodic capacity of TAS/MRC systems take advantage of high variability of severe fading conditions to get better ergodic capacities when the fading is more severe.

The remainder of this chapter is organized as follows. In the next section, we describe system and channel model. We derive the PDF and the MGF of received SNR. The expression for approximate SER for various modulation schemes is derived in section 4.2.1. The expressions for exact and asymptotic error probabilities of TAS/MRC systems for various modulation schemes over $\eta-\mu$ fading channels have been derived in section 4.2.2 and section 4.2.3 respectively. The expression for ergodic capacity is derived in section 4.3. In section 4.4, we present the analytical and simulation results with related discussions and the chapter is summarized in section 4.5.

## 4.1 System and Channel Model

### 4.1.1 System Model

The system model assumed in this chapter is same as that described in previous chapter. A MIMO system with $N_t$ antennas at transmitter side, $N_r$ antennas at the receiver side and single RF chain at the transmitter is under consideration. This allows only one antenna at transmitter to be active at a time. So, the transmission is done from the antenna that maximizes the instantaneous SNR at the receiver. Let the fading coefficients from $i^{th}$ transmitting antenna to $j^{th}$ receiving antenna is denoted by $h_{j,i}$ for $i \in (1,N_t)$ and $j \in (1,N_r)$. The antenna selection criterion for SC and MRC diversity schemes used in this chapter are discussed in section 3.1.

### 4.1.2 Channel Model

In this chapter, we assume the fading envelope $\left(\left|h_{j,i}\right|\right)$ to be $\eta-\mu$ distributed. We already discussed about the PDFs of $\eta-\mu$ distributed envelope and square variate in chapter 2. The PDF of $\eta-\mu$ distributed instantaneous SNR can be obtained by scaling of $\eta-\mu$ distributed random variable in (2.4) by a factor of average SNR, $\bar{\gamma}$ [18]. After suitable scaling, the PDF of received instantaneous SNR at each antenna can be given as

$$p_{\gamma_{\eta-\mu}}(\gamma)=\frac{2\sqrt{\pi}(\mu)^{\mu+\frac{1}{2}}h^{\mu}\gamma^{\mu-\frac{1}{2}}}{\Gamma(\mu)H^{\mu-\frac{1}{2}}(\bar{\gamma})^{\mu+\frac{1}{2}}}e^{\left(-\frac{2\mu\gamma h}{\bar{\gamma}}\right)}I_{\mu-\frac{1}{2}}\left(\frac{2\mu\gamma H}{\bar{\gamma}}\right) \tag{4.1}$$

where $\eta$ and $\mu>0$ are fading parameters, $h$ and $H$ are functions of the parameter $\eta$ as defined in Section 2.2.1.

The CDF of received SNR at any single antenna output for $\eta-\mu$ fading channels is given as

$$P_{\gamma_{\eta-\mu}}(x)=\frac{2\sqrt{\pi}(\mu)^{\mu+\frac{1}{2}}h^{\mu}}{\Gamma(\mu)H^{\mu-\frac{1}{2}}(\bar{\gamma})^{\mu+\frac{1}{2}}}\int_{0}^{x}\gamma^{\mu-\frac{1}{2}}e^{\left(-\frac{2\mu\gamma h}{\bar{\gamma}}\right)}I_{\mu-\frac{1}{2}}\left(\frac{2\mu\gamma H}{\bar{\gamma}}\right)d\gamma \tag{4.2}$$

The integral in the above expression can be solved by using series expansion of modified Bessel function and definition of incomplete Gamma function [63, 8.445, 3.351.1], i.e.

$$I_r(\omega)=\sum_{s=0}^{\infty}\frac{1}{s!\Gamma(r+s+1)}\left(\frac{\omega}{2}\right)^{r+2s} \tag{4.3}$$

$$\int_0^u e^{-\rho}x^{\xi}dx=\frac{\gamma_{inc}(\xi+1,u\rho)}{\rho^{\xi+1}} \tag{4.4}$$

where $\gamma_{inc}(\cdot,\cdot)$ is lower incomplete Gamma function.

Use of (4.3) and (4.4) in (4.2) and further mathematical simplifications leads to the expression of CDF as follows

$$P_{\gamma_{\eta-\mu}}(x)=\frac{2^{1-2\mu}\sqrt{\pi}}{h^{\mu}\Gamma(\mu)}\sum_{i=0}^{\infty}\frac{\gamma_{inc}\left(2\mu+2i,\frac{2\mu hx}{\bar{\gamma}}\right)}{i!\Gamma(\mu+i+0.5)}\left(\frac{H}{2h}\right)^{2i} \tag{4.5}$$

### 4.1.3 PDF and MGF of Received SNR after Antenna Selection

Each $\gamma_{t,ji}$ or $\gamma_{t,i}$ for $i \in (1,N_t)$ and $j \in (1,N_r)$ obtained from (3.1) or (3.2) are arranged in ascending order such that $\gamma_{t,(1)} \leq \gamma_{t,(2)} \leq \ldots \leq \gamma_{t,(N)}$ where $\gamma_{t,(\cdot)}$ is the random variable obtained after the arrangement in ascending order and $N = N_t N_r$ or $N_t$ for TAS/SC or TAS/MRC systems respectively. In TAS/MRC system, we select the transmitting antenna corresponding to the highest received SNR $\left(\gamma_{t,(N_t)}\right)$ when MRC diversity technique is used at the receiver. In TAS/SC, the transmit and receive antenna pair that maximizes the received SNR $\left(\gamma_{t,(N_t N_r)}\right)$ is selected. The PDF of SNR in such a system can be given by [59].

$$\begin{aligned} p_{\gamma_{t(N)}}(x) &= N\{P_{\gamma_t}(x)\}^{N-1} p_{\gamma_t}(x) \\ &= N\left[\frac{2^{1-2\mu}\sqrt{\pi}}{h^{\mu}\Gamma(\mu)}\sum_{i=0}^{\infty}\frac{\gamma\left(2\mu+2i,\frac{2\mu hx}{\overline{\gamma}}\right)}{i!\Gamma(\mu+i+0.5)}\left(\frac{H}{2h}\right)^{2i}\right]^{N-1} \\ &\quad\times\frac{2\sqrt{\pi}(\mu)^{\mu+\frac{1}{2}}h^{\mu}\gamma^{\mu-\frac{1}{2}}}{\Gamma(\mu)H^{\mu-\frac{1}{2}}(\overline{\gamma})^{\mu+\frac{1}{2}}}e^{\left(-\frac{2\mu\gamma h}{\overline{\gamma}}\right)}I_{\mu-\frac{1}{2}}\left(\frac{2\mu\gamma H}{\overline{\gamma}}\right) \end{aligned} \tag{4.6}$$

Using the following set of expressions

$$\gamma_{inc}(s,x) = \frac{x^s}{s}\Phi(s,s+1,-x) \tag{4.7}$$

$$\Phi(a,b,-x) = e^{-x}\Phi(b-a,b,x) \tag{4.8}$$

$$\Phi(a,b,x) = \sum_{k=0}^{\infty}\frac{(a)_k x^k}{(b)_k k!} \tag{4.9}$$

Above expressions are (9.236.4), (9.212.1) and (9.210.1) of [63]. Now, incomplete Gamma function can be represented in the series form as

$$\gamma_{inc}(s,x) = \frac{e^{-x}}{s}\sum_{k=0}^{\infty}\frac{x^{s+k}}{(s+1)_k} \tag{4.10}$$

where $(a)_n$ is Pochhammer symbol defined as $(a)_n = \frac{\Gamma(a+n)}{\Gamma(a)}$. So, the PDF and MGF of the received instantaneous SNR can be given as (4.11) and (4.12)

$$p_{\gamma_{t(N)}}(x) = 2N\ell \sum_{i,j} \frac{2^{j_\Sigma} H^{2i_\Sigma}}{h^{N\mu+2i_\Sigma} \prod_{p=1}^{N} (i_p! \Gamma(\mu'))} \frac{q e^{-\bar{\lambda} x} x^{r-1}}{\prod_{p=1}^{N-1} \left( (\mu+i_p)(2\mu')_{j_p} \right)} \tag{4.11}$$

$$\begin{aligned} M_\gamma(s) &= \int_0^\infty e^{-sx} p_{\gamma_{t(N)}}(x)\, dx \\ &= 2N\ell \sum_{i,j} \frac{2^{j_\Sigma} H^{2i_\Sigma} q \Gamma(r) (\bar{\lambda}+s)^{-r}}{h^{N\mu+2i_\Sigma} \prod_{p=1}^{N} (i_p! \Gamma(\mu')) \prod_{p=1}^{N-1} \left( (\mu+i_p)(2\mu')_{j_p} \right)} \end{aligned} \tag{4.12}$$

where

$$\sum_{i,j} = \sum_i \sum_j = \sum_{i_1=0}^{\infty} \sum_{i_2=0}^{\infty} \cdots \sum_{i_N=0}^{\infty} \sum_{j_1=0}^{\infty} \sum_{j_2=0}^{\infty} \cdots \sum_{j_{N-1}=0}^{\infty}, r = 2N\mu + 2i_\Sigma + j_\Sigma, \;\; i_\Sigma = \sum_{p=1}^{N} i_p,$$
$$j_\Sigma = \sum_{p=1}^{N-1} j_p, \mu' = \mu + i_p + \frac{1}{2}, \;\; \ell = \left( \frac{\sqrt{\pi}}{\Gamma(\mu)} \right)^N, \;\bar{\lambda} = \frac{2N\mu h}{\bar{\gamma}}, \text{ and } \;\mathrm{q} = \left( \frac{\mu \mathrm{h}}{\bar{\gamma}} \right)^{\mathrm{r}}$$

It should be noted that (4.11) applies to TAS/MRC as well as TAS/SC systems. For TAS/MRC $\gamma_t$ is $\eta - N_r\mu$ distributed as it is sum of $N_r$ i.i.d. $\eta-\mu$ square variates [19]. So, in (4.11), (4.12) and all subsequent expressions, $\mu$ shall be interpreted as $N_r\mu$ for TAS/MRC systems and $N_r$ becomes the number of antennas selected at the receiver, i.e. $N_r = 1$ for $(N_t, 1; N_r, 1)$ TAS/SC system.

## 4.2 Probability of Error

In this section, we derive expression for approximate and exact SER of TAS/MRC systems over $\eta-\mu$ fading channels for various modulation techniques. SER for a wireless communication system can be calculated by averaging the CPE over the PDF of received SNR. CPE for various

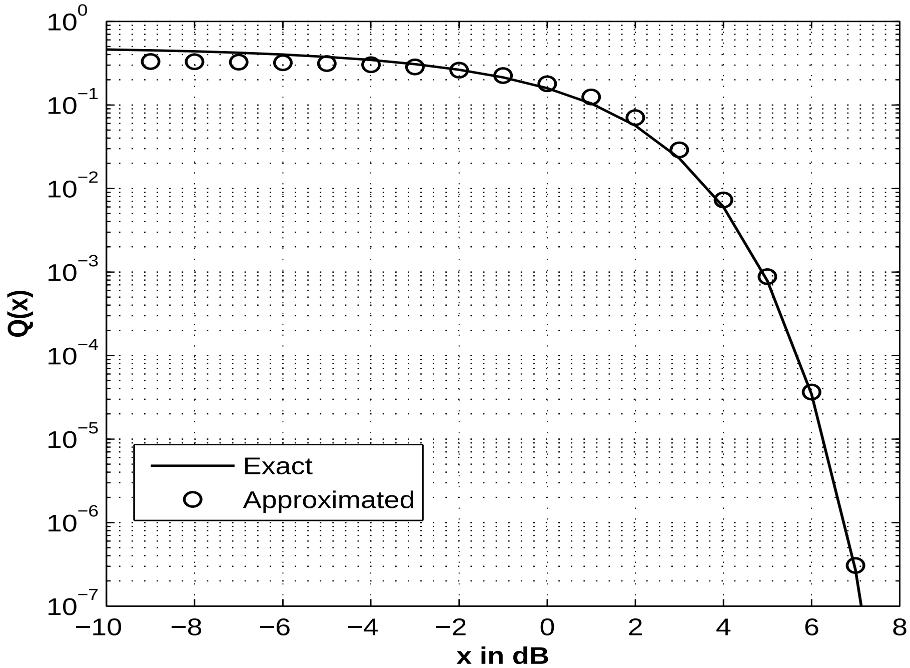


Figure 4.1: Plot to compare the values of exact and approximated Gaussian Q function

modulation schemes can be given by

$$P_e(\gamma) = aQ\left(\sqrt{b\gamma}\right) - cQ^2\left(\sqrt{b\gamma}\right) \tag{4.13}$$

where $Q(\cdot)$ is the Gaussian Q-function, $\gamma$ is SNR and $a$, $b$ and $c$ are modulation dependent parameters. The values of $a$, $b$ and $c$ are listed in Table 3.1 for different digital modulation techniques. The SER can be given by

$$\overline{P_e} = \int_0^\infty P_e(\gamma)\, p_{\gamma_{t(N)}}(\gamma)\, d\gamma \tag{4.14}$$

### 4.2.1 Approximate Probability of Error

To analyze approximate probability of error, the Gaussian Q-function is approximated as a sum of two exponential functions [64].

$$Q(\hbar) \approx \frac{1}{12}e^{-\frac{\hbar^2}{2}} + \frac{1}{4}e^{-\frac{2\hbar^2}{3}} \tag{4.15}$$

The approximated and exact values of Q-function are plotted in Figure 4.1 to confirm the validity of the above expression. It is observed that (4.15) gives a very accurate approximation for all values of $x$. For $x \geq -2$dB, the approximated and the exact values of Q-function are almost same.

Thus, using (4.13) and (4.15), approximate CPE can be given in the form of sum of exponential functions as

$$P_e(\gamma) \cong \frac{a}{12}e^{-\frac{b\gamma}{2}} + \frac{a}{4}e^{-\frac{2b\gamma}{3}} - \frac{c}{144}e^{-b\gamma} - \frac{c}{16}e^{-\frac{4b\gamma}{3}} - \frac{c}{24}e^{-\frac{7b\gamma}{6}} \tag{4.16}$$

where first two terms and last three terms represent first term and second term of (4.13) respectively.

Now, by averaging the above approximate CPE over the PDF of the received SNR, average approximate SER can be calculated as

$$\overline{P}_{e_{appr.}} \cong \sum_i \zeta_i \int_0^\infty e^{-\psi_i\gamma} p_{\gamma_{t(N)}}(\gamma)\,d\gamma \tag{4.17}$$

where $\zeta_1 = \frac{a}{12}$, $\zeta_2 = \frac{a}{4}$, $\zeta_3 = \frac{-c}{144}$, $\zeta_4 = \frac{-c}{16}$, $\zeta_5 = \frac{-c}{24}$, $\psi_1 = \frac{b}{2}$, $\psi_2 = \frac{2b}{3}$, $\psi_3 = b$, $\psi_4 = \frac{4b}{3}$, and $\psi_5 = \frac{7b}{6}$.

In the above expression, the integral of (4.17) fits the definition of MGF of the received SNR $M_\gamma(\psi_i)$. Thus, approximate SER can be given as the weighted sum of MGFs of received SNR. In this case, it can be given as

$$\overline{P}_{e_{appr.}} \cong \sum_i \zeta_i M_\gamma(\psi_i) \tag{4.18}$$

### 4.2.2 Exact Probability of Error

In this section, we derive expression for exact SER of TAS/MRC systems over $\eta-\mu$ fading channels for various modulation techniques. The exact SER can be evaluated as [61]

$$\overline{P}_e = \int_0^\infty \left[aQ\left(\sqrt{bx}\right) - cQ^2\left(\sqrt{bx}\right)\right] p_{\gamma_{t(N)}}(x)\,dx \tag{4.19}$$

$$= \underbrace{\frac{a}{\pi}\int_{0}^{\frac{\pi}{2}} M_{\gamma}\left(\frac{b}{2\sin^{2}\theta}\right)d\theta}_{I_1} - \underbrace{\frac{c}{\pi}\int_{0}^{\frac{\pi}{4}} M_{\gamma}\left(\frac{b}{2\sin^{2}\theta}\right)d\theta}_{I_2} \tag{4.20}$$

**Evaluation of $I_1$**

$I_1$ is the first term of (4.20), i.e.

$$I_1 = \frac{2aN}{\pi}\ell\sum_{i,j}\frac{2^{j_\Sigma}H^{2i_\Sigma}q\Gamma(r)\int_{0}^{\frac{\pi}{2}}\left(\bar{\lambda}+\frac{b}{2\sin^{2}\theta}\right)^{-r}d\theta}{h^{N\mu+2i_\Sigma}\prod_{p=1}^{N}(i_p!\Gamma(\mu'))\prod_{p=1}^{N-1}\left((\mu+i_p)(2\mu')_{j_p}\right)} \tag{4.21}$$

The above integral can be evaluated by bringing it in the form of (5A.3) of [61] as

$$I_1 = aN\ell\sqrt{\frac{\zeta}{\pi}}\sum_{i,j}\frac{2^{j_\Sigma}H^{2i_\Sigma}q\bar{\lambda}^{-r}\Gamma\left(r+\frac{1}{2}\right)}{h^{N\mu+2i_\Sigma}\prod_{p=1}^{N}(i_p!\Gamma(\mu'))}\frac{{}_2F_1\left(1,r+\frac{1}{2},r+1,\frac{1}{1+\zeta}\right)}{r(1+\zeta)^{r+\frac{1}{2}}\prod_{p=1}^{N-1}\left((\mu+i_p)(2\mu')_{j_p}\right)} \tag{4.22}$$

where $\zeta = \frac{b}{2\bar{\lambda}}$.

**Evaluation of $I_2$**

$I_2$ is the second term of (4.20), i.e.

$$I_2 = \frac{2cN}{\pi}\ell\sum_{i,j}\frac{2^{j_\Sigma}H^{2i_\Sigma}q\Gamma(r)\int_{0}^{\frac{\pi}{4}}\left(\bar{\lambda}+\frac{b}{2\sin^{2}\theta}\right)^{-r}d\theta}{h^{N\mu+2i_\Sigma}\prod_{p=1}^{N}(i_p!\Gamma(\mu'))\prod_{p=1}^{N-1}\left((\mu+i_p)(2\mu')_{j_p}\right)} \tag{4.23}$$

A detailed solution of above integral is given in Appendix A.2. However, substituting $\sin^2\theta = t/2$ in the above integral, following some mathematical simplifications and using [66, (7.2.4.42)], $I_2$ can be given as

$$I_2=\frac{\sqrt{2}cN}{\pi}\ell\sum_{i,j}\frac{2^{j_\Sigma}H^{2i_\Sigma}q\overline{\lambda}^{-r}\Gamma(r)}{h^{N\mu+2i_\Sigma}\prod_{p=1}^{N}(i_p!\Gamma(\mu'))}\frac{F_A^{(1)}\left(r+\frac{1}{2},\frac{1}{2},r,r+\frac{3}{2},\frac{1}{2},-\frac{1}{2\zeta}\right)}{\prod_{p=1}^{N-1}\left((\mu+i_p)(2\mu')_{j_p}\right)(1+2r)(2\zeta)^r} \tag{4.24}$$

where $F_A^{(1)}(a;b_1,b_2;c;x,y)$ is Appell Hypergeometric function of two variables and $\zeta=\frac{b}{2\overline{\lambda}}$.

### 4.2.3 Asymptotic Probability of Error

The asymptotic probability of error is a measure of performance analysis at high SNR conditions. In general, it is used to distinguish the system behavior at high SNR regime with a very easy evaluation method. From (4.22) and (4.24), it is clear that $I_2$ corresponds to the term containing squared Gaussian Q-function and it can be neglected at high SNR. The asymptotic error performance can be evaluated by assuming the values of all summation variables to be zero, i.e. ($i_1,\ i_2,\ \ldots,\ i_N=0$ and $j_1,\ j_2,\ \ldots,\ j_{N-1}=0$) in (4.22). The asymptotic probability of error can be given by

$$P_{e_{asympt}}=\frac{a\ell}{2}\sqrt{\frac{\zeta}{\pi}}\frac{\Gamma\left(2N\mu+\frac{1}{2}\right)}{h^{N\mu}\Gamma(\mu+\frac{1}{2})^N\mu^N}\frac{{}_2F_1\left(1,2N\mu+\frac{1}{2},2N\mu+1,\frac{1}{1+\zeta}\right)}{\left(\frac{\mu h}{\gamma}\right)^{-2N\mu}\overline{\lambda}^{2N\mu}(1+\zeta)^{2N\mu+\frac{1}{2}}} \tag{4.25}$$

Using (9.200) of [63], above expression can be simplified to obtain asymptotic probability of error as follows

$$P_{e_{asympt}}=\frac{a}{2\sqrt{\pi}}\left(\frac{\sqrt{\pi}}{\Gamma(\mu)}\right)^N\frac{(2N)^{-2N\mu}\Gamma\left(2N\mu+\frac{1}{2}\right)}{h^{N\mu}\mu^N\Gamma(\mu+\frac{1}{2})^N\left(1+\frac{b\overline{\gamma}}{4N\mu h}\right)^{2N\mu}} \tag{4.26}$$

Note that the above expression of asymptotic probability of error is in the form of elementary functions and can be easily evaluated using any of the commonly available computational tools.

Table. 4.1: Number of terms required for accuracy up to $5^{th}$ place of decimal digit in scientific notation of the result of (4.20)

| $\eta,\mu,N_t,N_r$ | SNR=5dB | | SNR=10dB | |
|---|---|---|---|---|
| | P | SER | P | SER |
| 1,0.5,2,2 | 10 | $1.98186\times10^{-2}$ | 7 | $9.27794\times10^{-4}$ |
| 0.5,1.25,2,1 | 18 | $6.92964\times10^{-2}$ | 11 | $5.49862\times10^{-3}$ |
| 0.8,1.5,3,1 | 18 | $4.58657\times10^{-2}$ | 11 | $1.52017\times10^{-3}$ |

## 4.3 Channel Capacity

In this section, we derive expression for ergodic channel capacity for TAS/MRC systems over $\eta-\mu$ fading channels. The ergodic capacity per unit bandwidth can be given as [61]

$$\frac{\bar{C}_{erg}}{B}=\int_0^\infty \log_2(1+\gamma)p_{\gamma_{t(N)}}(\gamma)\,d\gamma \tag{4.27}$$

Using (4.11) in the above expression and evaluating it by using the method discussed in [65] for integer values of $2\mu$, we get the ergodic capacity per unit bandwidth as

$$\frac{\bar{C}_{erg}}{B}=2N\ell\sum_{i,j}\frac{H^{2i_\Sigma}q\left(2^{j_\Sigma}\right)\Gamma(r)e^{\bar{\lambda}}\sum\limits_{\alpha=1}^{r}\frac{\Gamma(\alpha-r\bar{\lambda})}{\bar{\lambda}^{\alpha}}}{h^{N\mu+2i_\Sigma}\prod\limits_{p=1}^{N}(i_p!\Gamma(\mu'))\prod\limits_{p=1}^{N-1}\left((\mu+i_p)(2\mu')_{j_p}\right)} \tag{4.28}$$

## 4.4 Results and Discussion

We simulated TAS/MRC systems for various values of fading parameters ($\eta$ and $\mu$) for BER/SER and ergodic capacity. We truncated the infinite sum series of (4.22) and (4.24) while evaluating SER using (4.20) up to first $P$ terms such that it gives accurate result up to the $5^{th}$ place of decimal digit when the value is represented in scientific notation, i.e. in the form of $a\times10^b$. The value of $P$ and corresponding SER for some cases is tabulated in Table 4.1. It is observed that we can get accurate results up to 5 places of decimal by truncating the infinite sums to first

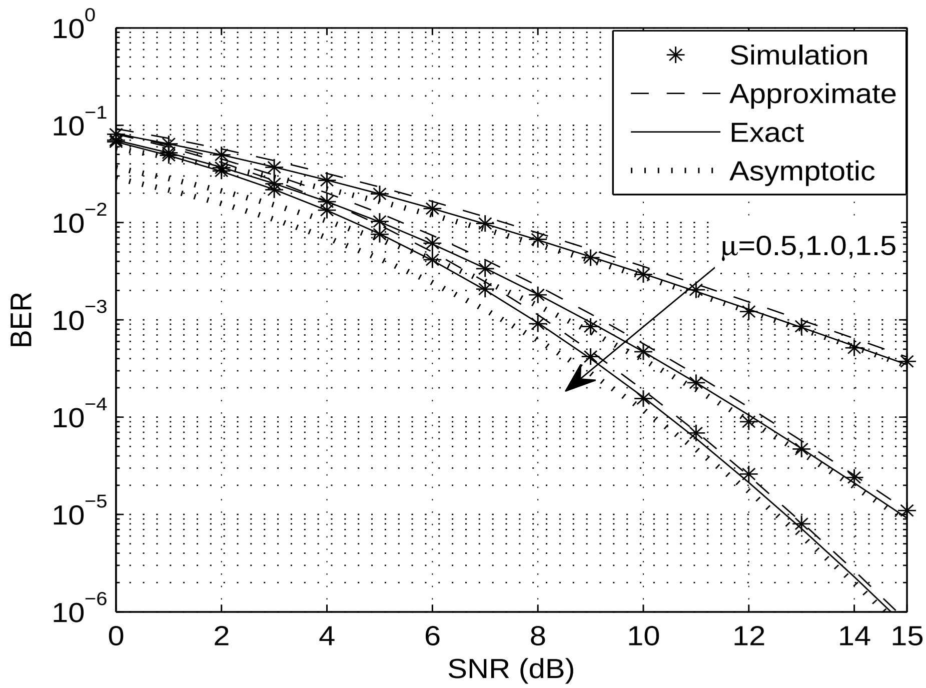


Figure 4.2: BER performance of (2,1;1) TAS/MRC system over $\eta - \mu$ fading channels for $\eta = 1$ with BPSK modulation

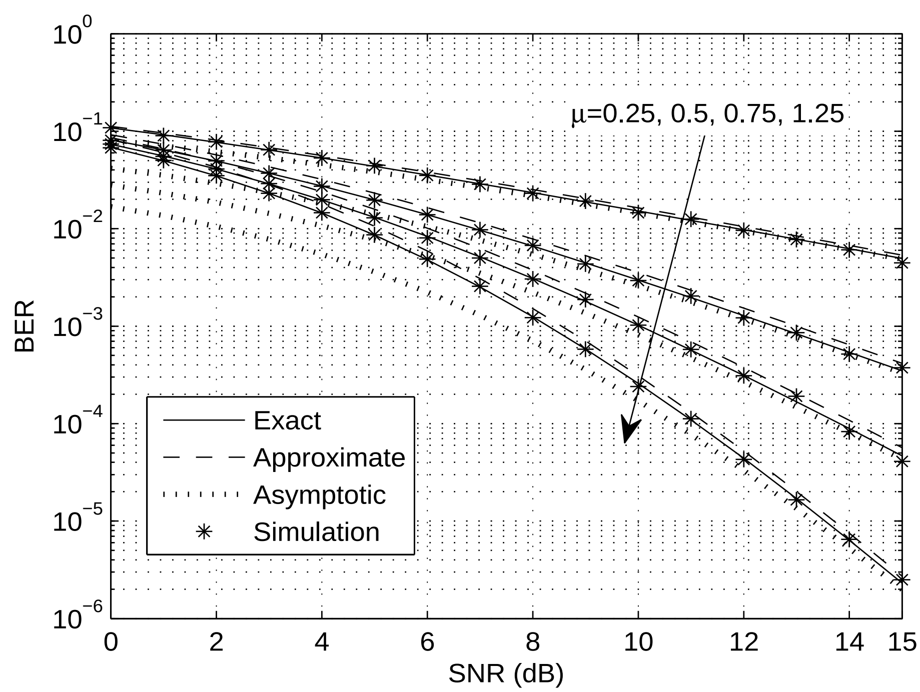


Figure 4.3: BER performance of (2,1;1) TAS/MRC system over $\eta - \mu$ fading channels for $\eta = 1$ including non integer values of $2\mu$ with BPSK modulation

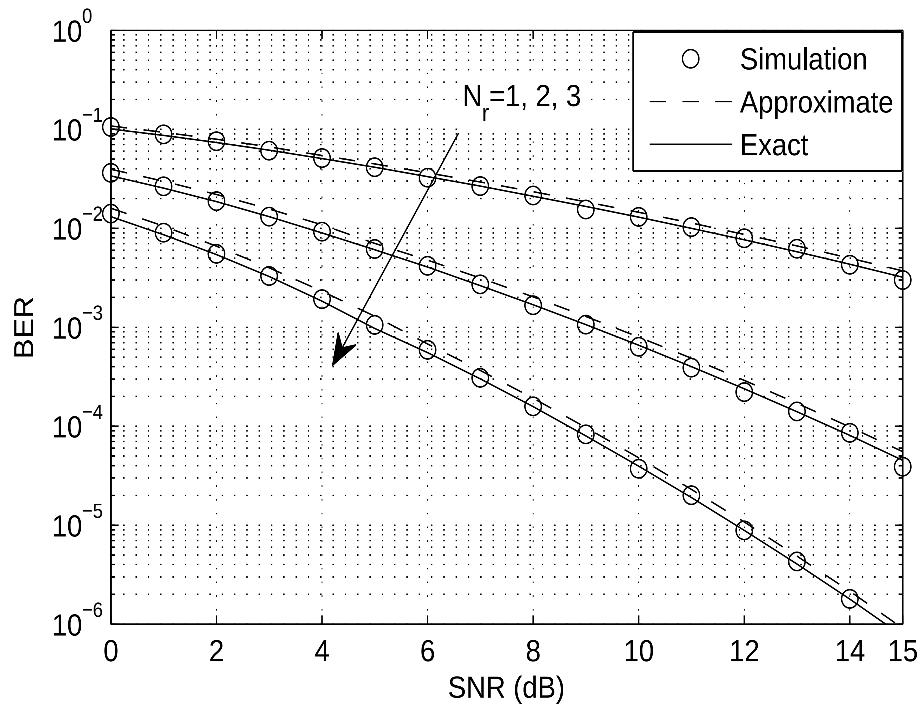


Figure 4.4: BER performance of (2,1;$N_r$) TAS/MRC system over $\eta-\mu$ fading channels for $\eta=0.01$ and $\mu=0.5$ with BPSK modulation

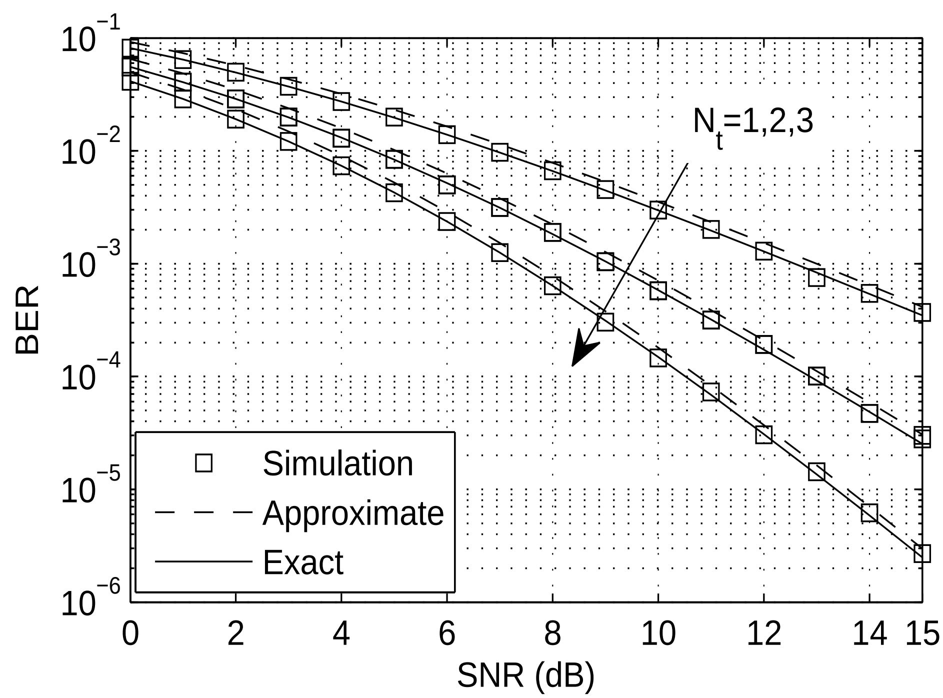


Figure 4.5: BER performance of ($N_t$,1;1) TAS/MRC system over $\eta-\mu$ fading channels for $\eta=1$ and $\mu=0.5$ with BPSK modulation

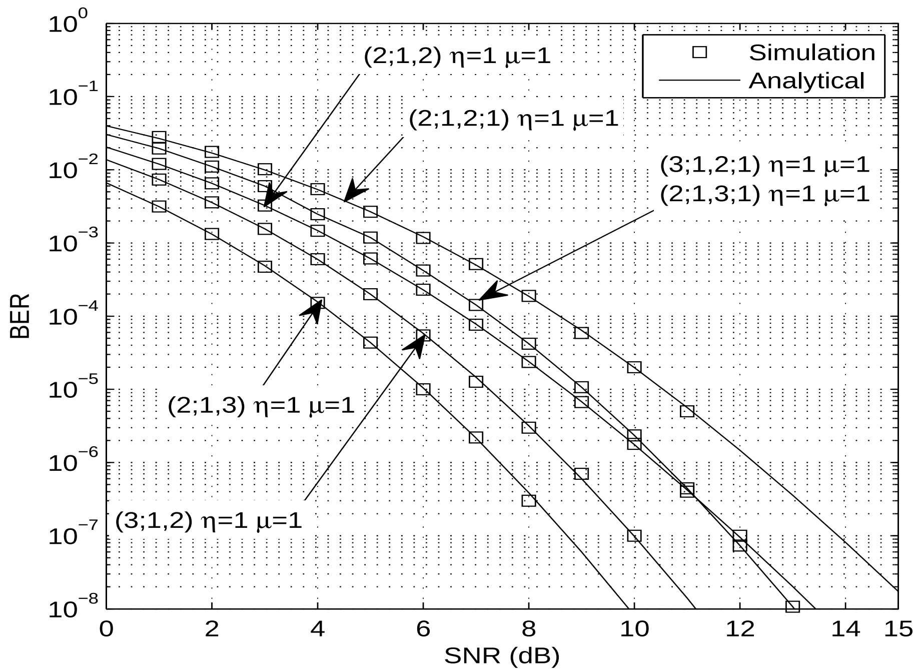


Figure 4.6: Performance Comparison of TAS/MRC and TAS/SC systems

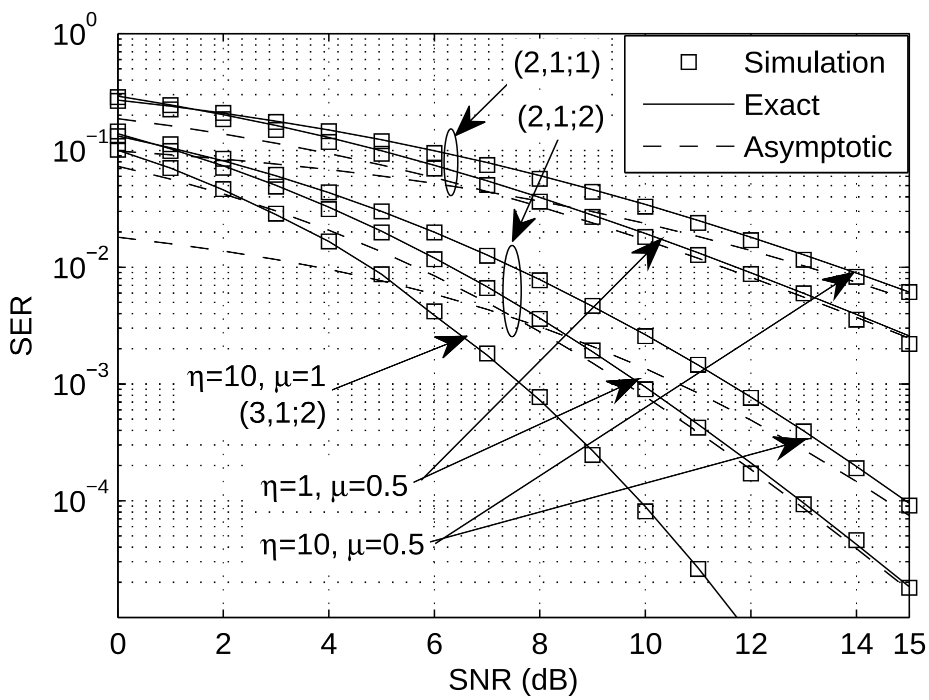


Figure 4.7: SER Performance $(N_t, 1; N_r)$ TAS/MRC with 4-QAM modulation for different values of fading parameters

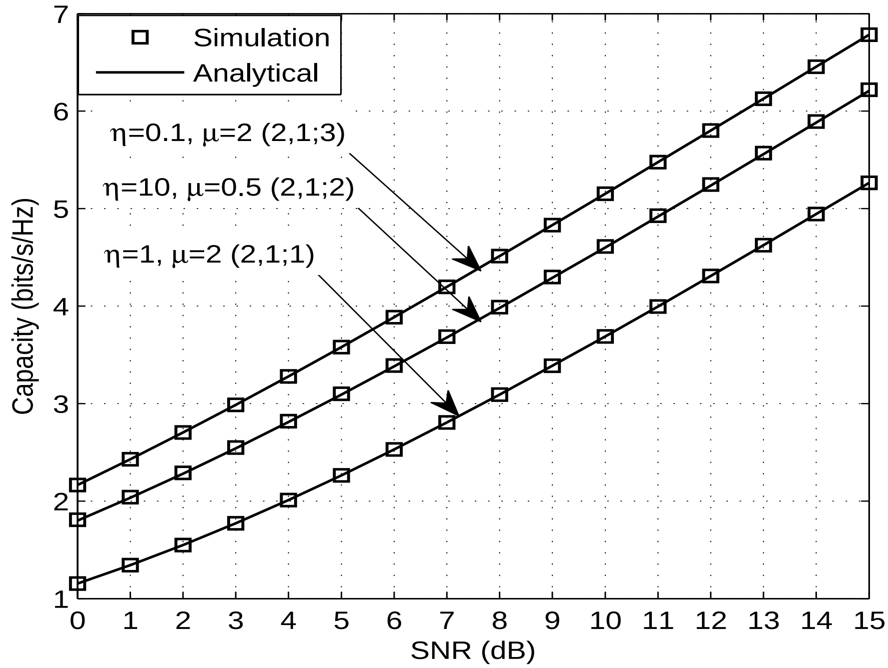


Figure 4.8: Capacity of $(2,1;N_r)$ TAS/MRC for different values of $\eta$ and $\mu$

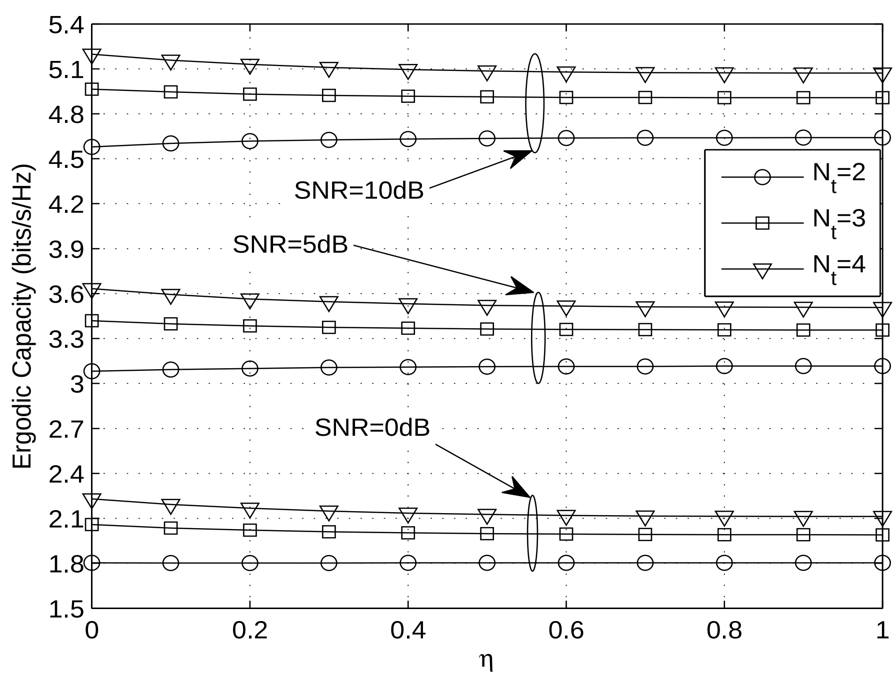


Figure 4.9: Capacity of $(N_t,1;2)$ TAS/MRC system for different values of $\eta$

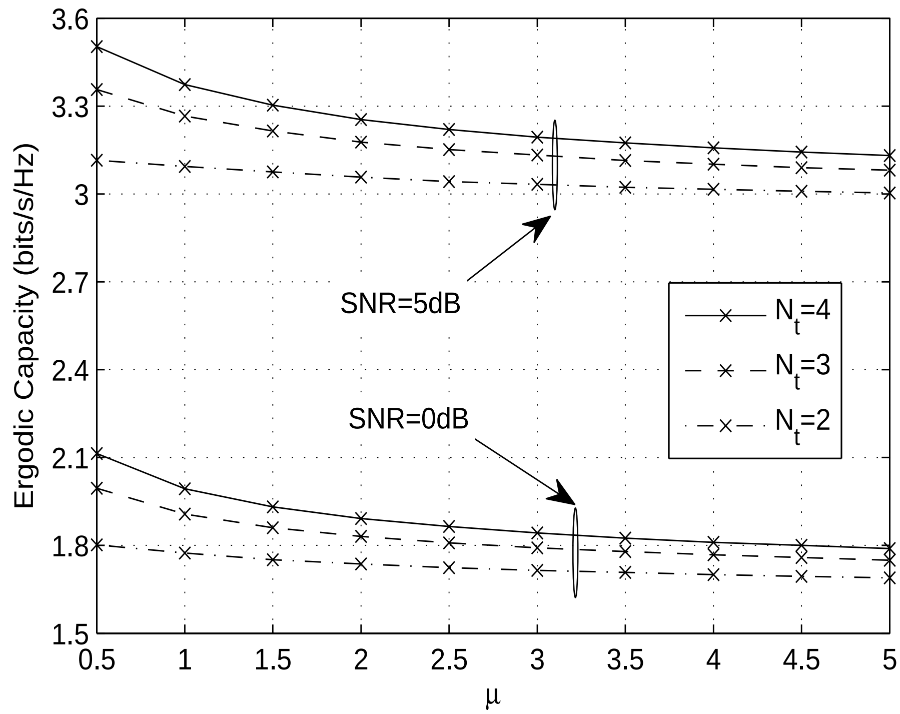


Figure 4.10: Capacity of $(N_t, 1; 2)$ TAS/MRC system for different values of $\mu$

20 terms, i.e. the first five places of decimal remains unchanged even on increasing the value of $P$ further.

In Figure 4.2, the results are shown for a (2,1;1) TAS/MRC system for Nakagami-m fading case with $\eta = 1$ and $\mu = m/2$ (a special case of $\eta-\mu$ fading). The analytical (exact, approximate and asymptotic) and simulation results of error performance are plotted for $m = 1, 2$ and 3 for BPSK modulation scheme. As the value of fading parameter, $m$ increases the severity of fading decreases and the BER performance of the system improves. It can be seen from the figure that the asymptotic BER performance is a lower bound and approximate BER is an upper bound to the exact BER performance. The analytical and simulation results can be observed to be in close agreement.

We simulated TAS/MRC system over $\eta-\mu$ fading channels to show that the derived expressions also applies equally well also to the fading conditions with non integer values of $2\mu$. The results are shown in Figure 4.3. It is observed that the numerical results are in close agreement with the Monte Carlo simulation results.

In Figure 4.4, the results are shown for a (2,1;$N_r$) TAS/MRC system for Hoyt (Nakagami-q) fading case with $\eta = 0.01$ and $\mu = 0.5$ (a special case of $\eta-\mu$ fading). The analytical (exact, approximate and asymptotic) and simulation results of error performance are plotted for $N_r$= 1, 2 and 3 for BPSK modulation scheme.

In Figure 4.5, the results are shown for a ($N_t$,1;1) TAS/MRC system for Rayleigh fading case with $\eta = 1$ and $\mu = 0.5$ (a special case of $\eta-\mu$ fading). The analytical (exact, approximate and asymptotic) and simulation results of error performance are plotted for $N_t$= 1, 2 and 3 for BPSK modulation scheme.

In Figure 4.6, the results are shown for a ($N_t$,1;$N_r$) TAS/MRC system and ($N_t$,1;$N_r$;1) TAS/SC system for $\eta = 1$ and $\mu = 1$. It compares the performance of TAS/MRC system and TAS/SC systems. The analytical (exact, approximate and asymptotic) and simulation results of error performance are plotted for BPSK modulation scheme. From figure, it can be observed that to achieve same BER of $10^{-4}$ (2;1,2) TAS/MRC require 2dB less SNR than (2;1,2;1) TAS/SC system. Similarly, to achieve the BER of $10^{-5}$, (2,1;3) TAS/MRC system require 3dB less SNR and (3,1;2) TAS/MRC require 3dB less SNR when compared with the performance of (2,1;3,1) or (3,1;2,1) TAS/SC system. It is important to note that the BER performance of ($N_t$,1;$N_r$,1) TAS/SC system is same as that of ($N_r$,1;$N_t$,1) TAS/SC system. Similarly, it is intuitive that the BER performance of ($N_t$,1;$N_r$,1) TAS/SC system is same as that of ($N_tN_r$,1;1,1) TAS/SC system or (1,1;$N_rN_t$,1) TAS/SC system.

In Figure 4.7, the results are shown for a ($N_t$,1;$N_r$) TAS/MRC system for different values of fading parameters $\eta$ and $\mu$ with 4-QAM modulation. Analytical and Monte Carlo simulation results are plotted for different number of transmit and receive antennas. The exactness of the analytical results can be seen through the close agreement of analytical and simulation results.

Simulations and numerical evaluations were done for the ergodic capacity of TAS/MRC systems over $\eta-\mu$ fading channels. The numerical and simulation results are plotted in Figure 4.8 for various values of fading parameters.

The variation of ergodic capacity with fading parameters $\eta$ and $\mu$ is also studied to investigate the effect of fading severity on the ergodic capacity. Figure 4.9 shows the variation of ergodic capacity for $0 \leq \eta \leq 1$ with $\mu = 0.5$ for SNR values of 0dB, 5dB and 10dB with $N_t$= 2, 3 and 4. It is observed that the ergodic capacity degrades with increasing value of $\eta$ for $N_t > 2$. This observation is similar to the findings of [26] for Hoyt fading channels.

The variation of ergodic capacity for $\eta = 1$ with different values of $\mu$ shows a degradation in capacity with increasing values of $\mu$. The simulation results of ergodic capacity are plotted in Figure 4.10 for ($N_t$,1;2) TAS/MRC system with different number of transmitting antennas for SNR values of 0dB and 5dB. It is observed that the capacity degrades with increasing values of $\mu$ irrespective of the number of transmitting antennas.

The observed degradations in ergodic capacity with fading parameters can be explained by the fact that with decreasing severity in fading it is highly likely that the instantaneous SNR will be less varying. In such a case, the PDF of the received SNR after TAS/MRC shifts towards left indicating a decrease in the average SNR at the receiver. However, this will not degrade the SER performance because this also narrows the PDF of the received SNR which improves the diversity order. The improved diversity order compensates the decrease in the average SNR at the receiver. Hence, an improvement in the SER is observed while the ergodic capacity degrades with decrease in the fading severity.

## 4.5 Summary

In this chapter, we derived expressions for exact, approximate and asymptotic SER and ergodic capacity of TAS/MRC systems with arbitrary number of transmitting and receiving antennas for various modulation schemes over $\eta-\mu$ fading channels. The derived expressions can also be applied for performance analysis of TAS/SC systems over $\eta-\mu$ fading channels. Monte Carlo simulations of TAS/MRC systems and TAS/SC systems are carried out for various values of fading parameters such that the special cases of $\eta-\mu$ fading model like Rayleigh, Nakagami-m and Hoyt fading scenario are covered. The SER performances of TAS/MRC and TAS/SC systems are compared and the superiority of TAS/MRC systems over TAS/SC systems is demonstrated. From extensive Monte Carlo simulation results, it is found that the ergodic capacity of TAS/MRC systems over $\eta-\mu$ fading channels improves as the value of $\eta$ decreases for $N_t \geq 3$ for $0 \leq \eta \leq 1$ while it degrades for increasing values of $\mu$ irrespective of the number of transmitting antennas for all $\mu \geq 0.5$.

# CHAPTER 5

# PERFORMANCE ANALYSIS OF TWO HOP MIMO COOPERATIVE COMMUNICATION SYSTEMS WITH SOURCE AND RELAY ANTENNA SELECTION

Cooperative relaying systems are known for extending the coverage area of wireless communication systems [67]. Cooperative relaying, in addition to achieve extended area coverage, inspired the researchers to germinate the idea of cooperative diversity scheme commonly known as cooperative communication (CC). In CC, a user transmits its own data to destination and in addition, also forwards the other users' data. It takes advantage of time diversity to improve the error performance of the system. Cooperative diversity schemes have been proposed as a robust system that increases capacity for both the users and to achieve an improved quality of service especially for next generation cellular systems [68, 69]. In CC, each of the user is known as a node. Nodes can be classified as source node, the node which generates information to be transmitted, destination node, the node to which the information is to be transmitted from the source node and relay node(s), the nodes which helps deliver the information from source to destination according the defined protocol. The most common protocols to be followed at relay

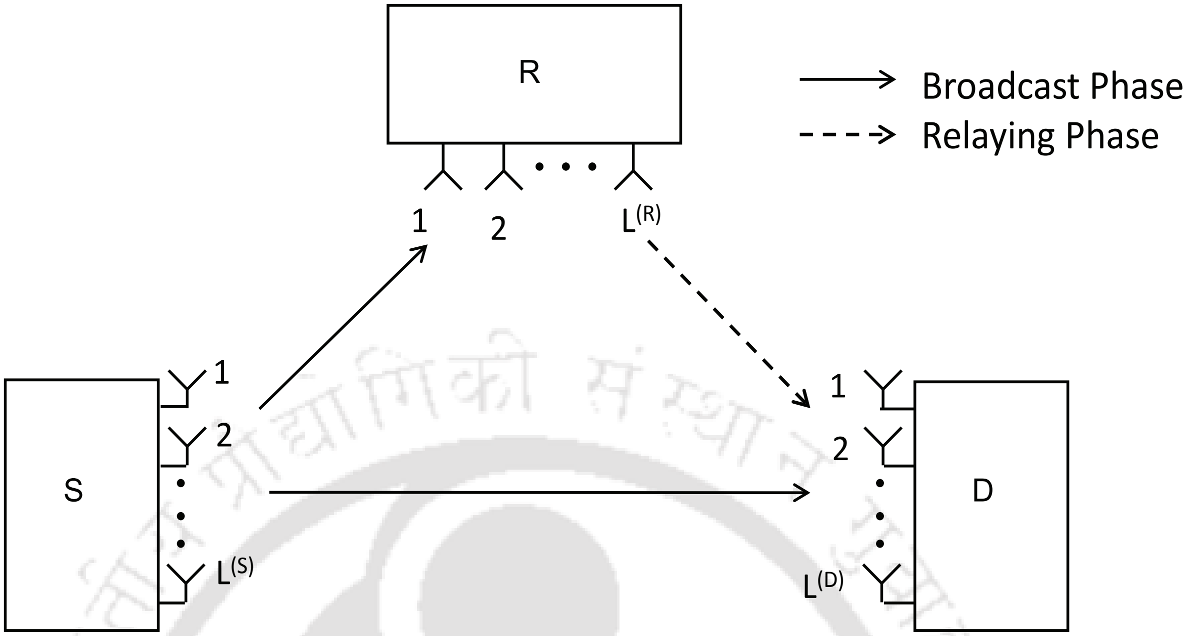


Figure 5.1: MIMO Based Cooperative Communication System

node(s) are:

(a) Amplify-and-forward (AF) protocol in which the the received signal is strengthened through amplification and the stronger signal is forwarded to destination or the next relay as per the situation.

(b) Decode-and-forward (DF) protocol in which the received signal is decoded and it is re-encoded using suitable modulation technique and transmitted to the destination in two-hop systems or next relay node in multi-hop systems.

A system model for MIMO CC systems is given in Figure 5.1. In MIMO CC systems, each node is having multiple antennas. CC systems have been widely studied for different performance metrics over various fading channels including multiple relays and even with multiple hop situations for various fading channel models.

TAS, proposed for two-hop CC systems in [1, 70], showed improved performance and achieved full diversity order. Initial works for the analysis of error performance of TAS based two-hop CC involves AF protocol at relay [39, 71] in which relay forwards an amplified signal to the destination. TAS based two-hop CC with DF relaying has been investigated in [44, 45, 72] of which only [44] investigated error performance of TAS CC systems. However, it assumes no presence of direct link between the source and the destination nodes.

In this chapter, based on the analysis of TAS/MRC systems over $\eta-\mu$ and $\kappa-\mu$ fading channels in Chapter 4 and Chapter 3, we derive infinite series expressions for end to end BER of two-hop relaying DF CC systems over generalized $\kappa-\mu$ and $\eta-\mu$ fading channels for BPSK modulation scheme. We consider antenna selection at source node and relay node as well such that the received SNR at the destination node is maximized. The results of analytical expressions are found to be in close agreement with the results of extensive Monte Carlo simulations of DF CC systems over $\kappa-\mu$ and $\eta-\mu$ fading channels for different values of fading parameters.

Further, this chapter is organized as follows. System and channel model along with the derivation of PDF and CDF of received SNRs are discussed in the next section. Detailed derivation of expressions for probability of error at the destination (end to end error probability) are derived in section 5.2. Simulation results with related discussions are described in section 5.3 and the chapter is summarized in section 5.4.

## 5.1 System and Channel Model

### 5.1.1 System Model

We consider a two-hop CC system with a source node (S) equipped with $L^{(S)}$ antennas, a destination node (D) equipped with $L^{(D)}$ antennas and a relay node (R) equipped with $L^{(R)}$ antennas. The source communicates with destination through relay node and the relay node is configured in half duplex DF relaying mode. The information is transferred from S to D in two time slots. In first time slot, information is broadcasted to R and D by S and in second time slot, R sends the information to D only if it can correctly decode the broadcasted information of S in the first time slot [67, Section 5.1]. At the end of the second time slot D performs MRC of the signals received in both the time slots. The information is transmitted from the antenna that maximizes the received SNR at D in both the time slots. The transmitting antennas of S and R those maximize SNR at D can be determined by

$$I^{(\Lambda)} = \underset{1\leq i\leq L^{(\Lambda)}}{\arg\max}\left\{C_i = \sum_{j=1}^{L^{(D)}}\left|h_{j,i}^{(\Lambda,D)}\right|^2\right\} \tag{5.1}$$

where $\Lambda \in \{\mathrm{S},\mathrm{R}\}$, $I^{(\Lambda)}$ denotes antenna index which corresponds to the transmitting antenna of node $\Lambda$ that maximizes the received SNR at node D and $h_{j,i}^{(\Lambda,D)}$ is the channel coefficient of the link between $i^{th}$ transmitting antenna of node $\Lambda$ and $j^{th}$ receiving antenna of node D.

### 5.1.2 Channel Model

We assume the fading envelope $\left(\left|h_{j,i}^{(\Lambda,\Theta)}\right|\right)$ to be independent and identical $\kappa-\mu$ distributed or $\eta-\mu$ distributed for $\Theta \in \{\mathrm{R},\mathrm{D}\}$. For MRC diversity combining at the receiver, it can be shown that the received instantaneous SNR for an arbitrary transmitting antenna of node $\Lambda$ will be $\kappa - L^{(\Theta)}\mu$ distributed or $\eta - L^{(\Theta)}\mu$ distributed [17–19].

The PDF of $\kappa - L^{(\Theta)}\mu$ distributed instantaneous SNR can be given as [17]

$$p_{\gamma_{\kappa-L^{(\Theta)}\mu}}(\gamma) = \frac{L^{(\Theta)}\mu(1+\kappa)^{\frac{L^{(\Theta)}\mu+1}{2}}\gamma^{\frac{L^{(\Theta)}\mu-1}{2}}}{\kappa^{\frac{L^{(\Theta)}\mu-1}{2}}\overline{\gamma}_{\Lambda\Theta}^{\frac{L^{(\Theta)}\mu+1}{2}}e^{L^{(\Theta)}\mu\kappa}}e^{-\frac{L^{(\Theta)}\mu(1+\kappa)\gamma}{\overline{\gamma}_{\Lambda\Theta}}}I_{L^{(\Theta)}\mu-1}\left(2L^{(\Theta)}\mu\sqrt{\frac{\kappa(1+\kappa)\gamma}{\overline{\gamma}_{\Lambda\Theta}}}\right) \tag{5.2}$$

where $\overline{\gamma}_{\Lambda\Theta}$ is the average SNR for the link between node $\Lambda$ and node $\Theta$.

The PDF of $\eta - L^{(\Theta)}\mu$ distributed instantaneous SNR can be given as [18]

$$p_{\gamma_{\eta-L^{(\Theta)}\mu}}(\gamma) = \frac{2\sqrt{\pi}\left(L^{(\Theta)}\mu\right)^{L^{(\Theta)}\mu+\frac{1}{2}} h^{L^{(\Theta)}\mu}\gamma^{L^{(\Theta)}\mu-\frac{1}{2}} e^{-\frac{2L^{(\Theta)}\mu\gamma h}{\overline{\gamma}_{\Lambda\Theta}}}}{\Gamma\left(L^{(\Theta)}\mu\right) H^{L^{(\Theta)}\mu-\frac{1}{2}}\left(\overline{\gamma}_{\Lambda\Theta}\right)^{L^{(\Theta)}\mu+\frac{1}{2}}} \times \sum_{i=0}^{\infty} \frac{1}{i!\Gamma\left(L^{(\Theta)}\mu-\frac{1}{2}+i+1\right)} \left(\frac{L^{(\Theta)}\mu\gamma H}{\overline{\gamma}_{\Lambda\Theta}}\right)^{L^{(\Theta)}\mu-\frac{1}{2}+2i} \quad (5.3)$$

The CDF of $\kappa-L^{(\Theta)}\mu$ and $\eta-L^{(\Theta)}\mu$ distributed instantaneous SNR can be given by (5.4) and (5.5) respectively from Chapter 3 and Chapter 4.

$$P_{\gamma_{\kappa-L^{(\Theta)}\mu}}(\gamma) = 1 - Q_{L^{(\Theta)}\mu}\left(\sqrt{2\kappa L^{(\Theta)}\mu}, \sqrt{\frac{2L^{(\Theta)}\mu\left(1+\kappa\right)\gamma}{\overline{\gamma}_{\Lambda\Theta}}}\right) \quad (5.4)$$

$$P_{\gamma_{\eta-L^{(\Theta)}\mu}}(x) = \frac{2^{1-2L^{(\Theta)}\mu}\sqrt{\pi}}{h^{L^{(\Theta)}\mu}\Gamma\left(L^{(\Theta)}\mu\right)} \sum_{i=0}^{\infty} \frac{\gamma_{inc}\left(2L^{(\Theta)}\mu+2i, \frac{2L^{(\Theta)}\mu h x}{\overline{\gamma}_{\Lambda\Theta}}\right)}{i!\Gamma\left(L^{(\Theta)}\mu+i+0.5\right)} \left(\frac{H}{2h}\right)^{2i} \quad (5.5)$$

### 5.1.3 CDF of Received SNR after Antenna Selection

Each $C_i$ for $i \in (1,2,...,L^{(\Lambda)})$ obtained from (5.1) for node S and node R are arranged in ascending order such that $C_{(1)} \leq C_{(2)}, \ldots \leq C_{(N)}$ where $C_{(l)}$ is the random variable obtained after the arrangement in ascending order and $N = L^{(\Lambda)}$. At both the nodes, we select the transmitting antenna corresponding to the highest received SNR, i.e. the antenna that corresponds to $\left(C_{L^{(\Lambda)}}\right)$ when MRC diversity technique is used at the receiver node. In such a system, assuming all $\left(\left|h_{j,i}^{(\Lambda,\Theta)}\right|\right)$'s to be i.i.d., the CDF of received SNR can be given by [59]

$$P^{\kappa-\mu}_{\gamma^{(\Lambda)}_{\Lambda D}}(\gamma) = \left\{P_{\gamma_{\kappa-L^{(\Theta)}\mu}}(\gamma)\right\}^N = \left(1 - Q_{L^{(\Theta)}\mu}\left(\sqrt{2\kappa L^{(\Theta)}\mu}, \sqrt{\frac{2L^{(\Theta)}\mu\left(1+\kappa\right)\gamma}{\overline{\gamma}_{\Lambda D}}}\right)\right)^N \quad (5.6)$$

$$P^{\eta-\mu}_{\gamma^{(\Lambda)}_{\Lambda D}}(\gamma) = \left\{P_{\gamma_{\eta-L^{(\Theta)}\mu}}(\gamma)\right\}^N = \left(\frac{2^{1-2L^{(\Theta)}\mu}\sqrt{\pi}}{h^{L^{(\Theta)}\mu}\Gamma\left(L^{(\Theta)}\mu\right)} \sum_{i=0}^{\infty} \frac{\gamma_{inc}\left(2L^{(\Theta)}\mu+2i, \frac{2L^{(\Theta)}\mu h\gamma}{\overline{\gamma}_{\Lambda D}}\right)}{i!\Gamma\left(L^{(\Theta)}\mu+i+0.5\right)} \left(\frac{H}{2h}\right)^{2i}\right)^N \quad (5.7)$$

where $\gamma_{\Lambda D}^{(\Lambda)} = \overline{\gamma}_{\Lambda D} C_{L^{(\Lambda)}}$ is the instantaneous SNR at D after performing transmit antenna selection at node $\Lambda$.

## 5.2 Probability of Error

The end to end CPE for two-hop DF relaying can be given as [67]

$$P_{bpsk}^{cond}(e) = \psi_b(\gamma_{SD})\,\psi_b(\gamma_{SR}) + \psi_b(\gamma_{SRD})\,[1 - \psi_b(\gamma_{SR})] \tag{5.8}$$

where $\gamma_{AB}$ is instantaneous SNR of link from node A to node B and $\psi_b(\gamma)$ is CPE for BPSK modulation scheme and is given by $\psi_b(\gamma) = Q(\sqrt{2\gamma})$ [61]. For i.i.d. fading channels, end to end average BER can be calculated as

$$\overline{P}_{bpsk}^{avg}(e) = \overline{\psi}_b(\overline{\gamma}_{SD})\,\overline{\psi}_b(\overline{\gamma}_{SR}) + \overline{\psi}_b(\overline{\gamma}_{SRD})\,[1 - \overline{\psi}_b(\overline{\gamma}_{SR})] \tag{5.9}$$

### 5.2.1 Calculation of $\overline{\psi}_b(\overline{\gamma}_{SR})$ for $\kappa - \mu$ Fading

The transmit antenna selection is done to maximize the received SNR at the destination in both the hops. Thus, the instantaneous SNR at the relay can be assumed to be $\kappa - L^{(R)}\mu$ distributed and average BER of S→R link can be calculated following the method discussed in [30] as

$$\overline{\psi}_b(\overline{\gamma}_{SR}) \cong \frac{1}{12} MGF(\overline{\gamma}_{SR}) + \frac{1}{4} MGF\left(\frac{4}{3}\overline{\gamma}_{SR}\right) \tag{5.10}$$

where

$MGF(x) = \left[\frac{L^{(R)}\mu(1+\kappa)}{L^{(R)}\mu(1+\kappa)+x}\right]^{L^{(R)}\mu} \exp\left[\frac{L^{(R)}\mu^2\kappa(1+\kappa)}{L^{(R)}\mu(1+\kappa)+x} - L^{(R)}\mu\kappa\right]$ is the moment generating function of $\kappa - L^R\mu$ distributed fading coefficients.

An expression for exact values of $\overline{\psi}_b(\overline{\gamma}_{SR})$ can be obtained following the steps of [36]. However, it involves numerical integration because the functions involving in the exact calculations are not available in the standard evaluation packages (Eg. MATLAB and Mathematica).

### 5.2.2 Calculation of $\bar{\psi}_b(\bar{\gamma}_{SR})$ for $\eta-\mu$ Fading

For the link from node S to node R, we do not apply TAS because at node S, the antenna is being selected to maximize SNR at node D. So, the average probability of error can be evaluated following the method discussed in [36]. It can be given by

$$\bar{\psi}_b(\bar{\gamma}_{SR}) = \frac{M_{\gamma_{\eta-L^{(R)}\mu}}(\bar{\gamma})}{2\sqrt{\pi}\left(2L^{(R)}\mu+\frac{1}{2}\right)_{\frac{1}{2}}} F_A^{(1)}\left(\frac{1}{2}, L^{(R)}\mu, L^{(R)}\mu, 2L^{(R)}\mu+1, A, B\right) \tag{5.11}$$

where $M_{\gamma_{\eta-L^{(R)}\mu}} = \left(\frac{4\left(L^{(R)}\mu\right)^2 h}{\left(\bar{\gamma}+2(h-H)L^{(R)}\mu\right)\left(\bar{\gamma}+2(h+H)L^{(R)}\mu\right)}\right)^{L^{(R)}\mu}$ is the MGF of $\eta-L^{(R)}\mu$ distribution, $A = \frac{2(h-H)L^{(R)}\mu}{\bar{\gamma}+2(h-H)L^{(R)}\mu}$ and $B = \frac{2(h+H)L^{(R)}\mu}{\bar{\gamma}+2(h+H)L^{(R)}\mu}$.

### 5.2.3 Calculation of $\bar{\psi}_b(\bar{\gamma}_{SD})$ for $\kappa-\mu$ Fading

The average BER of the link from S to D can be given by

$$\bar{\psi}_b(\bar{\gamma}_{SD}) = \int_0^\infty \psi_b(\gamma)\, p_{\gamma_{SD}^{(S)}}(\gamma)\, d\gamma = -\int_0^\infty \psi'_b(\gamma)\, P_{\gamma_{SD}^{(S)}}(\gamma)\, d\gamma \tag{5.12}$$

where $\psi'_b(\gamma)$ is the first derivative of CPE. For $\kappa-\mu$ fading, we use CDF based approach to evaluate probability of error as in Chapter 3. The average BER can be calculated by substituting (5.6) in (5.12)

$$\bar{\psi}_b(\bar{\gamma}_{SD}) = \frac{1}{2\sqrt{\pi}}\int_0^\infty \frac{e^{-\gamma}}{\sqrt{\gamma}}\left(1-Q_{L^{(D)}\mu}\left(\sqrt{2\kappa L^{(D)}\mu}, \sqrt{\frac{2L^{(D)}\mu(1+\kappa)\gamma}{\bar{\gamma}_{SD}}}\right)\right)^{L^{(S)}} d\gamma \tag{5.13}$$

To solve the above integral, $Q_{\ddot{m}}(\cdot,\cdot)$ can be represented in the form of infinite series for integer as well as non integer values of $\ddot{m}$ as in (3.15) and using (3.16). However, it is given below not to break continuity.

$$Q_{\ddot{m}}(\alpha,\beta) = 1 - e^{-\frac{\alpha^2+\beta^2}{2}} \sum_{r=\ddot{m}}^{\infty}\sum_{s=0}^{\infty} \frac{\left(\frac{\beta}{\alpha}\right)^r \left(\frac{\alpha\beta}{2}\right)^{r+2s}}{s!\,\Gamma(r+s+1)} \tag{5.14}$$

Using (5.14) in (5.13), the average BER can be given by

$$\bar{\psi}_b\left(\bar{\gamma}_{SD}\right)=\frac{1}{2\sqrt{\pi}}\sum_{R_{L^{(S)}}}\sum_{S_{L^{(S)}}}\frac{\left(\kappa L^{(D)}\mu\right)^{\sum_{i=1}^{L^{(S)}}s_i}\left(\frac{\ddot{K}}{L^{(S)}}\right)^{\ddot{\mu}}}{\left(1+\ddot{K}\right)^{\ddot{\mu}-\frac{1}{2}}}\frac{\Gamma\left(\ddot{\mu}+\frac{1}{2}\right)e^{-L^{(S)}\kappa L^{(D)}\mu}}{\prod_{i=1}^{L^{(S)}}s_i!\Gamma\left(s_i+r_i+L^{(D)}\mu+1\right)} \quad (5.15)$$

where $\ddot{K}=\frac{L^{(S)}L^{(D)}\mu(1+\kappa)}{\bar{\gamma}_{SD}}$, $\sum_{R_{L^{(S)}}}=\sum_{r_1=0}^{\infty}\sum_{r_2=0}^{\infty}\cdots\sum_{r_{L^{(S)}}=0}^{\infty}$, $\sum_{S_{L^{(S)}}}=\sum_{s_1=0}^{\infty}\sum_{s_2=0}^{\infty}\cdots\sum_{s_{L^{(S)}}=0}^{\infty}$ and $\ddot{\mu}=L^{(S)}L^{(D)}\mu+\sum_{i=1}^{L^{(S)}}r_i+\sum_{i=1}^{L^{(S)}}s_i$.

The fast convergence of (5.15) can be shown in the same manner as it is shown in Figure 3.1 of Chapter 3.

### 5.2.4 Calculation of $\bar{\psi}_b\left(\bar{\gamma}_{SD}\right)$ for $\eta-\mu$ Fading

For the link from node S to node D, TAS is applied at node S as per (5.1) so as to maximize the received SNR at node D. The received SNR in such case is the highest order statistics among $C_i$ for $i\in\{1,2,\ldots,N\}$, the PDF of which can be given by $p_{\gamma_{L^{(S)}}}=\frac{d}{dx}\left(P_{\gamma_{\eta-L^{(D)}\mu}}(x)^{L^{(S)}}\right)$ [59]. Using $\gamma_{inc}\left(\alpha,x\right)=\frac{e^{-x}}{\alpha}\sum_{k=0}^{\infty}\frac{x^{\alpha+k}}{(\alpha+1)_k}$ in (5.7), the PDF and MGF of received SNR after TAS can be given as

$$p_{\gamma_{\left(L^{(S)}\right)}}(x)=2L^{(S)}\ell\sum_{i,j}\frac{h^{-L^{(S)}L^{(D)}\mu}2^{j'_{\Sigma}}\left(\frac{H}{h}\right)^{2i'_{\Sigma}}\ddot{q}e^{-\lambda' x}x^{r'-1}}{\prod_{p=1}^{L^{(S)}}\left(i_p!\Gamma\left(\ddot{\mu}'\right)\right)\prod_{p=1}^{L^{(S)}-1}\left(\left(L^{(D)}\mu+i_p\right)\left(2\ddot{\mu}'\right)_{j_p}\right)} \quad (5.16)$$

$$M_{\gamma}(s)=2L^{(S)}\ell\sum_{i,j}\frac{h^{-L^{(S)}L^{(D)}\mu}2^{j'_{\Sigma}}\left(\frac{H}{h}\right)^{2i'_{\Sigma}}\ddot{q}\Gamma\left(r'\right)\left(\lambda'+s\right)^{-r'}}{\prod_{p=1}^{L^{(S)}}\left(i_p!\Gamma\left(\ddot{\mu}'\right)\right)\prod_{p=1}^{L^{(S)}-1}\left(\left(L^{(D)}\mu+i_p\right)\left(2\ddot{\mu}'\right)_{j_p}\right)} \quad (5.17)$$

where $\sum_{i,j}=\sum_{i_1=0}^{\infty}\sum_{i_2=0}^{\infty}\cdots\sum_{i_{L^{(S)}}=0}^{\infty}\sum_{j_1=0}^{\infty}\sum_{j_2=0}^{\infty}\cdots\sum_{j_{L^{(S)}-1}=0}^{\infty}$, $\lambda'=\frac{2L^{(S)}L^{(D)}\mu h}{\gamma}$, $r'=2L^{(S)}L^{(D)}\mu+2i_{\Sigma}+j_{\Sigma}$, $i'_{\Sigma}=\sum_{p=1}^{L^{(S)}}i_p$, $j'_{\Sigma}=\sum_{p=1}^{L^{(S)}-1}j_p$, $\ell=\left(\frac{\sqrt{\pi}}{\Gamma(\mu)}\right)^{L^{(S)}}$, $\ddot{\mu}'=L^{(D)}\mu+i_p+\frac{1}{2}$, and $\ddot{q}=\left(\frac{L^{(D)}\mu h}{\gamma}\right)^{r}$.

The average probability of error for BPSK modulation scheme in the form of MGF can be given by [73]

$$\bar{\psi}_b\left(\bar{\gamma}_{SD}\right) = \frac{1}{\pi}\int_0^{\frac{\pi}{2}} M_\gamma\left(\frac{1}{\sin^2\theta}\right)d\theta \tag{5.18}$$

From (5.18) and (5.17) and solving the integral in MATHEMATICA, the average probability can be given as

$$\begin{aligned}\bar{\psi}_b\left(\bar{\gamma}_{SD}\right) = L^{(S)}\ell\sum_{i,j}\frac{h^{-L^{(S)}L^{(D)}\mu}2^{j'_\Sigma}\left(\frac{H}{h}\right)^{2i'_\Sigma}\ddot{q}\Gamma(r')}{\prod_{p=1}^{L^{(S)}}\left(i_p!\Gamma\left(\ddot{\mu}'\right)\right)\prod_{p=1}^{L^{(S)}-1}\left(\left(L^{(D)}\mu+i_p\right)\left(2\ddot{\mu}'\right)_{j_p}\right)} \\ \left[\frac{(r')_{\frac{1}{2}}\left(\bar{\lambda}'+2\right)^{-r'}}{r'\sqrt{2\pi\left(\bar{\lambda}'+2\right)}}\left\{\bar{\lambda}'\ {}_2F_1\left(1, r'+\frac{1}{2}, -\frac{1}{2}, \frac{2}{\bar{\lambda}'+2}\right)\right.\right. \\ \left.\left. +\left(4\left(r'+1\right)-\bar{\lambda}'\right)\ {}_2F_1\left(1, r'+\frac{1}{2}, \frac{1}{2}, \frac{2}{\bar{\lambda}'+2}\right)\right\}+\frac{1}{\bar{\lambda}'^{r'}}\right]\end{aligned} \tag{5.19}$$

### 5.2.5 Calculation of $\bar{\psi}_b\left(\bar{\gamma}_{SRD}\right)$ for $\kappa-\mu$ and $\eta-\mu$ Fading

This is the case when node R is able to do correct decoding in the broadcast phase. In such a case, node D performs MRC of the received signal in first time slot and that in second time slot. Therefore, the calculation of $\bar{\psi}_b\left(\bar{\gamma}_{SRD}\right)$ remains same as the calculation of $\bar{\psi}_b\left(\bar{\gamma}_{SD}\right)$ with the substitutions $2L_r^{(D)}$ in place of $L_r^{(D)}$ and $\bar{\gamma}_{SRD} = \bar{\gamma}_{SD} + \bar{\gamma}_{RD}$ in place of $\bar{\gamma}_{SD}$ in (5.15) and (5.19) for $\kappa-\mu$ and $\eta-\mu$ fading respectively.

## 5.3 Simulation Results and Discussions

First of all, we compared BER performance of CC systems with TAS at different nodes and without TAS. For comparison, we assumed Rayleigh fading scenario and CC system with $L^{(S)} = L^{(R)} = 2$ and $L^{(D)} = 1$. In our analysis, the distance parameter has not been considered, so we keep equal average SNR for each link, i.e. $\bar{\gamma}_{SR} = \bar{\gamma}_{SD} = \bar{\gamma}_{RD}$ for all the results presented in this section. In Figure 5.2, the simulation results of BER for different combinations of TAS are shown. The results include BER of CC systems without TAS, TAS only at R to maximize the

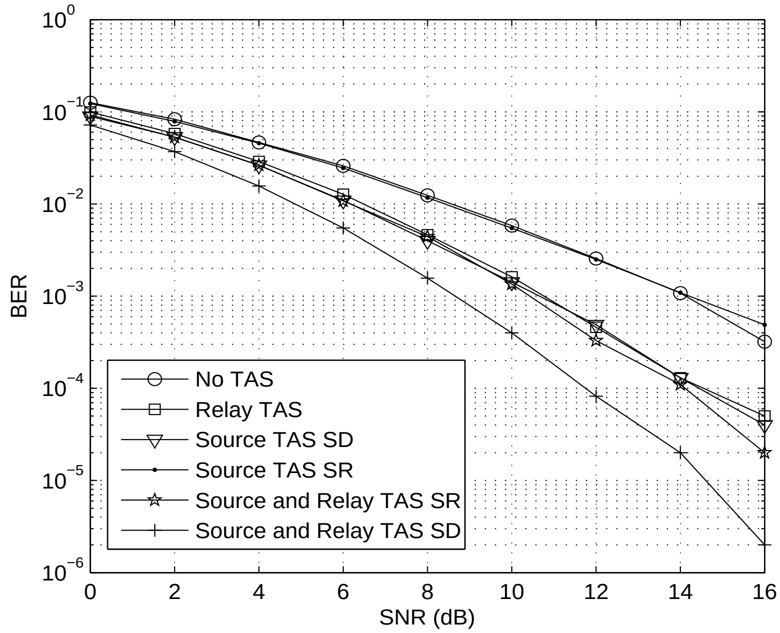


Figure 5.2: Comparison of BER performance of two hop TAS CC systems with different combinations of transmit antenna selection

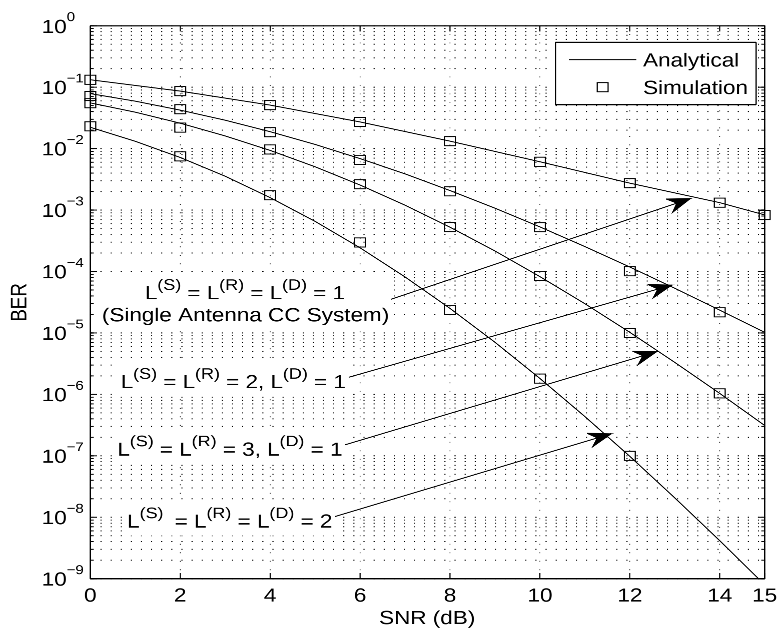


Figure 5.3: BER vs. SNR for two hop TAS CC systems with different number of transmit antennas for $\kappa = 0.5$ and $\mu = 1$

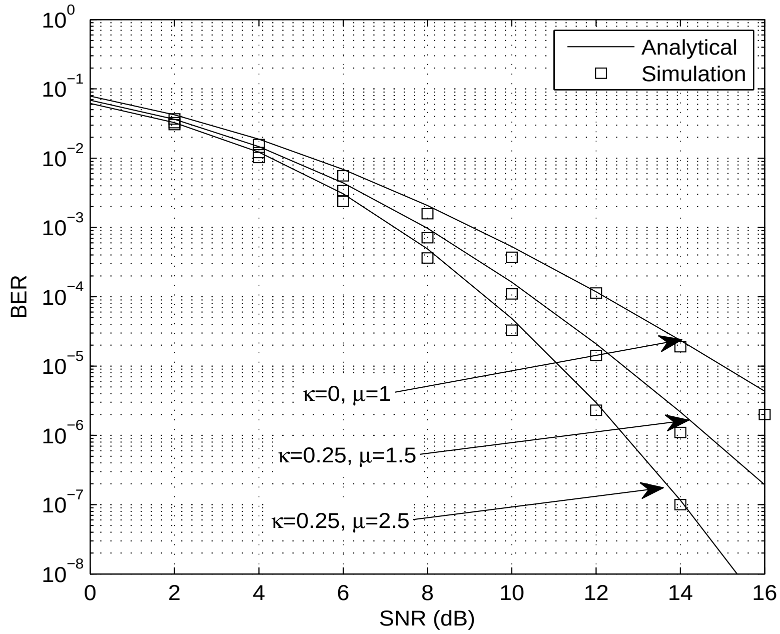


Figure 5.4: BER vs. SNR for two hop TAS CC systems with $L^{(S)} = L^{(R)} = 2$, $L^{(D)} = 1$ and different values of $\kappa$ and $\mu$

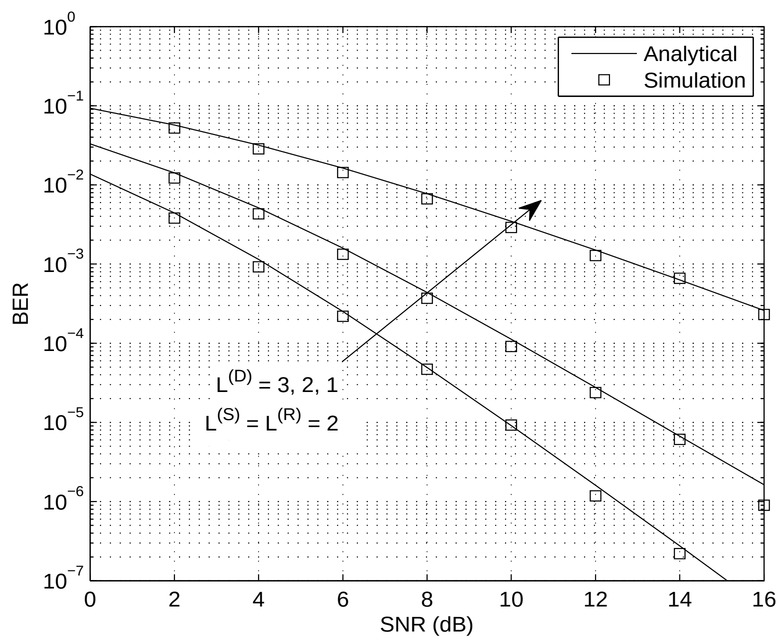


Figure 5.5: BER vs. SNR for two hop TAS CC systems with different number of receiver antennas for $\kappa = 0.25$ and $\mu = 0.5$

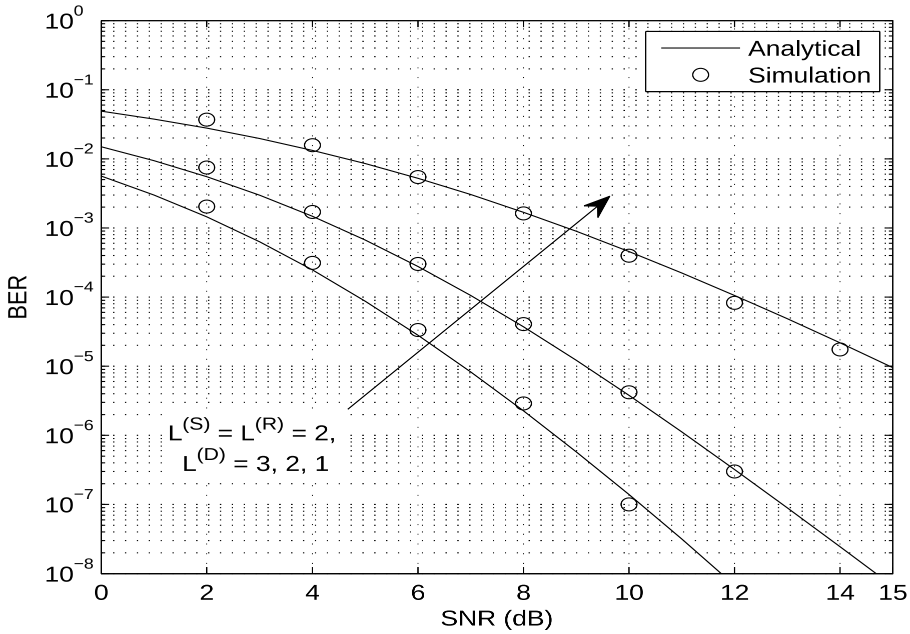


Figure 5.6: BER vs. SNR curve for TAS CC systems with BPSK modulation scheme and different $L^{(D)}$ ($\eta = 1, \mu = 0.5$).

received SNR at D (Relay TAS), TAS only at S to maximize the received SNR at D (Source TAS SD), TAS only at S to maximize the received SNR at R (Source TAS SR), TAS at S and R to maximize the received SNR at D (Source and Relay TAS SD) and TAS at S and R to jointly maximize the received SNR at R and D (Source and Relay TAS SR). In the case of Source and Relay TAS SR, the TAS is performed such that the antenna of S which maximizes the received SNR at R is activated in the first time slot and the antenna of R that maximizes the received SNR at D is activated in the second time slot. It is observed that the case in which TAS is performed at S and R such that the received SNR gets maximized at D gives the best BER performance among the combinations being considered. For simulations we have assumed equal transmit power allocation for node S in first time slot and node R in second time slot and $\bar{\gamma}_{SD} = \bar{\gamma}_{RD} = \bar{\gamma}_{SR}$.

We simulated the two-hop CC system for different number of transmitting and receiving antennas and different values of fading parameters. The results for error rate performance obtained from analytical expressions and Monte Carlo simulations can be observed in Figure 5.3 for TAS CC systems over $\kappa - \mu$ fading channels. It also shows the BER results for single

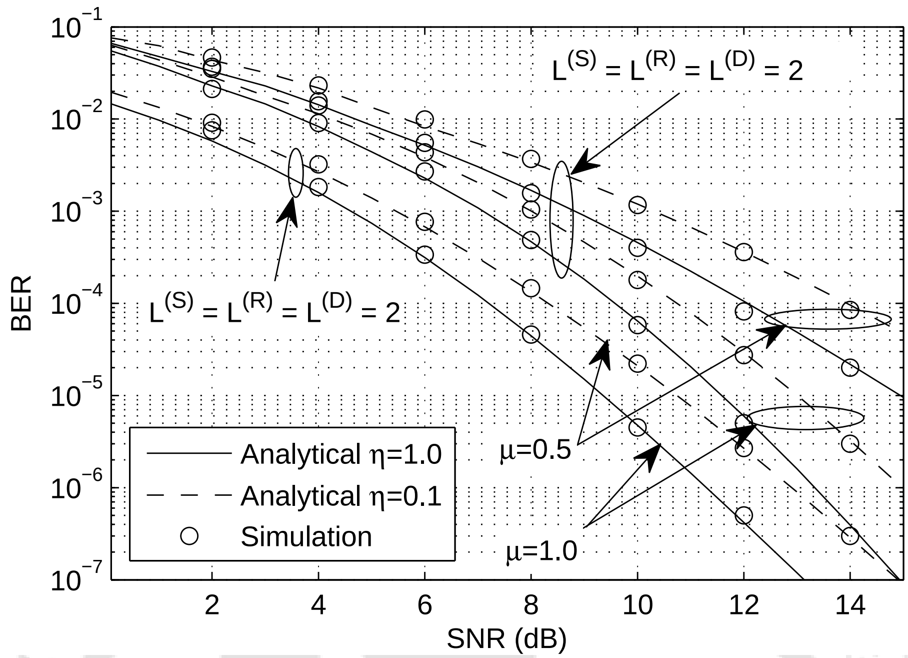


Figure 5.7: BER vs. SNR curve for TAS CC systems with BPSK modulation scheme and different values of fading parameters, $\eta$ and $\mu$.

antenna CC systems. The analytical results are calculated using (5.10) and (5.15) in (5.9). It is observed that CC systems give better performance when transmit antenna selection is used at source and relay nodes for all SNR values. In the same figure, it can be observed that the BER performance is better when the number of transmit antenna increases at source and relay node as well. It is observed that the infinite series involved in probability of error calculation converges fast enough such that first 10 terms give sufficient accuracy (<1% error). However, to maintain accuracy of our numerical results we used first 20 terms of the infinite summation in our numerical results.

Two-hop CC systems over $\kappa-\mu$ fading channels with antenna selection were also simulated to observe the effect of increased strength of LOS component and increasing values of $\mu$ on BER. The simulation and analytical results for different values of fading parameters, $\kappa$ and $\mu$ can be seen in Figure 5.4. An improvement in the BER performance can be observed with increasing values of $\kappa$ and $\mu$.

We have also simulated a two-hop CC systems over $\kappa-\mu$ fading channels to see the effect of

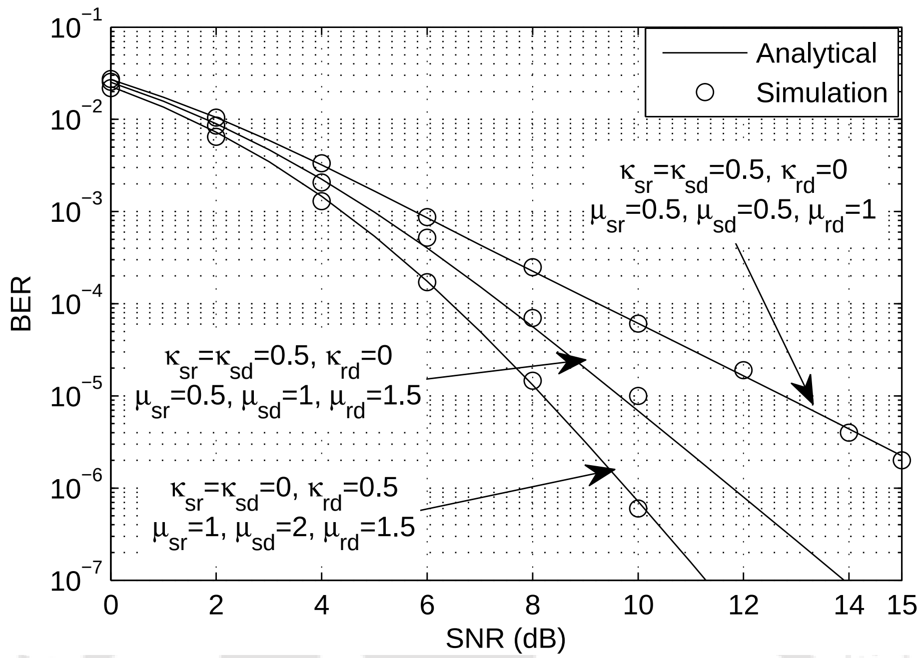


Figure 5.8: BER vs. SNR curve for TAS CC systems with BPSK modulation scheme and different values of fading parameters for different links

increasing number of antennas at the receiver (destination node). The simulation and analytical results are shown in Figure 5.5. It is observed that the performance improves with larger number of antennas at the receiver end with improved slope of BER curve as expected because of higher diversity gain for larger number of antennas.

The analytical and simulation results for two hop CC systems with TAS for different values of $L^{(D)}$ and fading parameters, $\eta = 1$ and $\mu = 0.5$ for BPSK modulation scheme are obtained and can be observed in Figure 5.6. It shows results for $L^{(S)} = L^{(R)} = 2$ and $L^{(D)} = 1, 2$ and 3. A close agreement between analytical and simulation results is observed and the performance improvement for larger number of antennas at the destination is observed on the account of multipath diversity. We show the BER performance of TAS CC systems for different values of fading parameters in Figure 5.7. It is observed that the BER performance degrades for decreasing values of $\eta$ which accounts for severe fading scenario and the BER performance improves for higher values of $\mu$.

The simulations of TAS CC systems with $L^{(S)} = L^{(R)} = L^{(D)} = 2$ are also performed for non identical values of fading parameters of different links. A close agreement between analytical and simulation results can be observed in Fig. 5.8.

## 5.4 Summary

In this chapter, we analyzed the performance of two-hop CC systems with MIMO nodes over generalized $\kappa-\mu$ and $\eta-\mu$ fading channels in which the source and relay nodes select transmit antenna to communicate with destination such that the received SNR at the destination node gets maximized. The analysis is presented for DF relaying protocol and presence of direct link from the source to the destination. We derived expressions for end to end BER with arbitrary transmitting and receiving antennas at each node for BPSK modulation scheme. Simulation results for various fading parameter values have been shown to validate the exactness of analytical expressions. The analytical and Monte Carlo simulation results are found to be in close agreement.

# CHAPTER 6

# MGF BASED APPROXIMATE SER CALCULATION OF SM MIMO SYSTEMS OVER GENERALIZED $\eta-\mu$ AND $\kappa-\mu$ FADING CHANNELS

SM systems also use single transmit antenna at a time to send information from transmitter to receiver. Hence, it is also a technique that overcomes disadvantages of MIMO like complex and bulky hardware due to multiple RF chains and mathematically complex detection processes. A technique called generalized SM has also been proposed in which multiple antennas are activated at a time [13]. Generalized SM gives better spectral efficiency as compared to SM systems but they do not overcome the disadvantages of MIMO systems. Unlike TAS, SM does not require any feedback from receiver to transmitter because the antenna selection in SM does not depend on the channel conditions but on the incoming data bits sequence. This simplifies the overall communication system. In return, the cost has to be paid in terms of diversity gain. SM MIMO systems can achieve diversity gains of the order of number of receiver antennas unlike TAS systems which are known to achieve full diversity order. However, SM MIMO systems can achieve better spectral efficiencies than TAS systems. In addition, it is already established that the detection process at receiver in SM MIMO systems is computationally less demanding as compared to VBLAST and Alamouti STBC schemes in [49].

In this chapter, we analyze the error performance of SM MIMO systems with suboptimal detection scheme over generalized $\eta-\mu$ and $\kappa-\mu$ fading channels for several modulation schemes. Closed form expressions for approximate SER performance of SM MIMO systems are derived for both the generalized fading models using MGF based approach and verified by Monte Carlo simulation results. We have also shown that using the approach of SER analysis over generalized fading channels presented in this chapter, we can analyze SER performance in any classical fading channels. Though the expressions for exact SER of SM MIMO systems over $\eta-\mu$ fading channels have been derived in [57, 74] but they involve evaluation of complicated mathematical functions like Hypergeometric functions. While the expressions for approximate SER derived in this chapter are in the form of elementary functions which are easy to evaluate which justifies the usefulness of our analysis. In addition, we also considered performance analysis of SM MIMO systems over $\kappa-\mu$ fading channels.

Further, this chapter is organized as follows. System model for SM MIMO under consideration is described in the next section. Spatial modulation system transmission, reception and channel models are also explained. In section 6.2, SER calculation using MGF based approach by deriving closed form expressions for approximate SER is explained. SER of SM MIMO systems for various fading channels as special case of $\eta-\mu$ and $\kappa-\mu$ fading channels is given in section 6.3. Results and related discussions of section 6.4 are followed by a brief summary in section 6.5.

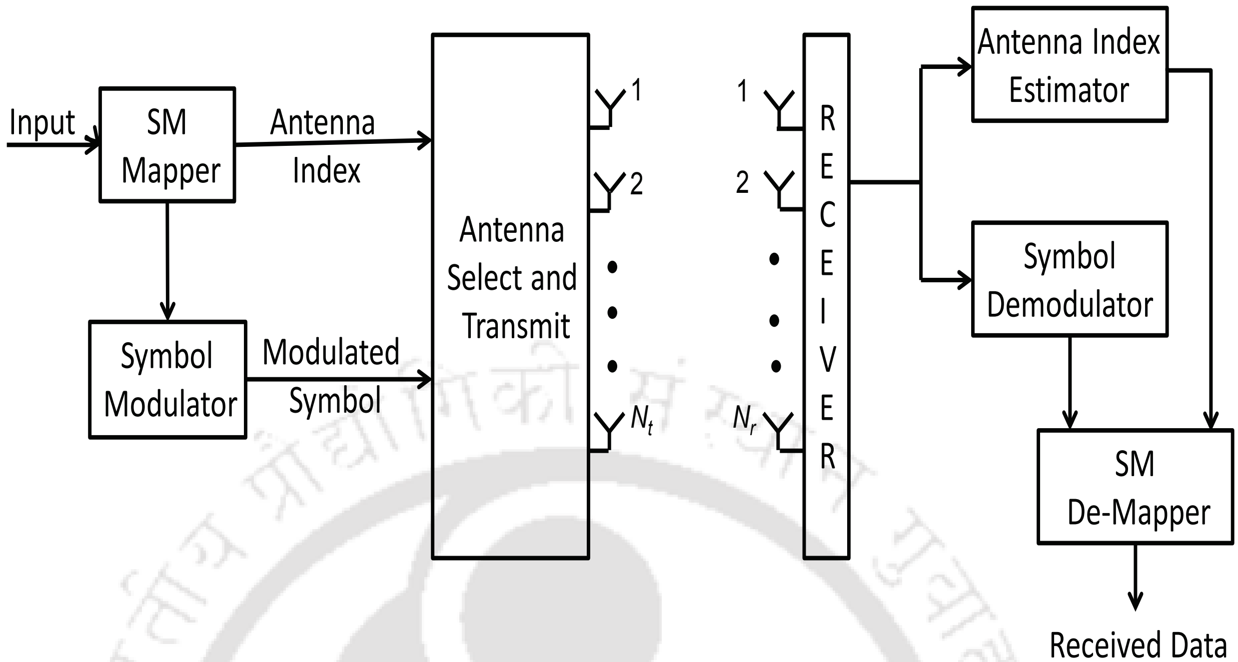


Figure 6.1: System Model of SM MIMO Systems

## 6.1 System Model

### 6.1.1 Spatial Modulation System

In SM, all the information bits are not transmitted physically. A part of information bits is mapped to transmit antenna indices (spatial constellation) and the antenna corresponding to mapped index is used to transmit information bits mapped to signal constellation. A system

Table. 6.1: SM mapping table for 3 bits/s/Hz with BPSK and QAM modulation schemes

| Input Bits | $N_t = 2, M = 4$ (QAM) | | $N_t = 4, M = 2$ (BPSK) | |
|---|---|---|---|---|
| | Antenna Number | Transmit Symbol | Antenna Number | Transmit Symbol |
| 000 | 1 | +1+j | 1 | -1 |
| 001 | 1 | +1-j | 1 | +1 |
| 010 | 1 | -1-j | 2 | -1 |
| 011 | 1 | -1+j | 2 | +1 |
| 100 | 2 | +1+j | 3 | -1 |
| 101 | 2 | +1-j | 3 | +1 |
| 110 | 2 | -1-j | 4 | -1 |
| 111 | 2 | -1+j | 4 | +1 |

model for SM MIMO is given in Figure 6.1. This SM MIMO system model considers an $N_t \times N_r$ MIMO system having $N_t$ antennas at transmitter side and $N_r$ antennas at the receiver side. For M-ary modulation scheme, each block of $\log_2(N_t)+\log_2(M)$ bits of information are mapped by the SM mapper to signal constellation and spatial constellations. $\log_2(N_t)$ bits of each block are mapped to points in spatial constellations which selects the antenna and $\log_2(M)$ bits are mapped in the signal constellation and modulated by symbol modulator using suitable digital modulation scheme. The digitally modulated signal constellation point is then transmitted from the antenna to which spatial constellation point is mapped. Thus, using SM, we effectively get spectral efficiency gain of $\log_2(N_t)$ bits/s/Hz without costing any extra bandwidth or power. Only one antenna depending on the incoming data bits is active at a time overcoming the problems of inter channel interference and the requirement of inter antenna synchronization. These are advantages of SM over V-BLAST and MIMO orthogonal frequency division multiplexing (OFDM) systems. At the receiver, transmit antenna index and transmitted symbol are estimated separately in suboptimal scheme [49]. SM de-mapper appends the estimated transmit antenna and detected symbol accordingly to regenerate the transmitted information bits. The Table 6.1 shows how the bits are mapped in spatial domain and the signal domain for spectral efficiency of 3 bits/s/Hz using BPSK and 4QAM schemes with 4 and 2 transmitter antennas respectively. The transmitted vector will have all zero elements except the one which will transmit the digitally modulated data bits as shown below.

$$\mathbf{x} = \begin{bmatrix} 0 & 0 & \cdots & \underset{k^{th}\ \ posistion}{\underset{\uparrow}{x_q}} & 0 & \cdots & 0 \end{bmatrix}^T \tag{6.1}$$

where $\mathbf{x}$ is the transmitted vector and $x_q$ is the digitally modulated symbol that is to be transmitted from the $k^{th}$ antenna.

### 6.1.2 SM Receiver

At receiver, overall detection needs two estimation processes. One for transmit antenna index estimation and the other for estimation of transmitted symbol. Using ML detection criteria, antenna index can be estimated as [50]

$$\hat{j} = \arg\max_{j} |\boldsymbol{h_j}^H \boldsymbol{y}| \tag{6.2}$$

where $\hat{j}$ is the estimated transmit antenna index, $\boldsymbol{h_j}$ is the $j^{th}$ column of channel matrix $\boldsymbol{H}$ and $\boldsymbol{y}$ is the received signal vector. In the above equation, $(\cdot)^H$ denotes complex conjugate transpose. Estimation of transmitted symbol is the same as the detection process for MRC diversity technique. It can be done using ML decoding technique,

$$x_{\hat{q}} = \arg\min_{q} \| \boldsymbol{h_{\hat{j}}} x_q \|^2 - 2Re\{\boldsymbol{h_j}^H \boldsymbol{y} x_q^*\} \tag{6.3}$$

where $x_{\hat{q}}$ is the estimated symbol from signal constellation space and $x_q$ is the transmitted symbol. The error in any of the detection process affects SER performance of the SM system.

### 6.1.3 Channel Model

In this chapter, we consider i.i.d. $\eta-\mu$ and $\kappa-\mu$ fading channel models to analyze the SER performance of SM systems. $\kappa-\mu$ fading channel distribution can be given as [17]

$$p(\omega) = \mu \left(\frac{1+\kappa}{\Omega_h}\right)^{\frac{\mu+1}{2}} \left(\frac{\omega}{\kappa}\right)^{\frac{\mu-1}{2}} \exp\left(-\frac{\mu(1+\kappa)\omega}{\Omega_h} - \kappa\mu\right) I_{\mu-1}\left(2\mu\sqrt{\frac{\kappa(1+\kappa)\omega}{\Omega_h}}\right) \tag{6.4}$$

where $\Omega_h = E(\omega)$, $E(\cdot)$ is expectation operator.

$\eta-\mu$ fading channel distribution can be given as [17]

$$p(\omega) = \frac{2\sqrt{\pi}h^{\mu}}{\Gamma(\mu)} \left(\frac{\mu}{\Omega_h}\right)^{\mu+\frac{1}{2}} \left(\frac{\omega}{H}\right)^{\mu-\frac{1}{2}} \exp\left(-\frac{2\mu h\omega}{\Omega_h}\right) I_{\mu-\frac{1}{2}}\left(\frac{2\mu H\omega}{\Omega_h}\right) \tag{6.5}$$

The definitions of fading parameters and discussions related to $\eta-\mu$ and $\kappa-\mu$ distributions are given in detail in Chapter 2.

## 6.2 Approximate SER Calculation

Let $P_a$ and $P_s$ be the respective probabilities of error in estimation of transmit antenna index and symbol from signal constellation. Then, assuming the two processes independent, probability of error can be given by [49]

$$P_e = P_a + P_s - P_a P_s \tag{6.6}$$

The process of symbol detection is the same as that for MRC. Using the general expression of conditional SER for any modulation scheme [2]

$$P_e(\gamma) = aQ(\sqrt{b\gamma}) - cQ^2(\sqrt{b\gamma}) \tag{6.7}$$

where $Q(\cdot)$ is Gaussian Q-function, $\gamma$ is instantaneous SNR, $a$, $b$ and $c$ are the modulation dependent parameters given in Table 3.1.

The Gaussian Q-function can be accurately approximated by the sum of exponential functions as [64]

$$Q(x) \cong \frac{1}{12}e^{-\frac{x^2}{2}} + \frac{1}{4}e^{-\frac{2x^2}{3}} \tag{6.8}$$

The approximated and exact values of Q-function are plotted in Figure 4.1. It is observed that (6.8) gives a very accurate approximation for all values of $x$. For $x \geq -2$ dB, the approximated and the exact values of Q-function are almost same.

Averaging the SER with respect to PDF of SNR, the average probability of error for MRC symbol detection can be given by

$$\begin{aligned} P_s \cong & a\left\{\frac{1}{12}MGF\left(\frac{b\overline{\gamma}}{2}\right) + \frac{1}{4}MGF\left(\frac{2b\overline{\gamma}}{3}\right)\right\} \\ & -\frac{c}{4}\left(\frac{1}{36}MGF\left(b\overline{\gamma}\right) + \frac{1}{4}MGF\left(\frac{4b\overline{\gamma}}{3}\right) + \frac{1}{6}MGF\left(\frac{7b\overline{\gamma}}{6}\right)\right) \end{aligned} \tag{6.9}$$

where $\overline{\gamma}$ is average SNR and $MGF(\cdot)$ is the moment generating function.

MGF of $\kappa-\mu$ distribution is given by [75]

$$MGF_{\kappa-\mu}(s) = \left(\frac{\mu(1+\kappa)}{\mu(1+\kappa)+s}\right)^{\mu} \cdot e^{\left(\frac{(\mu)^2\kappa(1+\kappa)}{\mu(1+\kappa)+s}-\mu\kappa\right)} \tag{6.10}$$

MGF of $\eta-\mu$ distribution is given by [75]

$$MGF_{\eta-\mu}(s) = \left(\frac{4\mu^2 h}{(2\mu(h-H)+s)(2\mu(h+H)+s)}\right)^{\mu} \tag{6.11}$$

In the antenna index estimation, we have $\boldsymbol{h_j^H y}$ for $j = 1,2,\ldots,N_t$ of which all will be noise except the one that corresponds to actual transmit antenna index. The conditional pairwise error probability can be calculated as [50]

$$P\left(x_{jq} \to x_{\hat{j}q}|\mathbf{H}\right) = P\left(d_{jq} > d_{\hat{j}q}|\mathbf{H}\right) = Q\left(\sqrt{\gamma_{eff}}\right) \tag{6.12}$$

where $P\left(x_{jq} \to x_{\hat{j}q}|\mathbf{H}\right)$ denotes the conditional probability of detecting $\hat{j}^{th}$ antenna index when symbol $x_q$ transmitted from antenna $j$. Unconditional average probability of error can be calculated by averaging the conditional pairwise error probability. For statistically independent $\eta-\mu$ and $\kappa-\mu$ MIMO channels, it can be shown that $\gamma_{eff}$ is $\eta-N_r\mu$ and $\kappa-N_r\mu$ distributed respectively [19, 57] and the average PEP can be given by

$$P_a = APEP(\overline{\gamma}) \cong \frac{1}{12}MGF\left(\frac{\overline{\gamma}}{2}\right) + \frac{1}{4}MGF\left(\frac{\overline{\gamma}}{3}\right) \tag{6.13}$$

APEP is calculated by approximating the Q-function by sum of exponential function as in (6.8) and averaging it over the PDF of $\kappa-N_r\mu$ and $\eta-N_r\mu$ distributions. MGFs of $\kappa-N_r\mu$ and $\eta-N_r\mu$ can be obtained from (6.11) and (6.10) respectively. The approximate unconditional probability of symbol error can be calculated by substituting (6.9) and (6.13) in (6.6).

## 6.3 SER of SM MIMO Systems for Various Fading Channels

In section 6.2, we analyzed SER performance of SM MIMO systems over generalized $\eta-\mu$ and $\kappa-\mu$ fading channels. The advantage of analyzing SER performance over generalized fading channels is that by taking special cases of the generalized fading channels we can evaluate the performance of the system in many well known fading channels.

### 6.3.1 Rayleigh Fading

Rayleigh fading channels can be represented as a special case of $\kappa-\mu$ and $\eta-\mu$ fading channel for ($\kappa=0,\ \mu=1$) and ($\eta=1,\ \mu=0.5$) respectively. $\eta=1$ implies that $h$ and $H$ in (6.5) bear the values 1 and 0 respectively. Using these particular values of $\kappa$ and $\mu$ in (6.10) and $\eta,\ \mu,\ h$ and $H$ in (6.11), we get the following expression which is the same as the MGF of Rayleigh distribution [61].

$$MGF_{Rayl}(\gamma)=\frac{1}{1+\gamma} \tag{6.14}$$

The SER performance in Rayleigh fading can be alternatively evaluated by substituting (6.14) in (6.9) and (6.13).

### 6.3.2 Rician Fading

Rician fading channels are suitable for LOS scenario in which there is a direct path from transmitter to receiver and many multipath components. Rician distribution can be modeled as a special case of $\kappa-\mu$ distribution for $\kappa=K$ and $\mu=1$ where $K$ is the ratio of power in LOS component to average power of scattered components. Using the values $\kappa=K$ and $\mu=1$ in (6.10), we can get the following expression which is the same as the MGF of Rician distribution [61].

$$MGF_{Rice}(\gamma)=\frac{1+K}{1+K+\gamma}e^{-\frac{K\gamma}{1+K+\gamma}} \tag{6.15}$$

The SER performance in Rician fading can be alternatively evaluated by substituting (6.15) in (6.9) and (6.13).

### 6.3.3 Nakagami-m Fading

Nakagami-m fading channels can also be modeled as special cases of the generalized fading channels. ($\kappa = 0,\ \mu = m$) and ($\eta = 1,\ \mu = m/2$) models Nakagami-m fading channel as a special case of $\kappa-\mu$ and $\eta-\mu$ fading channels respectively. Using these values of fading parameters in (6.10) and (6.11), we get the following expression which is the same as the MGF of Nakagami-m distribution [61].

$$MGF_{N-m}(\gamma) = \left(\frac{m}{m+\gamma}\right)^{m} \tag{6.16}$$

### 6.3.4 Nakagami-q Fading

Nakagami-q fading channels can be modeled as a special case of $\eta-\mu$ fading channels. ($\eta = q^2,\ \mu = 0.5$) models Nakagami-q fading channel as a special case of $\eta-\mu$ fading channel. From (6.11), for Nakagami-q fading, we get the following equation which is the MGF of Nakagami-q distribution [61].

$$MGF_{N-q}(\gamma) = \frac{(1+q^2)}{\left[(1+q^2)^2(1+2\gamma)+4q^2\gamma^2\right]^{0.5}} \tag{6.17}$$

Substituting (6.16) or (6.17) in (6.9) and (6.13), the SER performance can be evaluated over Nakagami-m or Nakagami-q fading respectively.

## 6.4 Results and Discussions

We performed simulations of $2\times2$ and $2\times4$ SM MIMO systems with 4-QAM modulation and 3bits/s/Hz. The SM MIMO systems were simulated for different special cases of generalized $\kappa-\mu$ and $\eta-\mu$ fading channels. Average SER values for different SNR levels are obtained from the simulations and plotted along with the approximate analytical SER. Figure 6.2 shows the results for $2\times2$ SM MIMO system considering Rician fading channel as special case of

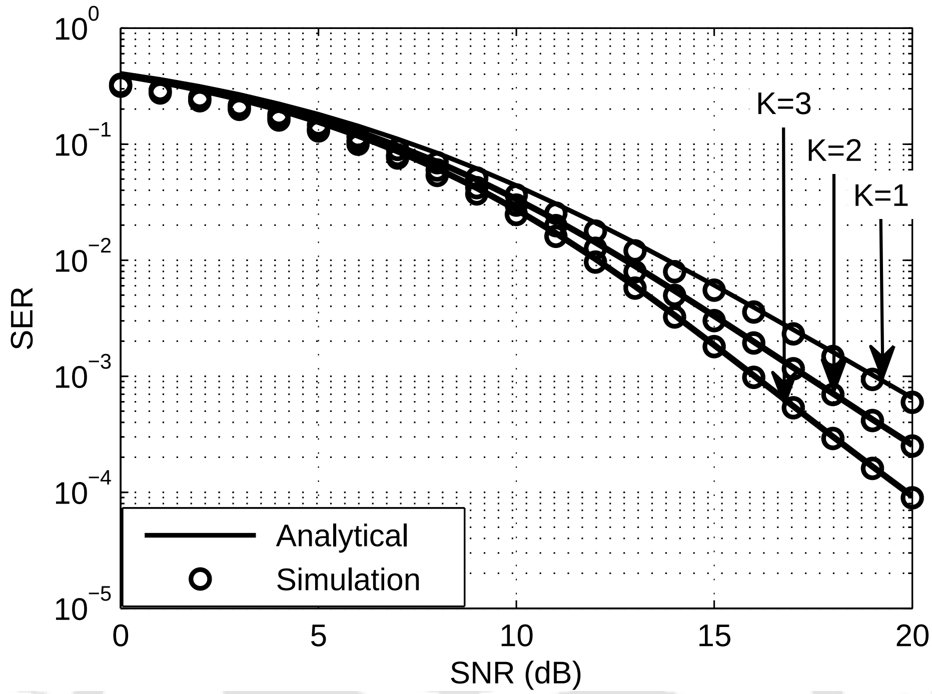


Figure 6.2: SER vs SNR (dB) for 2×2 SM MIMO system considering Rician fading as special case of $\kappa-\mu$ channels for $\kappa = K$ and $\mu = 1$

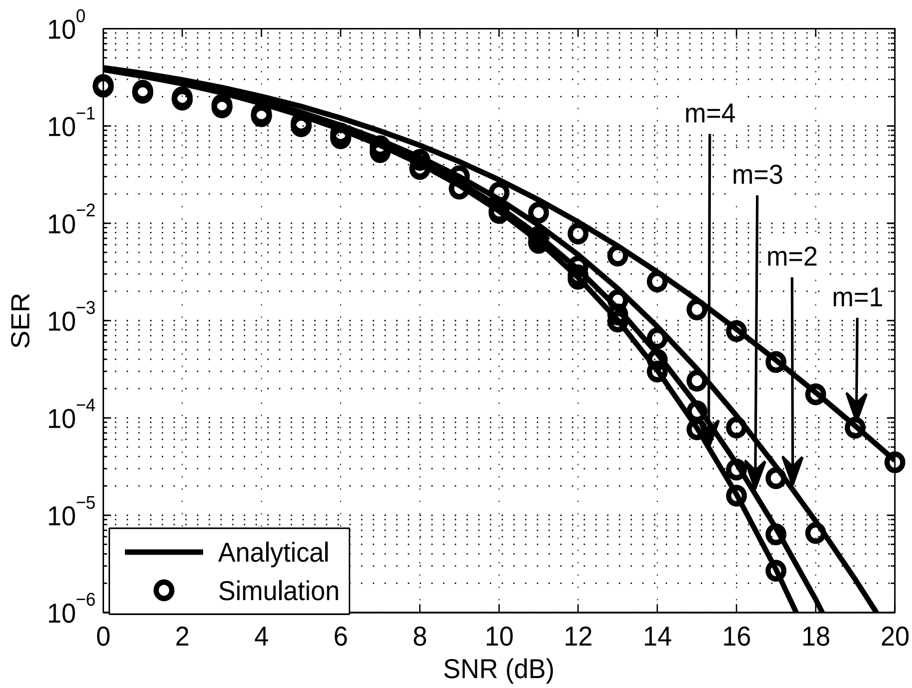


Figure 6.3: SER vs SNR (dB) for 2×4 SM MIMO system considering Nakagami-m fading as special case of $\kappa-\mu$ channels for $\kappa = 0$ and $\mu = m$

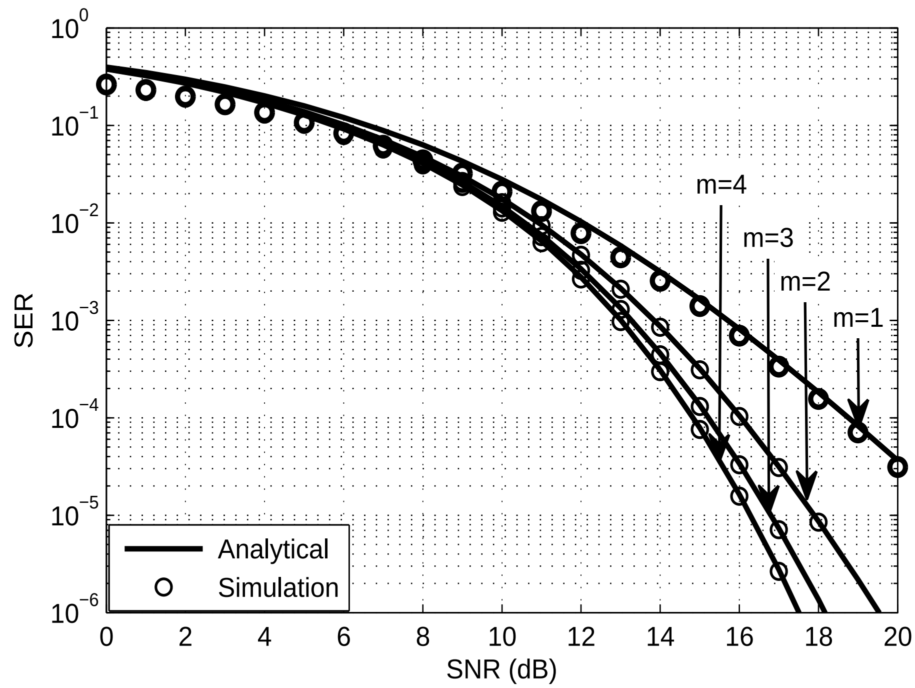


Figure 6.4: SER vs SNR (dB) for 2×4 SM MIMO system considering Nakagami-m fading as special case of $\eta-\mu$ channels for $\eta=1$ and $\mu=m/2$

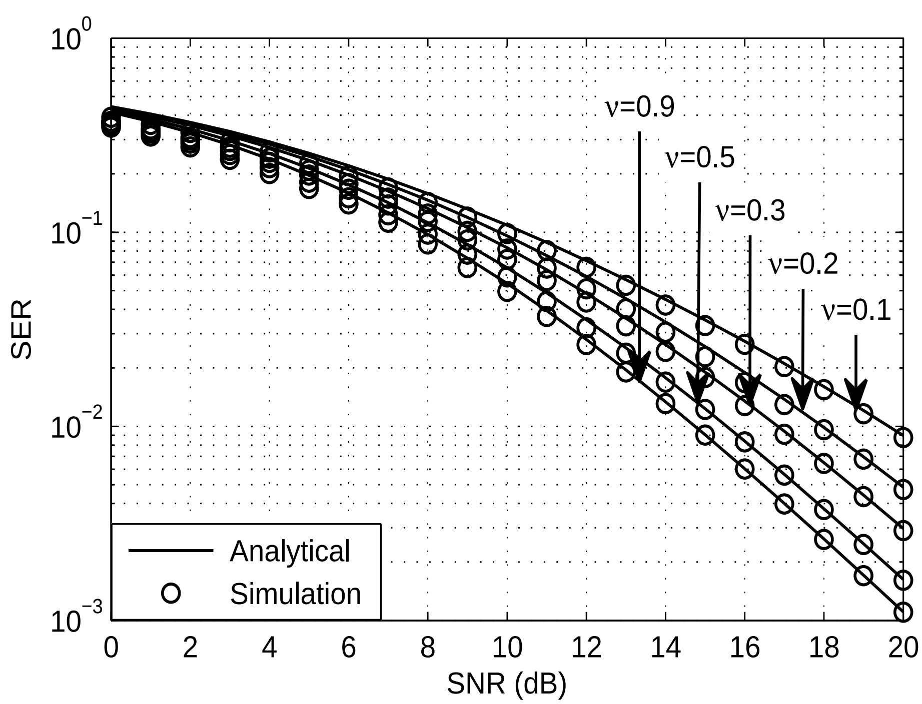


Figure 6.5: SER vs SNR (dB) for 2×2 SM MIMO system considering Nakagami-q fading as special case of $\eta-\mu$ channels for $\eta=\nu^2$ and $\mu=0.5$

$\kappa-\mu$ channel considering the values $\mu=1$ and $\kappa=K$. We have simulated the system for $K=1,\ 2$ and 3. The improved performance with increasing $K$ is observed. This improvement in the performance is on the account of stronger LOS component for higher values of $K$. However, for optimal detection scheme discussed in [50], the performance would degrade with stronger LOS components as observed in [76].

Figure 6.3 shows the SER vs SNR plot for Nakagami-m fading environment as special case of $\kappa=0$ and $\mu=m$. It also includes results for $m=1$ which represents Rayleigh fading channel as a special case of Nakagami-m fading channel and hence that of $\kappa-\mu$ fading channel. Figure 6.4 shows the performance of $2\times4$ SM MIMO system in Nakagami-m fading channels as a special case of generalized $\eta-\mu$ channels. The similarity in results shown in Figure 6.3 and Figure 6.4 show that the Nakagami-m fading environment can be well represented as special case of $\kappa-\mu$ and $\eta-\mu$ fading models. In both the figures, it is also observed that the SER performance improves with increasing values of fading parameter $m$ of Nakagami-m fading or $\mu$ of $\eta-\mu$ and $\kappa-\mu$ fading channels. This performance improvement is because of the fact that $\mu$ stands for the number of multipath clusters in the received signal [56, 57].

Nakagami-q or Hoyt distribution is a special case of generalized $\eta-\mu$ distribution for $\mu=0.5$ and $\eta=\nu^2$, where $\nu$ is the Nakagami-q fading parameter. The $2\times2$ SM MIMO system was simulated for plotting the SER Vs. SNR for Hoyt fading conditions. The results can be seen in Figure 6.5. The degradation in SER performance for decreasing values of $\nu$ is observed on the account of increased severity in the fading for smaller values of $\nu$ or $\eta$. It has been observed that in all the plots of Figures 6.2-6.5, the analytical results are in close agreement with the Monte Carlo simulation results and the approximated results are almost exact when SER$\leq 10^{-2}$. This validates the accuracy of the proposed approximate SER analysis.

## 6.5 Summary

In this chapter, we obtained closed form expressions for approximate SER performance of SM MIMO systems in generalized $\kappa-\mu$ and $\eta-\mu$ fading environments for several modulation schemes. The analytical closed form expressions of SER obtained could be employed for performance analysis of SM MIMO systems over any fading channel as long as the MGF of the fading channel statistics is available. Using the developed closed form expressions, the performance of SM MIMO systems for various special cases of generalized $\kappa-\mu$ and $\eta-\mu$ channels such as Nakagami-m, Rician, Nakagami-q and Rayleigh fading channels are obtained. In order to verify the accuracy of the closed form expression, simulations were carried out assuming 4-QAM modulation for symbol transmission and considering 2 transmit antennas to achieve transmission rate of 3 bits/s/Hz. The analytical results are in close agreement with Monte Carlo simulations carried out for different values of fading parameters and different number of antennas at the receiver.

# Chapter 7

# Transmit Antenna Selection in Spatial Modulation Systems

In the previous chapter, we discussed that SM MIMO systems transmit information from single antenna at a time and the index of transmit antenna is also a part of information. One of the possible problems with such SM MIMO systems is that the link of the antenna index used for communication may be completely down at certain time instant. It may result in loss of the complete block of $\log_2(N_t) + \log_2(M)$ bits of information. Keeping in consideration the recent advances of wireless communication systems, large MIMO systems and massive MIMO systems which contain hundreds and thousand of antennas, this amount of information might be very large [62, 77]. This problem can be overcome if one selects $S$ antennas out of $N_t$ transmitting antennas with the good links and apply SM on those $S$ selected antennas at the transmitter. Some of the researchers have worked in this direction and combined SM and TAS MIMO systems [16, 58]. We refer to those combined systems as TAS SM MIMO systems in the subsequent discussion of this chapter. In [16], it is shown that TAS SM MIMO systems give better BER performance than the conventional SM MIMO systems. In [58], N. Pillay, et. al. rectified the errors in formulation and Monte Carlo simulations of [16]. In [16, 58], Euclidean Distance Optimized Antenna Selection (EDAS) and Capacity Optimized Antenna Selection (COAS) are combined with SM MIMO system and SER performance results of simulation are reported. However, analytical results have not been reported.

In this chapter, we derived closed form expression for outage probability of TAS SM MIMO systems in flat Rayleigh fading environment. Our antenna selection is done based on Maximum Received Power (MRP) of useful signal which is equivalent to antenna selection at transmitter based on maximum received SNR. Analytical results are validated using Monte Carlo simulations and they are in close agreement.

The rest of the chapter is organized as follows: System model is described in the next section. In section 7.2, the derivation of PDF of the received SNR is elaborated. Then, closed form expression of OP of TAS SM MIMO systems is derived in section 7.3. Simulation and analytical results are shown and the chapter is summarized in section 7.4 and section 7.5 respectively.

## 7.1 System Model

We consider MIMO system with $N_t$ transmit and $N_r$ receive antennas with flat Rayleigh fading conditions. $S$ antennas are selected at transmitter which maximize the total received signal power $(S \leq N_t)$. For spatial modulation, $S$ has to satisfy the condition $S = 2^m$, where $m$ is a positive integer. Among $S$ selected antennas, an antenna is chosen at a time for symbol transmission according to incoming data bits as discussed in the previous chapter (see Table 6.1). The MRC combining is assumed at the receiver. The system is referred as $(N_t/S;N_r)$ MRP TAS SM MIMO system.

At any instant, if the symbol $x_q$ is transmitted from the single chosen antenna, the received signal vector is same as that for MRC receiver diversity. It can be given as:

$$\boldsymbol{y} = \boldsymbol{h_j} x_q + \boldsymbol{n} \tag{7.1}$$

where, $\boldsymbol{h_j}$ is the $j^{th}$ column of $N_r \times S$ channel matrix whose elements $h_{j,i}$ ($i = 1,2,\ldots,S$ and $j = 1,2,\ldots,N_r$) are assumed to be independent and identically Rayleigh distributed prior to antenna selection and $\boldsymbol{n}$ is an $N_r \times 1$ noise vector. The noise is assumed to be complex Gaussian distributed with variance $N_0$. It is assumed that either the set of $S$ antennas that maximize received useful signal power or channel state information is available at the transmitter through a feedback path from the receiver.

## 7.2 Order Statistics of Fading Coefficients

Antenna selection is done based on the magnitude of the parameter, $A_j$ [1]

$$A_j = \sum_{i=1}^{N_r} \left|h'_{i,j}\right|^2 \tag{7.2}$$

where each $h'_{i,j}$ ($i = 1, 2, ..., N_r$ and $j = 1, 2, ..., N_t$) is an entry of the $N_r \times N_t$ channel matrix **H**.

In Rayleigh MIMO channel, each $A_j$ is a sum of the squares of $2N_r$ Gaussian distributed random variables with zero mean which can be represented by a non-central Chi-squared distributed random variable with $2N_r$ degrees of freedom. So, the PDF of $A_j$ can be given as follows [73] :

$$f_{A_j}(x) = \frac{x^{N_r-1} e^{-x}}{\Gamma(N_r)}, x \geq 0 \tag{7.3}$$

and the CDF is given by

$$F_{A_j}(x) = 1 - e^{-x} \sum_{i=0}^{N_r-1} \frac{x^i}{i!}, x \geq 0 \tag{7.4}$$

To select $S$ antennas that give the maximum received power, $A_j$s are rearranged in ascending order and $S$ antennas that correspond to the highest values of $A_j$ are selected. According to order statics, the PDF of $A_{(\ddot{r})}$ such that $A_{(1)} \leq A_{(2)} \leq \cdots \leq A_{(N_t)}$ can be given by [59]

$$f_{A_{(\ddot{r})}}(x) = \frac{1}{B(\ddot{r}, N_t - \ddot{r} + 1)} \left\{F_{A_j}(x)\right\}^{\ddot{r}-1} \left\{1 - F_{A_j}(x)\right\}^{N_t - \ddot{r}} f_{A_j}(x) \tag{7.5}$$

where $\ddot{r} = N_t - S + 1$ and $B(.,.)$ is the Beta function.

So, the PDF of the received SNR can be given as

$$f_{\gamma}^{\ddot{r}}(x) = \frac{1}{N_t - \ddot{r} + 1} \sum_{i=\ddot{r}}^{N_t} \frac{1}{B(i, N_t - i + 1)} \left\{F_{A_j}(x)\right\}^{i-1} \left\{1 - F_{A_j}(x)\right\}^{N_t - i} f_{A_j}(x) \tag{7.6}$$

Substituting (7.3) and (7.4) in (7.6), the PDF of instantaneous received SNR ($\gamma_i$) can be given by

$$f_{\gamma_i}^{\ddot{r}}(x) = \frac{1}{(N_t - \ddot{r} + 1)} \sum_{i=\ddot{r}}^{N_t} \frac{1}{B(i, N_t - i + 1)} \left\{1 - e^{-x} \sum_{i=0}^{N_r - 1} \frac{x^i}{i!}\right\}^{i-1} \left\{e^{-x} \sum_{i=0}^{N_r - 1} \frac{x^i}{i!}\right\}^{N_t - i} \frac{x^{N_r - 1} e^{-x}}{\Gamma(N_r)}$$

$$= \frac{1}{(N_t - \ddot{r} + 1)\Gamma(N_r)} \sum_{i=\ddot{r}}^{N_t} \sum_{j=0}^{i-1} \sum_{t=0}^{\ddot{M}} \frac{\begin{pmatrix} i-1 \\ j \end{pmatrix} (-1)^j C_t(j, N_r)}{B(i, N_t - i + 1)} x^{N_r + t - 1} e^{-x(N_t - i + j + 1)} \tag{7.7}$$

where $\ddot{M} = (N_r - 1)(N_t - i + j)$ and $C_t(j, N_r)$ is the coefficient of $x^t$ in the expansion of

$$\left(\sum_{l=0}^{N_r - 1} \frac{x^l}{l!}\right)^{N_t - i + j} \tag{7.8}$$

## 7.3 Outage Probability

In this section, a closed form expression of outage probability for SM MIMO system with MRP TAS is derived considering Rayleigh fading conditions. The outage probability for an $(N_t/S; N_r)$ MRP TAS SM MIMO system can be given as

$$P_{out}(\overline{\gamma}, R) = \mathrm{P}_r \left\{\gamma_i < \frac{2^R - 1}{\overline{\gamma}}\right\} \tag{7.9}$$

where $R$ is the given rate of transmission and $\overline{\gamma}$ is the average SNR.

Assuming $\gamma_{th} = \frac{2^R - 1}{\overline{\gamma}}$, the outage probability in (7.9) can be given by

$$P_{out}\left(\overline{\gamma},R\right)=\frac{1}{\left(N_t-\ddot{r}+1\right)\Gamma\left(N_r\right)}\sum_{i=\ddot{r}}^{N_t}\frac{1}{B\left(i,N_t-i+1\right)}\sum_{j=0}^{i-1}\binom{i-1}{j}(-1)^j \times\sum_{t=0}^{\ddot{M}}C_t\left(j,N_r\right)\int_0^{\gamma_{th}}x^{N_r+t-1}e^{-x(N_t-i+j+1)}dx \tag{7.10}$$

Thus, the closed form expression for outage probability obtained after evaluating the integral in (7.10) is as given below [63]

$$P_{out}\left(\overline{\gamma},R\right)=\frac{1}{\left(N_t-\ddot{r}+1\right)\Gamma\left(N_r\right)}\sum_{i=\ddot{r}}^{N_t}\frac{1}{B\left(i,N_t-i+1\right)}\sum_{j=0}^{i-1}\binom{i-1}{j}(-1)^j \times\sum_{t=0}^{\ddot{M}}C_t\left(j,N_r\right)\frac{\gamma_{inc}\left(N_r+t,\gamma_{th}\left(N_t-i+j+1\right)\right)}{\left(N_t-i+j+1\right)^{(N_r+t)}} \tag{7.11}$$

The outage probability of SM MIMO systems without TAS in Rayleigh fading channels, $P_{out}(\overline{\gamma},R)_{noTAS}$ can be given as

$$\begin{aligned}P_{out}(\overline{\gamma},R)_{noTAS}&=\int_0^{\gamma_{th}}\frac{x^{N_r-1}e^{-x}}{\Gamma\left(N_r\right)}dx\\&=1-e^{-\gamma_{th}}\sum_{i=0}^{N_r-1}\frac{\gamma_{th}{}^i}{i!}\end{aligned} \tag{7.12}$$

The outage probabilities of MRP TAS SM MIMO systems with and without antenna selection are compared by evaluating (7.11) and (7.12) in the next section.

## 7.4 Simulation Results

MRP TAS SM MIMO system was simulated for $N_t=4,6$, $S=2$ and $N_r=2$ assuming 2 bits/s/Hz with BPSK modulation. The results of simulation are compared with the analytical results in

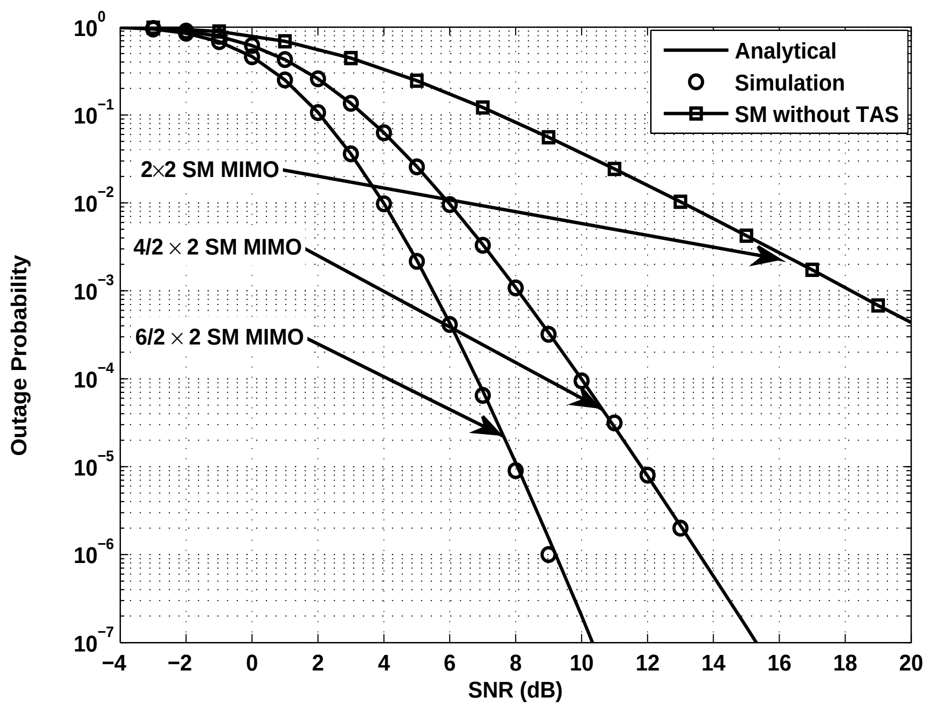


Figure 7.1: Outage Probability vs. SNR curve for MRP TAS SM MIMO systems with antenna selection (R=2 bits/s/Hz).

Figure 7.1. The results are also shown for an SM MIMO system without implementation of antenna selection. The improvements in the results are obtained using TAS with SM systems in the OP with added cost of larger number of antennas at transmitter and a feedback link that conveys channel state information or the set of antennas to be used for SM from receiver to the transmitter. Note that, with these additional complexities in the system, MRP TAS SM MIMO systems achieve diversity gain as obtained in [16].

## 7.5 Summary

A closed form expression for outage probability of MRP TAS SM MIMO systems is derived and validated using the simulation results. A significant improvement in the outage probability is observed for MRP TAS SM MIMO systems over conventional SM MIMO systems at the cost of larger number of antennas at the transmitter.

# CHAPTER 8

# CONCLUSIONS AND FUTURE WORK

In this thesis, we presented our work related to performance analysis of TAS and SM based MIMO wireless communication systems with application of TAS on MIMO CC systems. In this chapter, we summarize the thesis in the form of conclusions and also provide some suggestions for future work based on the presented works.

## 8.1 Conclusions

A brief summary of conclusions of the thesis are as follows.

In this thesis, we used CDF and MGF based methods to evaluate error performances of TAS and SM based MIMO wireless communication systems. CDF based error performance analysis is done for TAS/MRC systems over $\kappa-\mu$ fading channels and MGF based error performance analysis is done for TAS/MRC systems over $\eta-\mu$ fading channels and SM MIMO systems over $\kappa-\mu$ and $\eta-\mu$ fading channels. The expressions derived for TAS/MRC are also applicable to performance analysis of TAS/SC systems. We also presented the performance analysis of two hop CC systems with TAS at source and relay. The application of TAS on SM systems is studied and performance is evaluated in terms of OP. The specific contributions of the thesis are enlisted below.

1. Performance analysis of TAS/MRC systems over $\kappa-\mu$ fading channels

   (a) Expressions are derived for OP, SER and ergodic capacity. The expressions of OP are shown to be compact. SER expressions have been derived using CDF based approach.

   (b) The important observation is that the ergodic capacity degrades with improved LOS component.

2. Performance analysis of TAS/MRC systems over $\eta-\mu$ fading channels: expressions are derived for SER and ergodic capacity. SER expressions have been derived using MGF based approach.

3. Application of TAS to two hop CC systems and their performance analysis

   (a) Expressions are derived for BER of TAS based CC systems over $\kappa-\mu$ and $\eta-\mu$ fading channels using the analysis of TAS/MRC done in chapter 3 and chapter 4.

   (b) For error performance of DF CC systems, TAS at source and relay such that SNR at destination gets maximized in presence of direct link from source to destination was taken into consideration.

4. Approximate SER of SM MIMO systems over $\kappa-\mu$ and $\eta-\mu$ fading channels

   (a) Closed form expressions are presented in the form of elementary functions which are easy to evaluate compared to existing expressions for exact SER.

   (b) SER of SM MIMO systems over various fading channels has been presented as special cases of $\kappa-\mu$ and $\eta-\mu$ fading channels

5. Application of TAS to SM MIMO systems: Closed form expression for OP of SM MIMO systems with TAS based on MRP over i.i.d. Rayleigh fading channels is derived.

All the analytical expressions have been supported with results of Monte Carlo simulations. In each case, Monte Carlo simulation results are in closed agreement with the analytical results.

For infinite series expressions, it has been observed and verified that they can be evaluated by truncating to finite number of terms for sufficient accuracy in the results of their numerical evaluations.

## 8.2 Suggestions for Future Work

Some of the possible directions that can be taken up as extensions of this work are suggested as follows.

- Order statistics of correlated $\kappa - \mu$ and/or $\eta - \mu$ fading distributions and performance analysis of TAS/MRC systems.
- Performance analysis of multi-hop TAS CC systems with DF and/or AF forwarding protocols at relays
- Analytical expression for BER of MRP TAS SM MIMO systems may be derived for Rayleigh fading channels and can be extended to generalized fading channels.
- Performance analysis of TAS and/or SM based MIMO systems can be done in interference limited conditions.

# Appendix A

# Supplementary Materials

## A.1 Derivation of (3.8)

In (3.7), take the substitution

$$t = 1 - Q_{\mu}\left(\sqrt{2\kappa\mu}, \sqrt{\frac{2\mu(1+\kappa)x}{\overline{\gamma}}}\right) \quad \text{(A.1)}$$

Using (3.3) and (3.4) and the relation between PDF and CDF, we get

$$dt = \frac{\mu(1+\kappa)^{\frac{\mu+1}{2}} x^{\frac{\mu-1}{2}}}{\kappa^{\frac{\mu-1}{2}} \overline{\gamma}^{\frac{\mu+1}{2}} e^{\mu\kappa}} e^{-\frac{\mu(1+\kappa)x}{\overline{\gamma}}} I_{\mu-1}\left(2\mu\sqrt{\frac{\kappa(1+\kappa)x}{\overline{\gamma}}}\right) dx \quad \text{(A.2)}$$

Then, ignoring the limits of integral in (3.7) for a while, the indefinite integral is of the form

$$\int N t^{N-1} dt = t^{N}$$

Equation (3.8) can be obtained by putting the substituted value of $t$ and the limits of the integration in the above expression.

## A.2 Derivation of $I_2$ (4.24)

$$I_2 = \frac{2cN}{\pi}\ell\sum_{i,j}\frac{2^{j_\Sigma}H^{2i_\Sigma}q\Gamma(r)\int_0^{\frac{\pi}{4}}\left(\bar{\lambda}+\frac{b}{2\sin^2\theta}\right)^{-r}d\theta}{h^{N\mu+2i_\Sigma}\prod_{p=1}^{N}\left(i_p!\Gamma(\mu')\right)\prod_{p=1}^{N-1}\left((\mu+i_p)(2\mu')_{j_p}\right)} \tag{A.3}$$

The integral in the above expression is of the form

$$\begin{aligned} I &= \int_0^{\frac{\pi}{4}}\left(\bar{\lambda}+\frac{b}{2\sin^2\theta}\right)^{-r}d\theta \\ &=\bar{\lambda}^{-r}\int_0^{\frac{\pi}{4}}\left(\frac{\sin^2\theta}{\sin^2\theta+\zeta}\right)^{r}d\theta \end{aligned} \tag{A.4}$$

Substituting $\sin^2\theta = t/2$ in the above integral, the integral limits becomes 0 to 1 and

$$d\theta = \frac{dt}{4\sqrt{\frac{t}{2}}\sqrt{1-\frac{t}{2}}}$$

Now, the integral can be represented as

$$\begin{aligned} I &=\bar{\lambda}^{-r}\int_0^{1}\left(\frac{\frac{t}{2}}{\frac{t}{2}+\zeta}\right)^{r}\frac{dt}{4\sqrt{\frac{t}{2}}\sqrt{1-\frac{t}{2}}} \\ &=\frac{\bar{\lambda}^{-r}}{4}\int_0^{1}\left(\frac{t}{t+2\zeta}\right)^{r}\frac{dt}{\sqrt{\frac{t}{2}}\sqrt{1-\frac{t}{2}}} \\ &=\frac{\bar{\lambda}^{-r}}{2\sqrt{2}(2\zeta)^{r}}\int_0^{1}t^{r-\frac{1}{2}}\left(1+\frac{t}{2\zeta}\right)^{-r}\left(1-\frac{t}{2}\right)^{-\frac{1}{2}}dt \end{aligned} \tag{A.5}$$

Using [66, (7.2.4.42)], the above integral can be obtained in the form of Appell Hypergeometric function as

$$I = \frac{\bar{\lambda}^{-r}}{2\sqrt{2}(2\zeta)^{r}}F_A^{(1)}\left(r+\frac{1}{2},\frac{1}{2},r,r+\frac{3}{2},\frac{1}{2},-\frac{1}{2\zeta}\right) \tag{A.6}$$

Expression (4.24) can be obtained by using the above solution of integral in (4.23).

# REFERENCES


[1] Z. Chen, J. Yuan, and B. Vucetic, "Analysis of transmit antenna selection/maximal-ratio combining in rayleigh fading channels," *IEEE Transactions on Vehicular Technology*, vol. 54, no. 4, pp. 1312 –1321, July 2005.

[2] Y. Chen and C. Tellambura, "Distribution functions of selection combiner output in equally correlated Rayleigh, Rician, and Nakagami-m fading channels," *IEEE Transactions on Communications*, vol. 52, no. 11, pp. 1948–1956, 2004.

[3] A. Goldsmith, *Wireless Communications*, Cambridge University Press, 2005.

[4] G. Foschini and M. Gans, "On limits of wireless communications in a fading environment when using multiple antennas," *Wireless Personal Communications*, vol. 6, no. 3, pp. 311–335, 1998.

[5] A. Paulraj and T. Kailath, "Increasing capacity in wireless broadcast systems using distributed transmission/directional reception (DTDR)," *U.S. Patent*, 5 345 599, 1993.

[6] P. Wolniansky, G. Foschini, G. Golden, and R. Valenzuela, "V-BLAST: an architecture for realizing very high data rates over the rich-scattering wireless channel," in *Proceedings URSI International Symposium on Signals, Systems, and Electronics*, 1998, pp. 295–300.

[7] S. Alamouti, "A simple transmit diversity technique for wireless communications," *IEEE Journal on Selected Areas in Communications*, vol. 16, no. 8, pp. 1451–1458, 1998.

[8] V. Tarokh, N. Seshadri, and A. Calderbank, "Space-time codes for high data rate wireless communication: performance criterion and code construction," *IEEE Transactions on Information Theory*, vol. 44, no. 2, pp. 744–765, Mar 1998.

[9] E. Biglieri, R. Calderbank, A. Constantinides, A. Goldsmith, A. Paulraj, and H. V. Poor, *MIMO Wireless Communications*, Cambridge University Press, 2007.

[10] S. Sanayei and A. Nosratinia, "Antenna selection in MIMO systems," *IEEE Communications Magazine*, vol. 42, no. 10, pp. 68–73, 2004.

[11] J. Jeganathan, A. Ghrayeb, L. Szczecinski, and A. Ceron, "Space shift keying modulation for MIMO channels," *IEEE Transactions on Wireless Communications*, vol. 8, no. 7, pp. 3692–703, 2009.

[12] A. Molisch and M. Win, "MIMO systems with antenna selection," *IEEE Microwave*, vol. 5, no. 1, pp. 46–56, Mar 2004.

[13] A. Younis, N. Serafimovski, R. Mesleh, and H. Haas, "Generalised spatial modulation," in *Conference Record of the Forty Fourth Asilomar Conference on Signals, Systems and Computers (ASILOMAR)*, 2010, pp. 1498–502.

[14] Z. Chen, Z. Chi, Y. Li, and B. Vucetic, "Error performance of maximal-ratio combining with transmit antenna selection in flat Nakagami-m fading channels," *IEEE Transactions on Wireless Communications*, vol. 8, no. 1, pp. 424–431, Jan 2009.

[15] T. M. Duman and A. Ghrayeb, *Coding for MIMO communication systems*, John Wiley and Sons, 2007.

[16] R. Rajashekar, K. Hari, and L. Hanzo, "Antenna selection in spatial modulation systems," *IEEE Communications Letters*, vol. 17, no. 3, pp. 521–524, 2013.

[17] M. Yacoub, "The $\kappa-\mu$ distribution: a general fading distribution," in *Proceedings IEEE* $54^{th}$ *Vehicular Technology Conference, 2001*, vol. 3, 2001, pp. 1427–31.

[18] ——, “The $\eta-\mu$ distribution: a general fading distribution,” in *Proceedings IEEE* 52$^{nd}$ *Vehicular Technology Conference, 2000*, vol. 2, 2000, pp. 872–877.

[19] ——, “The $\kappa-\mu$ distribution and the $\eta-\mu$ distribution,” *IEEE Antennas and Propagation Magazine*, vol. 49, no. 1, pp. 68–81, 2007.

[20] N. Sollenberger, “Diversity and automatic link transfer for a TDMA wireless access link,” *in Proc. IEEE Global Telecommunications Conference, GLOBECOM ’93*, vol. 1, pp. 532–536, Nov 1993.

[21] S. Thoen, L. Van der Perre, B. Gyselinckx, and M. Engels, “Performance analysis of combined transmit-SC/receive-MRC,” *IEEE Transactions on Communications*, vol. 49, no. 1, pp. 5–8, Jan 2001.

[22] S. R. Meraji, “Performance analysis of transmit antenna selection in Nakagami-m fading channels,” *Wireless Personal Communications*, vol. 43, no. 2, pp. 327–333, Oct. 2007.

[23] A. Coskun and O. Kucur, “Performance analysis of joint single transmit and receive antenna selection in Nakagami-m fading channels,” *IEEE Communications Letters*, vol. 15, no. 2, pp. 211–213, February 2011.

[24] ——, “Performance analysis of joint single transmit and receive antenna selection in non-identical nakagami-m fading channels,” *IET Communications*, vol. 5, no. 14, pp. 1947–1953, Sept 2011.

[25] C.-C. Hung, C.-T. Chiang, N.-Y. Yen, and R.-C. Wu, “Outage probability of multiuser transmit antenna selection/maximal-ratio combining systems over arbitrary nakagami-m fading channels,” *IET Communications*, vol. 4, no. 1, pp. 63–68, January 2010.

[26] J. Pena-Martin, J. Romero-Jerez, and C. Tellez-Labao, “Performance of TAS/MRC wireless systems under Hoyt fading channels,” *IEEE Transactions on Wireless Communications*, vol. 12, no. 7, pp. 3350–3359, July 2013.

[27] H. Kim, H. Kim, N. Kim, H. Park, S. Seo, and J. Choi, “Efficient transmit antenna selection for correlated MIMO channels,” in *Proc. IEEE Wireless Communications and Networking Conference, WCNC*, April 2009, pp. 1–5.

[28] L. Yang, “Performance analysis of transmit antenna selection with MRC over correlated fast-fading channels,” in *Proc.* $4^{th}$ *International Conference on Wireless Communications, Networking and Mobile Computing, WiCOM ’08.*, Oct 2008, pp. 1–4.

[29] B.-Y. Wang and W.-X. Zheng, “BER performance of transmitter antenna selection/receiver-MRC over arbitrarily correlated fading channels,” *IEEE Transactions on Vehicular Technology*, vol. 58, no. 6, pp. 3088–3092, July 2009.

[30] D. Dixit and P. R. Sahu, “Performance of L-branch MRC receiver in $\eta-\mu$ and $\kappa-\mu$ fading channels for qam signals,” *IEEE Wireless Communications Letters*, vol. 1, no. 4, pp. 316–9, 2012.

[31] M. Milisic, M. Hamza, and M. Hadzialic, “Outage and symbol error probability performance of L-branch maximal-ratio combiner for generalized $\kappa-\mu$ fading,” in *Proc.* $50^{th}$ *International Symposium ELMAR*, vol. 1, Sept 2008, pp. 231–236.

[32] R. Subadar, T. Reddy, and P. R. Sahu, “Performance of an L-SC receiver over $\kappa-\mu$ and $\eta-\mu$ fading channels,” in *Proc. IEEE International Conference on Communications (ICC)*, May 2010, pp. 1–5.

[33] J. Zhang, Z. Tan, H. Wang, Q. Huang, and L. Hanzo, “The effective throughput of MISO systems over $\kappa-\mu$ fading channels,” *IEEE Transactions on Vehicular Technology*, vol. 63, no. 2, pp. 943–947, Feb 2014.

[34] J. Pena-Martin, J. Romero-Jerez, and C. Tellez-Labao, “Performance of selection combining diversity in $\eta-\mu$ fading channels with integer values of $\mu$,” *IEEE Transactions on Vehicular Technology*, vol. PP, no. 99, pp. 1–1, 2014.

[35] N. Y. Ermolova, “Moment generating functions of the generalized $\eta - \mu$ and $\kappa - \mu$ distributions and their applications to performance evaluations of communication systems,” *IEEE Communication Letters*, vol. 12, no. 7, 2008.

[36] ——, “Useful integrals for performance evaluation of communication systems in generalised $\kappa - \mu$ and $\eta - \mu$ fading channels,” *IET Communications*, vol. 3, no. 2, 2009.

[37] P. Yeoh, M. Elkashlan, N. Yang, D. da Costa, and T. Duong, “Unified analysis of transmit antenna selection in MIMO multirelay networks,” *IEEE Transactions on Vehicular Technology*, vol. 62, no. 2, pp. 933–939, Feb 2013.

[38] G. Brante, I. Stupia, R. D. Souza, and L. Vandendorpe, “Outage probability and energy efficiency of cooperative MIMO with antenna selection,” *IEEE Transactions on Wireless Communications*, vol. 12, no. 11, pp. 5896–5907, November 2013.

[39] Y. Gao and J. Ge, “Outage probability analysis of transmit antenna selection in amplify-and-forward MIMO relaying over Nakagami-m fading channels,” *Electronics Letters*, vol. 46, no. 15, pp. 1090–1092, July 2010.

[40] J. Li, Q. Zhang, Q. Li, L. Luo, and J. Qin, “Joint single transmit and receive antenna selection for MIMO cognitive radios without channel state information,” *Electronics Letters*, vol. 49, no. 13, pp. 848–850, June 2013.

[41] I.-H. Lee, H. Lee, and H.-H. Choi, “Exact outage probability of relay selection in decode-and-forward based cooperative multicast systems,” *IEEE Communications Letters*, vol. 17, no. 3, pp. 483–486, March 2013.

[42] H. Yu, I.-H. Lee, and G. Stuber, “Outage probability of decode-and-forward cooperative relaying systems with co-channel interference,” *IEEE Transactions on Wireless Communications*, vol. 11, no. 1, pp. 266–274, January 2012.

[43] G. Li, J. Chen, Y. Huang, and G. Ren, "Outage performance of multiple-input multiple-output decode-and-forward relay networks with the Nth-best relay selection scheme in the presence of co-channel interference," *IET Communications*, vol. 8, no. 15, pp. 2762–2773, October 2014.

[44] X. Jin, J.-S. No, and D.-J. Shin, "Source transmit antenna selection for MIMO decode-and-forward relay networks," *IEEE Transactions on Signal Processing*, vol. 61, no. 7, pp. 1657–1662, April 2013.

[45] H. Guo, J. Ge, and M. Gao, "Transmit antenna selection for two-hop decode-and-forward relaying," *Electronics Letters*, vol. 47, no. 18, pp. 1050–1052, September 2011.

[46] P. L. Yeoh, M. Elkashlan, and I. Collings, "MIMO relaying: Distributed TAS/MRC in nakagami-m fading," *IEEE Transactions on Communications*, vol. 59, no. 10, pp. 2678–2682, October 2011.

[47] ——, "Exact and asymptotic SER of distributed TAS/MRC in MIMO relay networks," *IEEE Transactions on Wireless Communications*, vol. 10, no. 3, pp. 751–756, March 2011.

[48] R. Mesleh, H. Haas, C. W. Ahn, and S. Yun, "Spatial modulation - a new low complexity spectral efficiency enhancing technique," in *Proceedings First International Conference on Communications and Networking in China*, 2006, pp. 1–5.

[49] R. Mesleh, H. Haas, S. Sinanovic, C. W. Ahn, and S. Yun, "Spatial modulation," *IEEE Transactions on Vehicular Technology*, vol. 57, no. 4, pp. 2228–41, 2008.

[50] J. Jeganathan, A. Ghrayeb, and L. Szczecinski, "Spatial modulation: optimal detection and performance analysis," *IEEE Communications Letters*, vol. 12, no. 8, pp. 545–7, 2008.

[51] J. Wang, S. Jia, and J. Song, "Signal vector based detection scheme for spatial modulation," *IEEE Communications Letters*, vol. 16, no. 1, pp. 19–21, January 2012.

[52] N. Pillay and H. Xu, "Comments on "signal vector based detection scheme for spatial modulation"," *IEEE Communications Letters*, vol. 17, no. 1, pp. 2–3, January 2013.

[53] A. Younis, S. Sinanovic, M. Di Renzo, R. Mesleh, and H. Haas, "Generalised sphere decoding for spatial modulation," *IEEE Transactions on Communications*, vol. 61, no. 7, pp. 2805–2815, July 2013.

[54] M. Di Renzo and H. Haas, "Bit error probability of space modulation over nakagami-m fading: Asymptotic analysis," *IEEE Communications Letters*, vol. 15, no. 10, pp. 1026–1028, October 2011.

[55] J. Luna-Rivera, M. Gonzalez-Perez, and D. Campos-Delgado, "Improving the performance of spatial modulation schemes for MIMO channels," *Wireless Personal Communications*, vol. 77, no. 3, pp. 2061–2074, 2014.

[56] M. Di Renzo and H. Haas, "Bit error probability of SM-MIMO over generalized fading channels," *IEEE Transactions on Vehicular Technology*, vol. 61, no. 3, pp. 1124–1144, March 2012.

[57] O. S. Badarneh and R. Mesleh, "Spatial modulation performance analysis over generalized $\eta-\mu$ fading channels," in $24^{th}$ *IEEE International Symposium on Personal Indoor and Mobile Radio Communications (PIMRC)*, Sept 2013, pp. 886–890.

[58] N. Pillay and H. Xu, "Comments on "antenna selection in spatial modulation systems"," *IEEE Communications Letters*, vol. 17, no. 9, pp. 1681–1683, 2013.

[59] H. A. David and H. N. Nagaraja, *Order Statistics*, $3^{rd}$ ed. New York: Wiley Interscience, 2003.

[60] G. L. Stuber, *Principles of Mobile Communication*. Kluwer Academic Publishers, Second Edition, 2002.

[61] M. K. Simon and M. S. Alouini, *Digital Communication over Fading Channels*, 2nd ed. New York: Wiley, 2005.

[62] A. Chockalingam and B. S. Rajan, *Large MIMO Systems*, Cambridge University Press, 2014.

[63] I. S. Gradshteyn and I. M. Ryzhik, *Table of Integrals, Series, and Products*, $7^{th}$ ed. New York: Academic Press, 2007.

[64] M. Chiani, D. Dardari, and M. K. Simon, "New exponential bounds and approximations for the computation of error probability in fading channels," *IEEE Transactions on Wireless Communications*, vol. 2, no. 4, pp. 840–5, 2003.

[65] M.-S. Alouini and A. Goldsmith, "Capacity of rayleigh fading channels under different adaptive transmission and diversity-combining techniques," *IEEE Transactions Vehicular Technology*, vol. 48, no. 4, pp. 1165–1181, Jul 1999.

[66] A. P. Prudnikov, I. A. Brychkov, O. I. Marichev, and G. G. Gould, *Integrals and series. Volume 3, More special functions*. Amsterdam, Paris, New York: Gordon and Breach science publ, 1986.

[67] K. J. R. Liu, A. Kwasinski, W. Su, and A. K. Sadek, *Cooperative Communications and Networking*. Cambridge University Press, First Edition, New York, 2008.

[68] A. Sendonaris, E. Erkip, and B. Aazhang, "User cooperation diversity. Part I. System description," *IEEE Transactions on Communications*, vol. 51, no. 11, pp. 1927–1938, Nov 2003.

[69] ——, "User cooperation diversity. Part II. Implementation aspects and performance analysis," *IEEE Transactions on Communications*, vol. 51, no. 11, pp. 1939–1948, Nov 2003.

[70] S. Peters and R. Heath, "Nonregenerative MIMO relaying with optimal transmit antenna selection," *IEEE Signal Processing Letters*, vol. 15, pp. 421–424, 2008.

[71] H. Suraweera, P. Smith, A. Nallanathan, and J. Thompson, “Amplify-and-forward relaying with optimal and suboptimal transmit antenna selection,” *IEEE Transactions on Wireless Communications*, vol. 10, no. 6, pp. 1874–1885, June 2011.

[72] M. Ju, H.-K. Song, and I.-M. Kim, “Joint relay-and-antenna selection in multi-antenna relay networks,” *IEEE Transactions on Communications*, vol. 58, no. 12, pp. 3417–3422, December 2010.

[73] J. G. Proakis, *Digital Communications*, $3^{rd}$ ed. New York: McGraw-Hill, 1995.

[74] R. Mesleh, O. Badarneh, A. Younis, and H. Haas, “Performance analysis of spatial modulation and space-shift keying with imperfect channel estimation over generalized $\eta - \mu$ fading channels,” *IEEE Transactions on Vehicular Technology*, vol. 64, no. 1, pp. 88–96, Jan 2015.

[75] N. Ermolova, “Moment generating functions of the generalized $\eta - \mu$ and $\kappa - \mu$ distributions and their applications to performance evaluations of communication systems,” *IEEE Communications Letters*, vol. 12, no. 7, pp. 502–4, 2008.

[76] M. Koca and H. Sari, “Performance analysis of spatial modulation over correlated fading channels,” in *IEEE Vehicular Technology Conference (VTC Fall)*, Sept 2012, pp. 1–5.

[77] E. Larsson, O. Edfors, F. Tufvesson, and T. Marzetta, “Massive MIMO for next generation wireless systems,” *IEEE Communications Magazine*, vol. 52, no. 2, pp. 186–195, February 2014.

# List of Publications

### Journal Publications

1. **Kumbhani B.** and Kshetrimayum R. S., " Outage Probability Analysis of Spatial Modulation Systems with Antenna Selection," *IET Electronics letters*, vol. 50, Issue 2, pp. 125-126, Jan 2014.

2. Kulkarni M., Choudhary L., **Kumbhani B.** and Kshetrimayum R. S., "Performance analysis comparison of transmit antenna selection with maximal ratio combining and orthogonal space time block codes in equicorrelated Rayleigh fading multiple input multiple output channels," *IET Communications*, vol. 8, Issue 10, pp. 1850-1858, July 2014.

3. **Kumbhani B.** and Kshetrimayum R. S., "Error Performance of Two-hop Decode and Forward Relaying Systems with Source and Relay Transmit Antenna Selection," *IET Electronics letters*, vol. 51, Issue 6, pp. 530-532, Mar 2015.

4. **Kumbhani B.** and Kshetrimayum R. S., "Analysis of TAS/MRC based MIMO systems over $\eta-\mu$ Fading Channels,", *IETE Technical Review*, vol. 32, Issue 4, 2015, pp. 252-259.

5. **Kumbhani B.** and Kshetrimayum R. S., "MGF based approximate SER calculation of SM MIMO systems over generalized $\eta-\mu$ and $\kappa-\mu$ fading channels," *Wireless Personal Communications* vol. 83, Issue 3, 2015, pp. 1903-1913.

6. **Kumbhani B.** and Kshetrimayum R. S., "Performance Analysis of MIMO systems with Antenna Selection over Generalized $\kappa-\mu$ Fading Channels," *IETE Journal of Research*, (accepted). DOI: 10.1080/03772063.2015.1082444

## Conference Publications

1. **Kumbhani B.**, Mohandas V. K., Singh R. P., Kabra S. and Kshetrimayum R. S., "Analysis of Space-Time Block Coded Spatial Modulation in Correlated Rayleigh and Rician Fading Channels," *in Proc. IEEE DSP*, Singapore, July 2015, pp. 516-520.

2. Kumar N., **Kumbhani B.** and Kshetrimayum R. S., "Performance analysis of MIMO based Cooperative Communication in $\kappa - \mu$ Fading Channels," *in Proc. IEEE ReTIS*, Kolkata, India, July 2015, pp. 520-525.

3. **Kumbhani B.** and Kshetrimayum R. S., "Source and Relay Transmit Antenna Selection in Two Hop Cooperative Communication Systems over $\kappa - \mu$ Fading Channels," *submitted to NCC 2016*.

# Bio-Data

| | | |
|---|---|---|
| 1 | Name: | Brijesh Kumbhani |
| 2 | Date of Birth: | 2-Sep-88 |
| 3 | Educational Qualifications: | May-2010 B.E. in Electronics and Communications Engineering (75.3%), Dharamsinh Desai University, Nadiad, India<br><br>June-2015 Ph.D (Thesis submitted, 9.37/10 CGPA), Indian Institute of Technology Guwahati, India |
| 4 | Permanent Address: | S/O S. H. Kumbhani<br>District: Amreli<br>At-Post: Lakhapadar<br>Gujarat, India<br>Pincode-365635 |
| 5 | Contact Address: | Room No B-256<br>Barak Hostel<br>Indian Institute of Technology Guwahati<br>North Guwahati 781 039<br>Assam, India |
| 6 | Contact Number | (+91)-9085304103 |